

THESIS

OBJECTIVE ANALYSIS OF EXTREME PRECIPITATION EVENTS IN DIVERSE
GEOGRAPHIC REGIONS

Submitted by

Nathan Robert Kelly

Department of Atmospheric Science

In partial fulfillment of the requirements

For the degree of Master of Science

Colorado State University

Fort Collins, Colorado

Spring 2018

Master's Committee:

Advisor: Russ S. Schumacher

Kristen L. Rasmussen

Peter A. Nelson

Copyright by Nathan Robert Kelly 2018

All Rights Reserved

ABSTRACT

OBJECTIVE ANALYSIS OF EXTREME PRECIPITATION EVENTS IN DIVERSE GEOGRAPHIC REGIONS

Extreme precipitation events are a focus of much research in the atmospheric science community today. These events are extraordinarily impactful to society, damaging critical infrastructure and in the worst cases taking lives. The factors that lead to these destructive events are not the same everywhere, dependent on each regions unique geography and climatology. There are two critical ingredients to precipitation: moisture and lift. However, there are many synoptic patterns that can combine these two ingredients in the right proportions, resulting in an extreme storm. This thesis addresses the relationship between lift and moisture, and relates these two variables to the patterns that produce them, in a way that can be applied to any region of the world.

To accomplish this task the synoptic patterns must be categorized. This is done in an objective way, using a global reanalysis product (namely MERRA-2) so as to be applicable to any area around the globe. The period 1980 to 2016 is analyzed, and an extreme precipitation event is defined here as an event that exceeds the 99.9th percentile of running 24-hour precipitation sums. Two domains are analyzed, one covering Argentina, and another covering northeast Colorado and part of the high plains to the north and east. Principal Component Analysis (PCA) is the objective method employed to investigate the variability within extreme precipitation events. PCA gives an indication as to what variables input into the analysis have the most impact on the variability of the dataset as a whole. This allows for an analysis of what

variables are most different in different extreme events and what variables are about the same across events. PCA is performed on two different sets of variables at each grid point in both the northern Colorado and Argentina. Two points are selected for further analysis herein; these are 40.5N 104.375W (near Greeley, Colorado) and 31.5S 63.75W (near Córdoba, Argentina).

At the northern Colorado gridpoint it is clear that there are two very distinct modes of extreme 24 hour precipitation. The first is a convective mode that is characterized at upper levels by a large ridge aloft with a small embedded shortwave. The second is a synoptic mode commonly associated with the most intense snowstorms in the region; a cutoff low approaching from the southwest. The convective mode is associated with more precipitable water than the synoptic mode, whereas in the synoptic mode the upper air features are able to contribute significantly to the lifting of air and cause extreme precipitation with a relative dearth of moisture. In Argentina, the primary variability seems to be in the position of a surface trough in the lee of the Andes as a large scale upper level trough impinges on the Andes crest. The first mode has this lee trough more directly contributing to lift and allowing the low level jet and associated moisture to reach farther south. The second involves the position of the lee trough farther north, which allows the south Atlantic high to push flow from the Atlantic upslope into the Sierra de Córdoba, initiating convection. The overlap between 1-hour and 24-hour extremes is also explored for Argentina, confirming the convective nature of much of this precipitation and illustrating just how important these convective episodes are to the production of extreme precipitation.

ACKNOWLEDGMENTS

I would like to thank Dr. Russ Schumacher and the entire Schumacher research group for their support and help throughout this project. Thanks also to my committee, Dr. Kristen Rasmussen and Dr. Peter Nelson for their help and understanding. Dr. Chris Kummerow deserves thanks and credit for his helpful suggestions regarding Chapter 10, which began as a class project in his Atmospheric Water Cycle class. I would also like to acknowledge the Science Olympiad academic competition for providing me an outlet for my interest in science that went deeper than my school coursework. Thank you to my family for supporting and nurturing that interest and being a constant source of support for me in all my endeavors. Most of all thanks to my wonderful wife, Aura Lee, who has been an immense support and inspiration for me ever since the day I met her.

TABLE OF CONTENTS

ABSTRACT	ii
ACKNOWLEDGMENTS	iv
LIST OF FIGURES	vii
CHAPTER 1 INTRODUCTION	1
1.1 Statement of the Problem.....	1
1.2 Objectives and Scope of Research.....	2
CHAPTER 2 Background.....	5
2.1 Introduction.....	5
2.2 History: Early Days.....	5
2.3 Other Classifications of Extreme Precipitation.....	7
2.4 South American Convection and Extreme Precipitation	10
2.5 Colorado Convection and Extreme Precipitation	13
2.6 Summary	15
CHAPTER 3 DATA	16
3.1 MERRA-2.....	16
3.2 Stage IV	23
3.3 Domain.....	24
CHAPTER 4 Methods	26
4.1 Choosing Period and Threshold.....	26
4.2 Principal Component Analysis	30
4.3 ClickHist	33
CHAPTER 5 timing at selected gridpoints	34
5.1 Introduction.....	34
5.2 Córdoba, Argentina.....	34
5.3 Mendoza, Argentina.....	38
5.4 Northern Colorado	42
5.5 Conclusion	44
CHAPTER 6 Analysis of Two Events.....	46
6.1 Introduction.....	46
6.2 Precipitable Water Scenario.....	47
6.3 Synoptic Scenario	49
6.4 Comparison of Quantitative Amounts	51
6.5 Summary	56
CHAPTER 7 PCA of Extreme events with common meteorological variables.....	58
7.1 Introduction.....	58
7.2 Northern Colorado (40.5 North 104.375 West).....	59
7.3 Córdoba, Argentina (31.5S 63.75W).....	64
7.4 Conclusion	70
CHAPTER 8 pca of meteorological variables directly correlated with lift.....	71
8.1 Introduction.....	71
8.2 Northern Colorado	72
8.3 Córdoba, Argentina.....	73

8.4 Summary	74
CHAPTER 9 Events in Context.....	75
9.1 Introduction.....	75
9.2 Precipitable Water.....	75
9.3 Low Level Divergence.....	77
9.4 Conclusion	79
CHAPTER 10 analyses of 1-hr and 24-hr overlap	80
10.1 Introduction.....	80
10.2 Results.....	80
10.3 Conclusions.....	87
CHAPTER 11 summary and conclusions.....	89
11.1 Summary.....	89
REFERENCES	91

LIST OF FIGURES

FIGURE 2-1	1911 FLOOD IN DURANGO.....	7
FIGURE 2-2	STORM TRACKS.....	12
FIGURE 2-3	SEASONALITY OF COLORADO EXTREMES.....	14
FIGURE 3-1	MODEL PRECIPITATION.....	18
FIGURE 3-2	AVERAGE VALUES ABOVE THE 99TH PERCENTILE.....	19
FIGURE 3-3	OBSERVATION CORRECTED PRECIPITATION.....	20
FIGURE 3-4	TOPOGRAPHY.....	23
FIGURE 4-1	THRESHOLD VALUES.....	28
FIGURE 4-2	HISTOGRAM OF UNIQUE EVENTS.....	29
FIGURE 4-3	PCA EXAMPLE.....	32
FIGURE 5-1	TIME SERIES; CÓRDOBA.....	35
FIGURE 5-2	EVENTS PER MONTH CÓRDOBA.....	36
FIGURE 5-3	UTC TIME VS HOURLY PRECIPITATION.....	37
FIGURE 5-4	TIME SERIES; MENDOZA.....	38
FIGURE 5-5	EVENTS PER MONTH; MENDOZA.....	40
FIGURE 5-6	AN “EXTREME EVENT”.....	41
FIGURE 5-7	TIME SERIES; COLORADO.....	42
FIGURE 5-8	EVENTS PER MONTH; COLORADO.....	43
FIGURE 5-9	UTC TIME VS HOURLY PRECIPITATION; COLORADO.....	44
FIGURE 6-1	2D HISTOGRAM PRECIPITATION VS PRECIPITABLE WATER.....	47
FIGURE 6-2	PRECIPITABLE WATER Z-SCORE.....	48
FIGURE 6-3	WEATHER MAP FOR THE SEPTEMBER FLOODING EVENT.....	50
FIGURE 6-4	WEATHER MAP FOR THE APRIL EVENT.....	51
FIGURE 6-5	MERRA-2 PRECIPITATION; APRIL 2009 EVENT.....	53
FIGURE 6-6	MERRA-2 PRECIPITATION; SEPTEMBER 2013 EVENT.....	54
FIGURE 6-7	STAGE IV PRECIPITATION; APRIL 2009 EVENT.....	55
FIGURE 6-8	STAGE IV PRECIPITATION; SEPTEMBER 2013 EVENT.....	56
FIGURE 7-1	PLOT OF PC1 LOADINGS; COLORADO.....	60
FIGURE 7-2	CONFIDENCE INTERVALS; COLORADO.....	61
FIGURE 7-3	500HPA HEIGHT; BOTTOM 25% OF PCS.....	62
FIGURE 7-4	500HPA HEIGHT; TOP 25% OF PCS.....	62
FIGURE 7-5	PRECIPITABLE WATER; BOTTOM 25% OF PCS.....	63
FIGURE 7-6	PRECIPITABLE WATER; TOP 25% OF PCS.....	63
FIGURE 7-7	PC1 LOADINGS; CÓRDOBA.....	65
FIGURE 7-8	SIGNIFICANCE PLOT FOR THE CÓRDOBA PCA.....	65
FIGURE 7-9	SEA LEVEL PRESSURE AND 10M WIND; BOTTOM 25% OF PCS.....	66
FIGURE 7-10	SEA LEVEL PRESSURE AND 10M WIND; TOP 25% OF PCS.....	67
FIGURE 7-11	PRECIPITABLE WATER; BOTTOM 25% OF PCS.....	68
FIGURE 7-12	PRECIPITABLE WATER; TOP 25% OF PCS.....	69
FIGURE 8-1	PCA OF LIFT VARIABLES; COLORADO.....	72
FIGURE 8-2	LIFT VARIABLE LOADINGS AT CÓRDOBA.....	74
FIGURE 9-1	PRECIPITABLE WATER; NORTHERN COLORADO.....	76

FIGURE 9-2	PRECIPITABLE WATER; CÓRDOBA.....	77
FIGURE 9-3	10M WIND DIVERGENCE FOR NORTHERN COLORADO.....	78
FIGURE 9-4	10M WIND DIVERGENCE FOR CÓRDOBA.....	78
FIGURE 10-1	1-HOUR TO 24-HOUR AMOUNT RATIO MAP.....	82
FIGURE 10-2	24-HOUR PERIODS WITHOUT A 1-HOUR PERIOD.....	83
FIGURE 10-3	CUMULATIVE PRECIPITATION FROM CÓRDOBA.....	84
FIGURE 10-4	CUMULATIVE PRECIPITATION FROM 35.5S 64.375W.....	84
FIGURE 10-5	500HPA COMPOSITE COMPARISON; CÓRDOBA.....	85
FIGURE 10-6	500HPA COMPOSITE COMPARISON; 35.5S 64.375W.....	86
FIGURE 10-7	PRECIPITABLE WATER COMPOSITE COMPARISON; CÓRDOBA.....	86
FIGURE 10-8	PRECIPITABLE WATER COMPOSITE COMPARISON; 35.5S 64.375W.....	87

CHAPTER 1 INTRODUCTION

1.1 Statement of the Problem

The Goldilocks of weather phenomena, rain can be fickle. Too little, and drought can cripple a region. Too much, and floods can wash away lives and livelihoods. Look no further than Cape Town, South Africa during February 2018, when taps were in danger of running dry within months. A sudden storm during the month brought welcome rain that pushed back the day the city's water will run out, but also caused nine flash flooding deaths. This thesis examines those situations in which the delicate balance humanity has with precipitation is tilted toward the heavy side. What atmospheric patterns lead to extreme precipitation, and are these patterns similar in different regions? Does extreme precipitation in a given area almost always occur under the same patterns, or can multiple patterns produce extreme conditions?

These questions will be answered specifically for Colorado and Argentina. These locations were chosen for their relative geographic similarity, with both situated on the east side of north- south-oriented mountain ranges having similar climates. Furthermore, comparing Colorado to Argentina allows for comparison of a thoroughly studied region to a somewhat less studied one. Argentina is the focus of the upcoming RELAMPAGO field campaign which will closely observe summertime convective precipitation processes in the Córdoba and Mendoza regions. This thesis will build towards the research that will be conducted in the field as meteorologists seek to understand the processes at work in the deepest thunderstorms on Earth (Zipser et al. 2006).

1.2 Objectives and Scope of Research

The goal of this research is to produce objective categorization of extreme precipitation events in these two regions using a method that can be generalizable to the entire globe. By impartially identifying relevant patterns in a way generalizable for any location on the globe this research aims to extend knowledge of how these events occur. Beyond the scope of this research for now is speculating on how these events may change in a changing climate. However, using the baseline knowledge that this research provides will enable a better hypothesis as to how a warmer climate may impact extreme events.

Extreme precipitation occurs where it rains harder for longer, that is: total precipitation equals precipitation duration multiplied by precipitation rate (Doswell et al. 1996). Both duration and rate are affected by two fundamental variables that affect precipitation: moisture and lift. The effect of a warmer climate on moisture is well known, because a warmer atmosphere can hold more water, total water vapor content will increase assuming a constant relative humidity, requiring more evaporation (Flohn et al. 1990). Pan evaporation has not increased, however, but this may be a result of more terrestrial evaporation leading to more humidity in the air and therefore less evaporation from the pan (Ohumura and Wild 2002). An increase in moisture is predicted by a slab ocean model incorporating predicted increases in greenhouse gasses (Rose and Rencurrel 2015). Satellite observations portray increasing moisture in the air, but a slower increase in actual precipitation after instrumentation effects are accounted for (Wentz et al. 2007; personal communication with author). Stephens and Ellis (2008) support this disparity between moisture and precipitation increases using a collection of climate models used for the IPCC AR4 report, finding that on a global scale precipitation is primarily controlled by radiative loss from the column. Radiative loss from the column is in turn predicted to decrease. The

decrease in radiative loss is due to a slight decline in low troposphere relative humidity, reducing low and mid-level cloud amount while leaving high clouds relatively unchanged. This leads to a warmer column with less instability, and therefore less precipitation. This decrease in instability leads to the next portion of the equation, lift. This part of this equation is far less certain. Even for the most predictable source of lift, the passage of Rossby wave, there is currently much uncertainty (Barnes and Polvani 2013, Francis 2017). Rossby waves depend on the differential warming between the arctic and tropics, and the response to warming of these waves could greatly impact synoptic forcing for lift.

Mesoscale sources of lift are also quite uncertain in future climate, a fact exacerbated because unlike Rossby waves they occur at smaller scales than global climate models. Some research has been done that addresses this problem by climate models to determine changes in larger scale variables known to be favorable for severe convection (Púčik et al. 2017, Allen et al. 2014, Trapp and Hoogewind 2016). These studies all covered different regions (Europe, Australia and the United States respectively) but all found an increase in favorable convective environments largely associated with higher convective available potential energy (CAPE) due to higher low level temperature and moisture. Note the contrast to Stephens and Ellis, which found warmer columns that would imply less CAPE on a global average scale. Trapp and Hoogewind (2016) also ran downscaled models that showed no significant differences in storm morphology compared to current climate. Thus determining the relative contributions of moisture and lift to historical events as represented in reanalysis will allow potential for further insight into what could be expected in the future. A region where moisture is the primary control on extreme precipitation could have a very different response than a region where the primary control is lift. Analysis of extreme events in the past can therefore contextualize these events for better

understanding of how they may change in the future. Furthermore, knowledge of these patterns will also aid RELAMPAGO forecasters for extreme rain during the field campaign that is set to take place there in November and December 2018.

CHAPTER 2 BACKGROUND

2.1 Introduction

This study is of course not the first to consider the problem of extreme precipitation in Colorado or Argentina. Many researchers have come before, building a large body of knowledge in service to both society and the ideal of advancing human understanding of our environment. This review of the published literature will provide an overview of the background from which the work in this thesis was born. A brief history of the early days of meteorology in Colorado and Argentina is provided. The section then shifts to an overview of previous synoptic classifications of patterns that produce extreme precipitation, and further insight on the mechanisms that produce extreme rain.

2.2 History: Early Days

The late 1800's, with the rapid advances in both transportation and communication technology, brought about a flowering of knowledge about climate and weather due to the newfound ability to place observing stations in remote places, and communicate with them via telegraph. A Monthly Weather Review (MWR) article from November 1897 titled 'Recent Publications' lists a compendium of Argentine climatological data, "Ligeros apuntes sobre el clima de la Republica Argentina," published in 1889 (Smith 1897). A further MWR article describes successful efforts to create a sufficient network of stations and telegraph rights in the country to produce daily 2pm weather maps. (C.A. 1902). By 1917 understanding of the weather in the country had advanced sufficiently that H. Helm Clayton was able to publish a review of

Argentine weather that notes that “10 types [of circulations] 4 of high pressure and 6 of low pressure, have been recognized in Argentina . . . In Summer the cyclones linger over the hot arid plains between Mendoza and Santiago.” The article also displays the growing recognition in the field of meteorology at the time that “the movements of the cyclones seem to be controlled by two factors: (1) The upper drift . . . and (2) the sea level pressure over large areas” (Clayton 1917). However, since that time period, there has been relatively little research in Argentine precipitation, and especially how that precipitation compares to North American precipitation. A synopsis of the recent research that has been done regarding precipitation in Argentina will be presented in the following section.

Meanwhile, in Colorado, an attempt was made at seasonal forecasting for precipitation. The effort was inconclusive, noting that the precipitation in one season does not give much predictive insight to the precipitation of the following season (Brandenburg 1900). In 1911 Brandenburg details a serious flood that occurred in the San Juan Mountains as a result of October precipitation falling in the form of rain instead of snow. (Brandenburg 1911). Figure 2-1 shows an image of this historic flood from Durango, CO. There are many more examples, but these few are presented here to underline the rich and long history of atmospheric research in these regions. In the intervening decades many other researchers have followed in the footsteps of these pioneers investigating the cyclones that produce the most interesting and impactful weather, including extreme precipitation.

Jumping forward about 50 years, in 1967 a study was published by Charles Stidd that used the monthly average of precipitation at 60 Nevada weather stations to investigate the largest modes of annual variability in precipitation amount. This study used the same technique used to produce this thesis, principal component analysis. However the study is much simpler, because

“a 12X12 matrix that had to be diagonalized. This was too much of a job for our IBM 1620 to handle efficiently and it was sent to the Western Data Processing Center.” Nonetheless, the study was an important first foray into the use of objective methods to categorize precipitation.



Figure 2-1 1911 flood in Durango. 5.5 hours after the photo, water was up to the top of the arches. Photo from the archives of the Durango Herald.

2.3 Other Classifications of Extreme Precipitation

Maddox et al. (1979) sought to classify synoptic patterns associated with flash flooding across the United States. This was motivated by a series of destructive flash floods throughout the 1970's that severely impacted both life and property. The authors subjectively sifted through 150 cases of flash floods, as defined by flash flood storm reports over the period 1973 to 1977 throughout the continental United States. These they separated into four patterns, western, mesohigh, frontal, and synoptic composing 21%, 34%, 25% and 20% of events respectively. For the western events it is noted that since there is far less data availability for events in the Rocky Mountains and farther west, nothing conclusive can be drawn. The authors do mention that other

than strong synoptic events, many western events could be credibly classified as one of the three other types, albeit with orographic modification. Western events were further explored by Maddox et al. (1980), which showed that weak shortwave troughs moving around large ridges were an important component in the non-synoptic western events. Mesohigh events resulted from the nearly stationary outflow boundary of a previous thunderstorm or complex of thunderstorm lifting moist air flowing in from the south. Frontal events are very similar to mesohigh events, except that the focus for lift in this case is a synoptic scale frontal boundary rather than thunderstorm outflow. Since these events include significant veering winds with strong westerly winds aloft, storms often form and then move along the front, inundating the flooding area with thunderstorm after thunderstorm. The last type of event is the synoptic type. This is again similar to the other two types in that warm moist air is being lifted over some sort of frontal boundary. The difference in this case is that the areal coverage is larger, and the system is more progressive and associated with a strong upper level trough. Together, these classifications provide insight into why flash floods occur in specific atmospheric situations. Limitations to this particular approach to classification include the lack of detail and incomplete coverage that using only the flash flood report database entails, as well as the subjective nature to the classifications since the scenarios are all broadly similar.

Stevenson and Schumacher (2014) also embarked on a classification of the causes of precipitation extremes. This study utilized Stage IV data, a multi-sensor precipitation product composed of radar and gauges interpolated to a 4km grid, and considered the 100 year recurrence interval at locations in the continental United States east of the Rockies. Classifying the discovered events into categories, this study found that 63% of such events are due to a mesoscale convective system (MCS), 30% were synoptic in nature, and 7% were tropical. This is

of course not to say that there are certain synoptic conditions favourable for the growth of extreme rain producing MCS, as described in the preceding paragraph. This study also notes that in the stage IV data there is not much overlap between hourly and 24 hour exceedances of a given recurrence interval. Only 16% of one hour points corresponded to a 24 hour point. This is likely due to the relatively high resolution of the stage IV dataset, which allows for large precipitation amounts in an hour associated with a single thunderstorm to be accurately identified in a way that is not possible in MERRA-2.

Another more objective effort aimed at prediction was undertaken by Garavaglia et al. (2014). They sought empirical predictors of months with extreme values using gauge precipitation data and NCEP/NCAR reanalysis. To do this they used just two variables: 500hPa height and water vapor convergence. Using these variables three indices were created, one to indicate the amount of troughing over the South American continent and two others consisting of eastern and western region water vapor convergence. The La Plata basin was split into three regions, and in each of these regions the authors found high correlations between troughing and moisture convergence and the probability of a month of extreme precipitation, with the probability of detection over climatology improving 50%.

This thesis seeks to build on these earlier efforts in a few ways. One, it will be objective, so that researcher opinion will not be necessary in classification. Objectiveness will improve on differentiating atmospheric scenarios that seem similar, and allow the method to be entirely generalizable and repeatable. Second, it will use a longer record than was available to either of these earlier papers by using the full MERRA-2 reanalysis record. The limitation of this study compared to these previous studies is the relatively coarse resolution of MERRA-2 data compared to gridded gauge or remote sensing data.

2.4 South American Convection and Extreme Precipitation

Argentina has some of the most intense thunderstorms on Earth, as described by data from the Tropical Precipitation Measurement Mission (TRMM) satellite (Zipser et al. 2006). Most of the extreme precipitation events in Argentina's La Plata basin, in the northeast of the country bordering Brazil and Uruguay, stem from large MCS (Cavalcanti 2012). Though not specifically mentioned in the paper, judging by the description and composite figures, these events would appear to fall within the same categories as Maddox, with a major mechanism being the lifting of the warm moist low level jet from the Amazon being lifted over some boundary. This conclusion is supported by the fact that 41% of days with a strong low level jet (LLJ) produced an MCS, while only 12% of days without one did (Salio et al. 2007). Occurrences of MCS were also observed to have a mutually reinforcing relationship with the LLJ, which explains why an MCS was observed in conjunction with such a high proportion of strong LLJ events (Saulo et al. 2007). The Andes were also found to be a significant contributor to the favorable convective environment, as simulations with a reduced Andes crest produced less CAPE (due to a weaker LLJ) and more CIN (leading to more intense storms after breaking of the cap) than the control simulation with the real world Andes topography (Rasmussen and Houze 2016). Durkee et al. (2009) described the general characteristics of the MCS that form in the region. They found that, especially at the upper tail of the distribution, cloud shield size and duration of these MCS are larger than their counterparts in the United States. Also, MCS in Argentina had a much larger contribution to total precipitation, 50% vs 20%. This is particularly true in the warm season. Figure 2-2, taken from Durkee et al.'s figure 7, illustrates the climatologically favored locations of MCS by adding up all the number of storm tracks that passed over a given point. It can be seen from the map that the highest concentration of storms is

near the Andes where they form with diminishing concentrations to the east where they move on diverging paths depending on ambient conditions. This model of initiation, growth and eastward movement as a wide stratiform region was furthered by work that showed using TRMM radar data the evolution of convective mode throughout the life cycle of the storm (Rasmussen 2011). Building on this MCS research, Rasmussen et al. 2015, again using TRMM data, reported that the fraction of South American subtropical precipitation from MCSs with extreme characteristics (defined as a >10km echo at > 40dbz, area coverage > 50000km², and/or 40dbz > 1000km²) exceeded 80%. This result was despite the percentage of defined raining areas classified as extreme comprising less than 4% of the dataset containing all rain events. With the north-central region of Argentina receiving so much precipitation from MCSs, it is expected that patterns that lead to extreme precipitation will be patterns that are favorable for MCS development and propagation.

As one may expect, extreme precipitation from these storms is most common in conjunction with El Niño due to the strengthening of the subtropical jet and initiation of eastward propagating Rossby waves in the east-central Pacific. Both of these occurrences strengthen the low level jet that transports moisture from the Amazon and tropical Atlantic southward into Argentina (Grimm and Tedeschi 2009). Convection is also moderated by the South Atlantic convergence zone. Factor analysis of the precipitation at Sao Paulo, Brazil resulted in two distinct axes of variance, weak and strong South Atlantic Convergence Zone (SACZ), and oceanic vs continental convection (Carvalho 2002). Factor analysis is similar to PCA, but not exactly the same. It seeks a prediction of an unmeasurable variable using measurable variables, while PCA is meant to boil down a large matrix into a single time series. Regarding this study it should also be noted that Sao Paulo is far to the northeast of the main region of interest for this

study. However, as this study describes, the SACZ can have impacts far beyond just the narrow region it directly occurs in, through its influence on the subtropical jet stream. Indeed a 2-year cycle of precipitation variability can be observed in west-central Argentina, which agrees with an El Nino timescale. Additionally, since the mid 1970's the impact of ENSO on Argentinian precipitation seems to have increased, though this may just be an artifact of more stations and better record keeping (Agosta and Compagnucci 2011). These results agree with earlier work by Penabla and Vargas (2004), who also note that wet years oscillate on an annual cycle, with the very wettest years occurring on the back of lower frequency cycles.

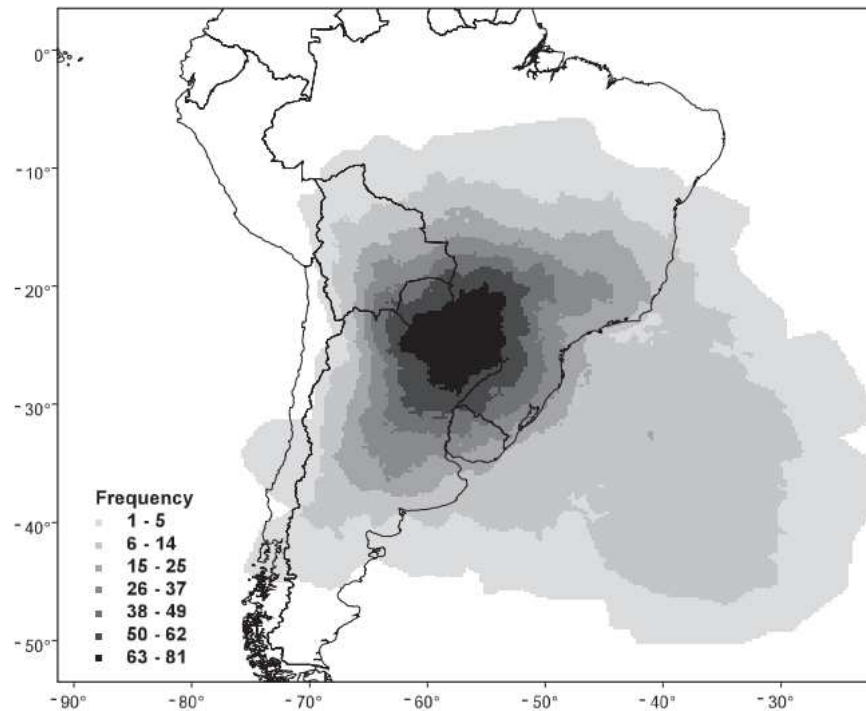


Figure 2-2 Plot showing number of times an MCC storm track crossed the location from October to May 1998-2007. From Durkee et al. (2009)

2.5 Colorado Convection and Extreme Precipitation

Much of the recent work on extreme precipitation in Colorado has centered around the recent September 2013 flood, and for good reason, as it resulted in over two billion dollars in damage. The flood was characterized by both an exceptional areal coverage and long duration. Doswell et al. 1996 discuss different storm morphologies by their contribution to rain rate and duration. The 2013 flood involved record amounts of precipitable water for that kind of year in Colorado. So unusual was the situation that warm rain processes dominated, and the radar precipitation retrievals from the event had to be corrected to use a tropical reflectivity precipitation relation, while at the same time continuous upslope flow created an environment for a long duration of rainfall (Gochis et al. 2015). However, this being merely one flood event, albeit of epic historical proportions, the question remains how representative it may be of other extreme rain events. This is in contrast to two other heavily studied Colorado events, the 1997 Northern Colorado flood and the 1976 Big Thompson Canyon flood (Maddox et al. 1977, Peterson et al. 1999), which were characterized by higher rainfall rates over a shorter period of time, as they were associated with single storms that remained over the same area for several hours. Figure 2-3 shows the seasonal distribution of extreme precipitation, especially in the mountains, is not as clearly correlated to the climatologically wettest months, as evidenced by the late summer floods. Many stations can receive extreme precipitation outside of the climatologically wettest months of springtime. In the case of the Front Range in the September 2013 flood, the monsoonal pattern of July and August held over into September, and the ingredients came together for a historic flood. These results show that for Colorado and the high plains, extreme precipitation is a year round risk (Mahoney et al. 2015).

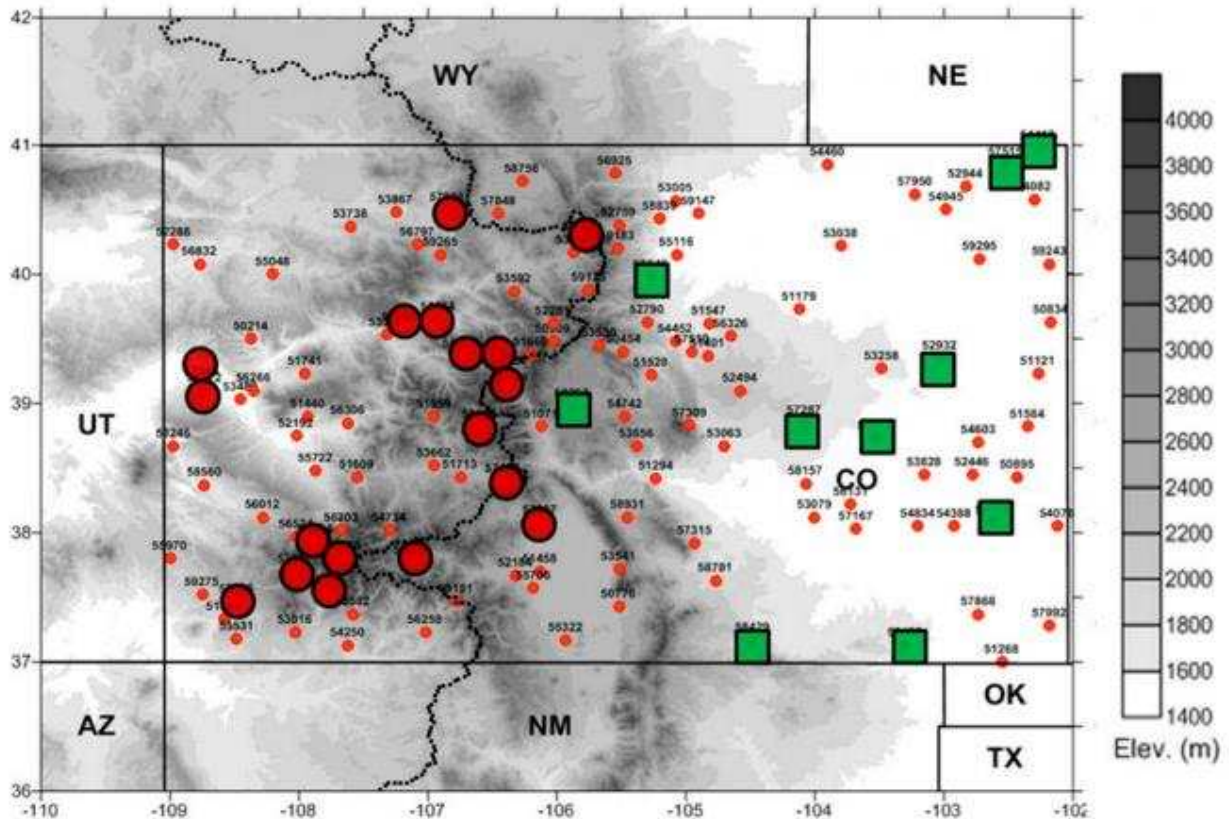


Figure 2-3 Red circles denote stations where less than 40% of the top 10 daily rain events occurred during the three wettest months of the year and more than 40% in the driest six months; Green squares denote where more than 90% occurred in the wettest three months and none in the driest six. Red dots are stations that fit neither criteria. From Mahoney et al. (2015)

When investigating events in the western United States as a whole, ENSO again plays a large role. This is particularly true of the events to the west of the Cascades and Sierra Nevada, far outside the domain of this study, but effects are also felt further inland at reduced magnitude. EOF analysis (the spatial version of PCA analysis) was used to identify patterns in wintertime precipitation by Schubert et al. (2008). They found that the EOF pattern favored (West Coast, Midwest, Gulf Coast or East) depended significantly on ENSO phase. Jiang et al. (2016) note two distinct regions of ENSO related variability in the western United States, a southwest and northwest region, with a transition zone in between. These zones were defined with several

metrics (total precipitation, days with greater than 10mm, consecutive dry days, five day precipitation, amount of precipitation per rainy day, and amount of annual precipitation contributed by rain above the 95th percentile), with eastern Colorado either falling in the southwest region or transition zone. These studies show the influence of ENSO on precipitation in the western United States.

2.6 Summary

As we have seen, extreme precipitation is a complex problem, especially in the presence of orography, as is the case in Colorado and Argentina. Ocean teleconnection patterns can provide favorable environments for extreme precipitation, but local weather patterns must also be favorable. This can occur through a favorable convective environment or favorable orography, and combinations of the two can produce a particularly impactful event, as occurred along the Front Range in September 2013. In many cases it is an MCC that persists for several hours that is the cause of the most extreme totals, especially in Argentina. This research seeks to build on this long tradition of investigation that began in the 1800's and been rejuvenated in the past two decades.

CHAPTER 3 DATA

3.1 MERRA-2

This study primarily utilizes an atmospheric reanalysis product. Reanalysis is a method that implements a model to produce a quasi-observational dataset. Producing such a dataset allows for a continuous record on a gridded domain over a long period of time, mitigating the issues found in observational datasets such as missing data or simply not enough observations for good coverage. The model is run by implementing a wide variety of available datasets in the data assimilation scheme to create an initialization state of the model. The initialization state is then stored as the state of the atmosphere at that moment in time. In this way observational data are gridded and refined by the model so that there are no missing data, providing a continuous and coherent record of global weather. This is very important to a study like this one that requires a continuous record with a guarantee of model stability throughout. This mitigates the effect of potentially systematically biased observational datasets. Pitfalls of reanalysis can include discontinuities in fields related to changes in available observational systems, and that areas without a lot of observations can involve large amounts of interpolation. Because of the computing requirements involved in producing a long term record with the model, the resolution of the reanalysis in both the vertical and horizontal is relatively course, at ~50km in the horizontal and 72 model layers in the vertical. Near the ground the vertical resolution is every 15hPa up to 800hPa, 25mb to 675hPa, 37.5hPa to 337.5hPa. Above that level the pressure increments tighten again as the distance in meters between pressure levels increases exponentially with height. As new satellite systems have come on line there is less need for

interpolation in data sparse areas. For a philosophical discussion of the strengths and weaknesses of reanalyses in relation to other ways of analyzing observations, see Parker (2016); Hoffman (2017), and Parker (2017). This section will discuss the relative strengths and weaknesses of the MERRA-2 reanalysis used in this study. Also included is a brief discussion of the NCEP Stage IV precipitation analysis, which is used to compare with MERRA-2 for a few events in the Colorado domain.

MERRA-2 reanalysis utilizes the Goddard Earth Observing System version 5.12.4 as the underlying modeling system (Bosilovich et al. 2015, Gelaro et al. 2017). The resolution is 0.5 degrees in latitude and 0.625 degrees in longitude with 72 model levels and full global coverage. Temporal resolution is one or three hours depending on variable. MERRA-2 provides a significant improvement on the first version of MERRA, particularly in the representation of the water cycle. This is partially done through observation correction of model produced precipitation where such observations are available. Both satellite and rain gauges are used for these corrections, so there is not a serious deficiency in gauge sparse regions. By correcting precipitation with observations rather than relying on model precipitation the model is then better able to represent important soil moisture processes that feed back onto the atmosphere. Model precipitation is retained as a sink for atmospheric water.

Representation of the water cycle is also improved by using the dry mass of the atmosphere as a constraint. Since the dry mass of the atmosphere does not change significantly, especially on the model timescales, the integration is done to ensure that dry mass is conserved and the only changes in atmosphere mass come from changes in water vapor content. Because of this, spurious jumps in total column water do not occur in conjunction with changes in observational inputs with nearly the same intensity in MERRA-2 as they do in MERRA. Figure

1, shows this increased stability in the model precipitation with time in the MERRA-2 model precipitation product. This study will use the observation corrected product, further mitigating these issues. This is important because the entire 1980 to 2016 data record will be used for this study, meaning that reducing fluctuations purely due to observing system is crucial to avoid sudden jumps in the data record unrelated to real changes in the Earth system.

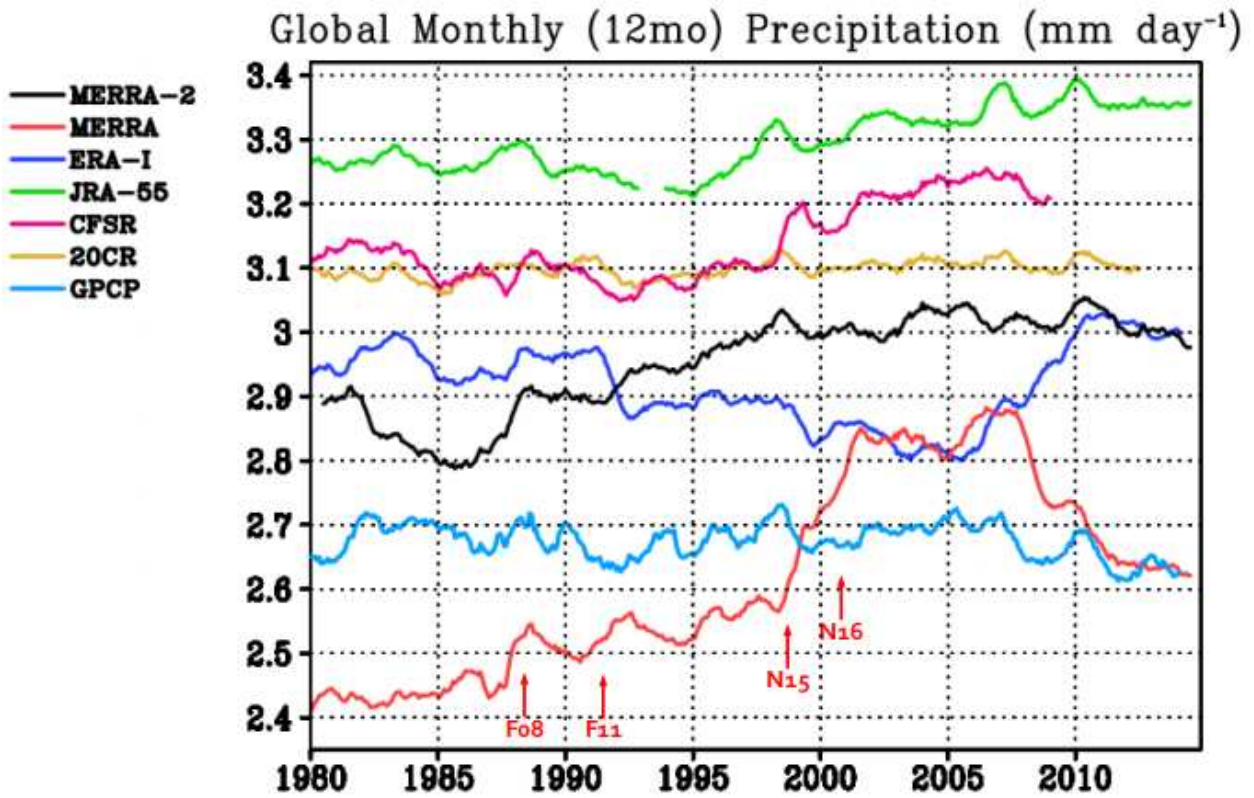


Figure 3-1 MERRA-2 model precipitation compared to other reanalysis products to show the improved stability of precipitation in the model. Arrows pointing to the MERRA line indicate when a new precipitation product was assimilated. Reproduction of Bosilovich et al. 2015 figure 6-4

The later years of the MERRA-2 record benefit from being able to assimilate increased satellite observations, including satellite radio occultation and aerosol measurements. Radio occultation utilizes the precise timing of Global Positioning System satellite signals as they pass through the atmosphere to derive the density. From this density, temperature and water content

can be inferred. This technology has allowed an unprecedented number of space borne measurements of atmospheric profiles. Due to the lower cost and therefore greater number of platforms in orbit, the radio occultation technique is able to provide far greater coverage both spatially and temporally of the globe than radiosondes or polar orbiting satellites. Aerosol measurements from space allow the model to simulate how the aerosols affect radiation interactions and how this warming and cooling feeds back onto the atmosphere. Aerosol optical

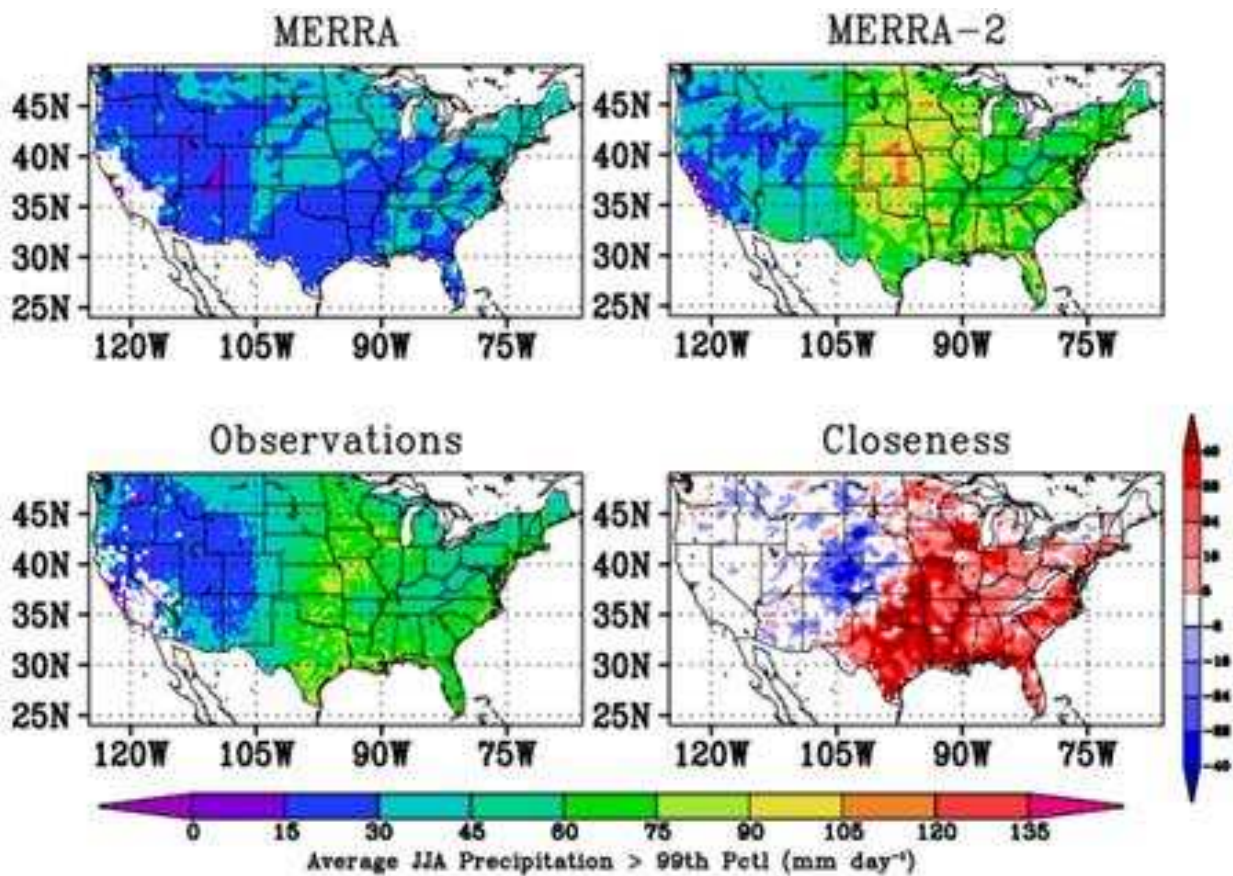


Figure 3-2 The average value of the 99th percentile for June, July and August for MERRA, MERRA-2 and the CPC gauge dataset. Closeness shows whether MERRA (blue) or MERRA-2 (red) is closer to the observation value. From Bosilovich et al. 2015

depth is directly assimilated and from this the model physics is able to compute radiation interactions with the aerosols, as well as other variables such as aerosol transport and concentration. See Randles et al. 2017 for further discussion of this assimilation. Taken together, these newly assimilated satellite measurements provide a much clearer picture of atmospheric profiles, which are crucial for the accurate representation of the weather.

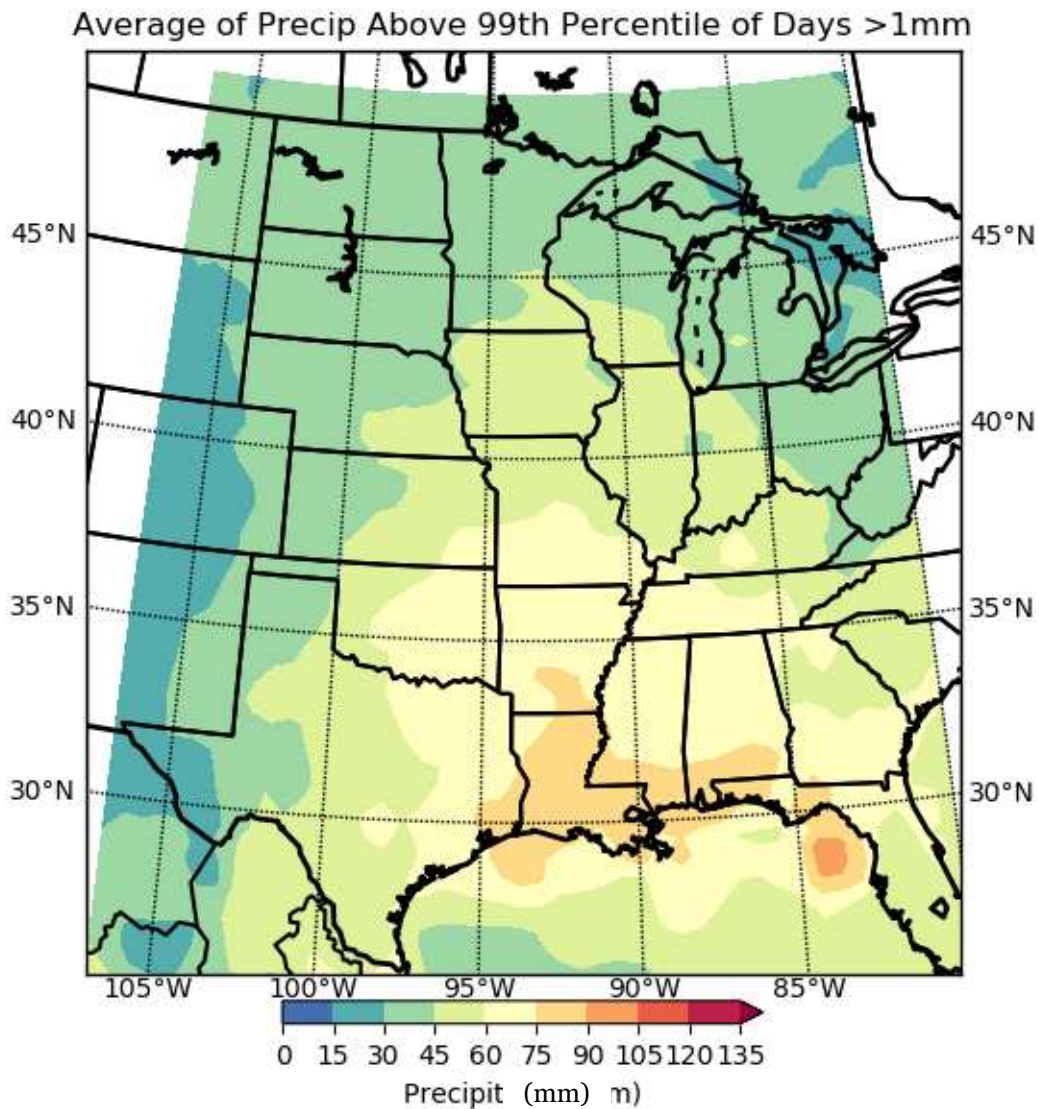


Figure 3-3 Average amount of precipitation above the 99th percentile of wet days (>1mm) from the observation corrected MERRA-2 precipitation dataset. Breaks in the color bar are the same as in Figure 3-2 for easier comparison.

Also of interest to this study is the ability of MERRA-2 to represent observed extreme events. This it also does far better than MERRA, which tends to smooth out precipitation, particularly at the extremes. Figure 3-2 shows the average of all precipitation above the 99th percentile on wet days, defined as greater than 1mm in 24 hours. It can be seen that MERRA-2 is closer both in amount and in spatial distribution to the observations than MERRA, partially due to the fact that MERRA has many more wet days than MERRA-2 due to spurious drizzle (Bosilovich et al. 2015). MERRA-2 does, however, overestimate the average amount of precipitation above the 99th percentile on wet days (which are defined as days with more than 1mm of rainfall) in the central and northern plains. In this region MERRA-2 is closer to the observations than MERRA, while farther to the west on the high plains MERRA is closer to the observations. Bosilovich et al. note that “the patterns of extreme precipitation in MERRA-2 are much more comparable to the observations than MERRA.” Again, these values are the model precipitation before any observation correction is applied. The values used to determine events in this thesis are the observation corrected values. Figure 3-3 shows the equivalent plot of the average amount of precipitation above the 99th percentile of wet days for the observation corrected precipitation. This map much more closely matches the observation panel in the lower left of Figure 3-2. Influence from the gridded gauge observations can be seen in such details as the local maxima in south central Texas and the local minima on the Illinois–Indiana border. Where the datasets do not match, MERRA-2 shows lower average extreme amounts. The largest such underestimated area stretches from southeast Kansas into southern Minnesota. The difference in amount is to be expected given the coarse spatial resolution of the reanalysis and the largely convective nature of top end rainfall events on the Plains. It is clear from these results that applying the observation correction produces an increased fidelity to the observations.

Therefore the MERRA-2 data is suitable for an analysis of extremes, particularly because of the reasonable match of the spatial patterns of observations to observation corrected reanalysis results. This study is not looking specifically at the small scale precipitation and associated patterns that are not represented well at the ~60km resolution found in MERRA-2. Therefore, the quantitative amount of MERRA-2 corrected precipitation is less important than spatial pattern because it is assumed that the quantitative amount will be self-consistent within the reanalysis (larger events in real life will be larger in the reanalysis, even if the absolute amount of precipitation in the reanalysis is lower than real life). There is no reason to believe that spatial variability would necessarily be consistent with observations in this same way, so it is encouraging that the spatial patterns correlated between the two datasets. This point about the quantitative amount will be seen later in comparison to Stage IV quantitative precipitation analysis.

Figure 3-4 shows the representation of Argentine and Colorado topography in the MERRA-2 grid, highlighting the spatial resolution. It can be seen that topography is certainly quite smoothed out by the grid, but that key features are left intact. Note especially the Palmer Divide and Cheyenne Ridge in Colorado, which can be distinguished from the Platte river valley that separates them. These features are smoothed out a little, but not completely washed out by the MERRA-2 resolution, meaning that upslope and downslope flows relating to them are represented in the model. The Andes are also properly represented as a relatively thin mountain range, especially on the southern end. Crucial for convective initiation in the RELAMPAGO Córdoba domain, the Sierras de Córdoba are also visible between 30 and 35°S latitude to the east of the Andes crest. Beyond the obvious large features of the Andes and the Rockies, the more

subtle features also have large influences on precipitation, so it is encouraging to see them represented in the model terrain, albeit in a coarse, smoothed manner.

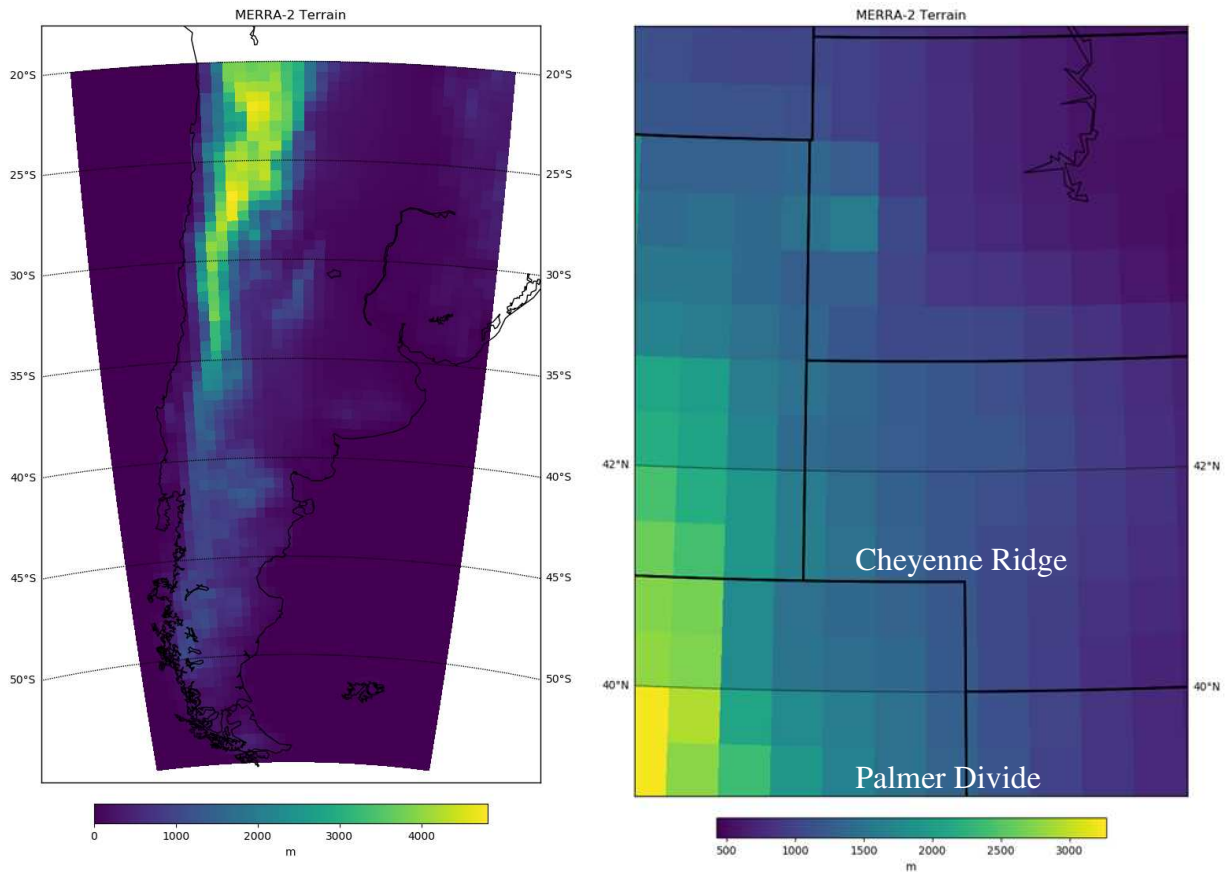


Figure 3-4 Representation of the topography of the Argentina (left) and Colorado (right, with state borders) regions of study in the MERRA-2 grid. The color scales are different between the panels, with peak elevations in the Andes reaching above 5000m.

3.2 Stage IV

The NCEP Stage IV analysis (Lin and Mitchell 2005; Nelson et al. 2016) is a precipitation analysis product that combines gauge and radar precipitation estimates. The product is produced on a 4-km grid with hourly resolution throughout the CONUS. Quality control of the data is performed by the River Forecast Centers before the data is aggregated at the National

Center for Environmental Prediction (NCEP). The result is a relatively high-resolution dataset of observed precipitation that can easily be used for case study purposes and comparing to other datasets, as this study will do.

3.3 Domain

Two domains are analyzed in this work, one on the high plains of the continental United States and one encompassing the whole of Argentina. These domains can be seen in Figure 3-3, which illustrates the model terrain within the domains. The domains were chosen as a relatively small domain in Colorado as a testbed of sorts for the method, as well as a larger domain for application that encompasses Argentina. These domains have interesting similarities to each other, as they are both situated in the rain shadow of a major north and south mountain range. When comparing the RELAMPAGO domain (roughly, this refers to east of the Andes between 30 and 35 south) specifically, many similarities can be found. Both of these areas experience a similar amount of annual precipitation and therefore a similar pattern of vegetation. They also rely on a low-level jet from a moisture rich region (the Amazon for Argentina, the Gulf of Mexico for Colorado) for most of the moisture supply for precipitation, especially in the summer. Significant differences also exist. The Andes are a much different mountain range than the Rockies, being both much narrower and taller, which affects variables such as the amount of convective inhibition (CIN) due to subsidence warming in the lee, and CAPE due to the taller mountains resulting in a stronger LLJ (Rasmussen and Houze 2016). The ocean is always much closer in Argentina and can add supplementary moisture to the main Amazonian source. (Grimm and Tedeschi 2009). Also, much of Argentina lies closer to the subtropics than the mid-latitudes proper, which means that the weather there is much more strongly affected by things such as the

placement of the subtropical high (Carvalho 2002).. Due to both these similarities and differences, these two regions provide a fascinating insight into the morphology of extreme precipitation.

Reanalysis data provides a tool to use to analyze heavy precipitation occurring of a relatively wide area, as is the goal of this study. It provides a stable platform for gridded analysis of the weather over a climate scale period. Using the best observations available, it provides a clearer picture than any one observational dataset alone. The resolution is good enough to depict key terrain features in both domains, which is critical to precipitation processes in mountainous regions. Furthermore, this is an exciting opportunity to utilize the relatively recently released MERRA-2 dataset, which improves greatly over its predecessor, especially in the area of precipitation. Stage IV analysis provides a higher resolution platform to compare performance of the reanalysis to, giving a sense of how well the reanalysis model can reproduce events that are strongly influenced by sub-gridscale processes

CHAPTER 4 METHODS

4.1 Choosing Period and Threshold

Beginning with perhaps the most fundamental problem, what accumulation time period to consider, this study selected 24 hours. This was implemented through the time period 1980-2016 by creating running sums of each 24-hour period in the data record, such that each 24-hour period shares 23 hours in common with the immediately preceding 24 hour period. Amalgamating the precipitation data in this way allows for no potential extreme event to be cut in half by an arbitrary time of day cutoff. When defining extreme, a balance was sought that would provide a large enough sample size for meaningful analysis, yet small enough that the word “extreme” can be meaningfully applied. An objective categorization is sought that will allow for the method’s use throughout the globe and not confined to the two present regions of interest. A percentile threshold satisfies these requirements. For this study the 99.9th percentile of all the running 24-hour sums (including zeros) is applied. The percentile threshold is then applied to the whole dataset of summed periods. The 24-hour period for extremes was chosen because 24 hours will capture the peak of most events and most often encompass an entire event, especially in areas where extreme precipitation is more often convective and relatively short lived. Combined with the running sums, this ensures that no potentially interesting events based on the percentile threshold are passed over. Furthermore, extremes on shorter time scales are often much smaller spatially, at a resolution that MERRA-2 cannot fully resolve. Therefore, a running 24 hour period provides a longer time scale for accumulation that likely also involves a larger

spatial scale, as Stevenson and Schumacher 2014 observed more spatial coherence in 24 hour extremes than one hour extremes.

This leads to the next question, which threshold to consider as “extreme”. Extreme events have been defined in many different ways in the literature, including fixed precipitation thresholds (Junker et al. 1999), estimated return periods or recurrence intervals (e.g., Stevenson and Schumacher 2014), and percentiles (Groisman et al. 2004). Considering the large regions of interest, and the lack of established recurrence interval thresholds in South America, we will use a percentile framework in this study. In this framework, the percentile that is chosen must encompass enough events for a meaningful sample, but not so many as to render the description of these events as extreme meaningless. A number of different percentiles were tested, keeping in mind that the method for combining the precipitation record retained the hours with no precipitation, which even in relatively wet regions is most of them. The percentiles tested were 95, 99, 99.9 and 99.99. Maps of the value of each of these thresholds for Argentina can be found in Figure 4-1. Especially 95, but also 99, were found to contain far too many points for the purposes of this investigation due to most raining times falling above the 95th percentile at many points in Argentina. At the 95th percentile, many arid to semi-arid regions have nearly all of their precipitation classified as extreme by this threshold. The 99th percentile was better, but still contained too many points to take as a reasonably quantification of extreme. 99.99th percentile left too few observations, usually only identifying the most extreme one or two events in the record. This left the 99.9th percentile, which was selected for this analysis.

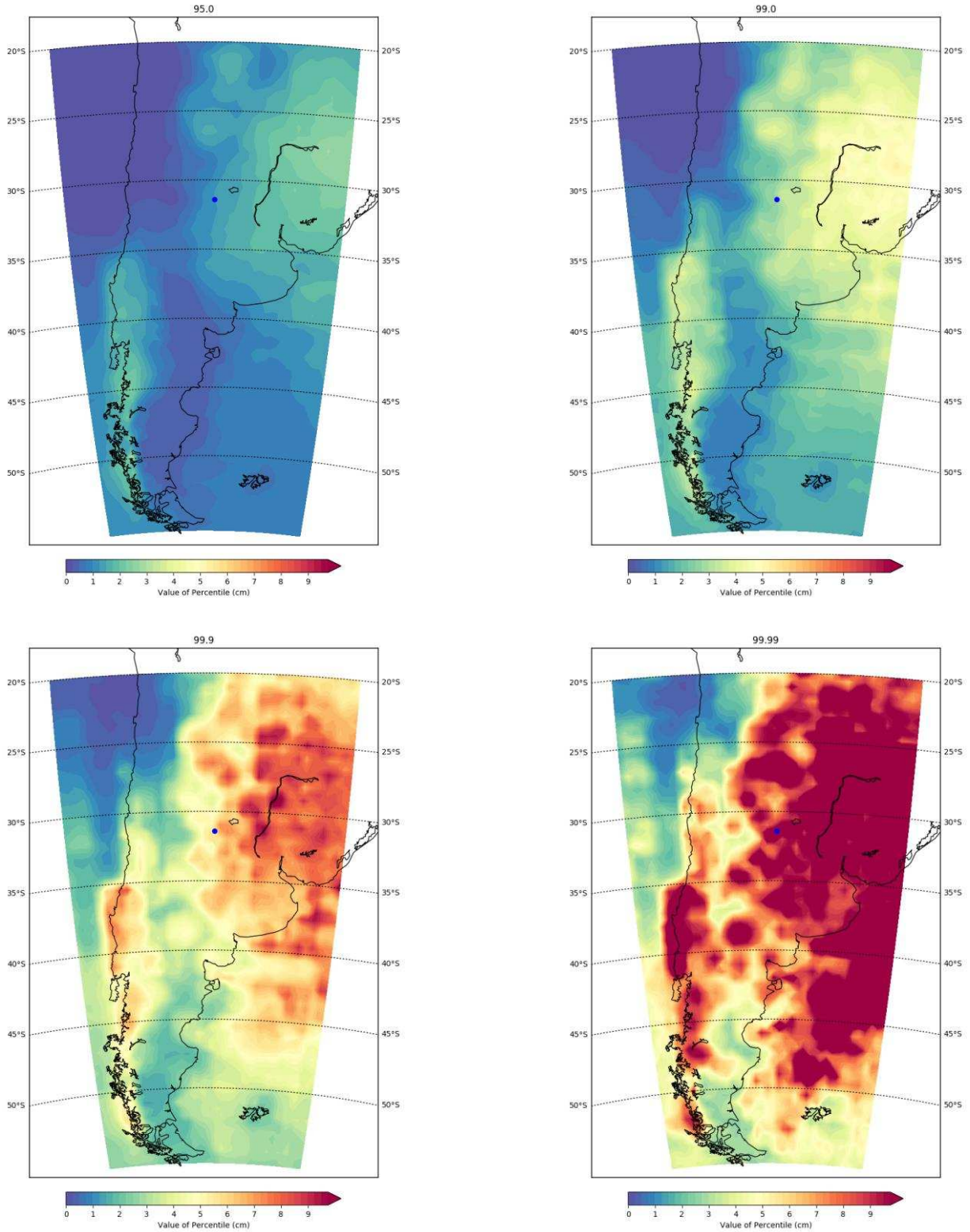


Figure 4-1 Maps of threshold value for 95th percentile (top left) 99th percentile (top right) 99.9th percentile (lower left) 99.99th percentile (lower right). Blue dot denotes Córdoba, Argentina.

Taking only points above the 99.9th percentile produces 325 summed 24-hour periods at each gridpoint over the 37-year period. Because of the nature of the process, many of these periods overlap and it is necessary to determine how many unique events exist in the database to ensure there are enough for analysis. A unique event was defined as a continuous run of overlapping 24 hour periods that were all above the 99.9th percentile. Figure 4-2 shows a histogram of number of unique events at each Colorado and Argentina gridpoint. Separate histograms for Argentina and Colorado were also produced but are both similar in shape to the combined plot. This shows a minimum of nine unique events with a mode around 22. The statistical significance of individual gridpoints will be explored in the following sections, where it will be seen that these numbers of unique events are sufficient for a meaningful analysis of the characteristics of these events, rather than producing a mere case study of one or two.

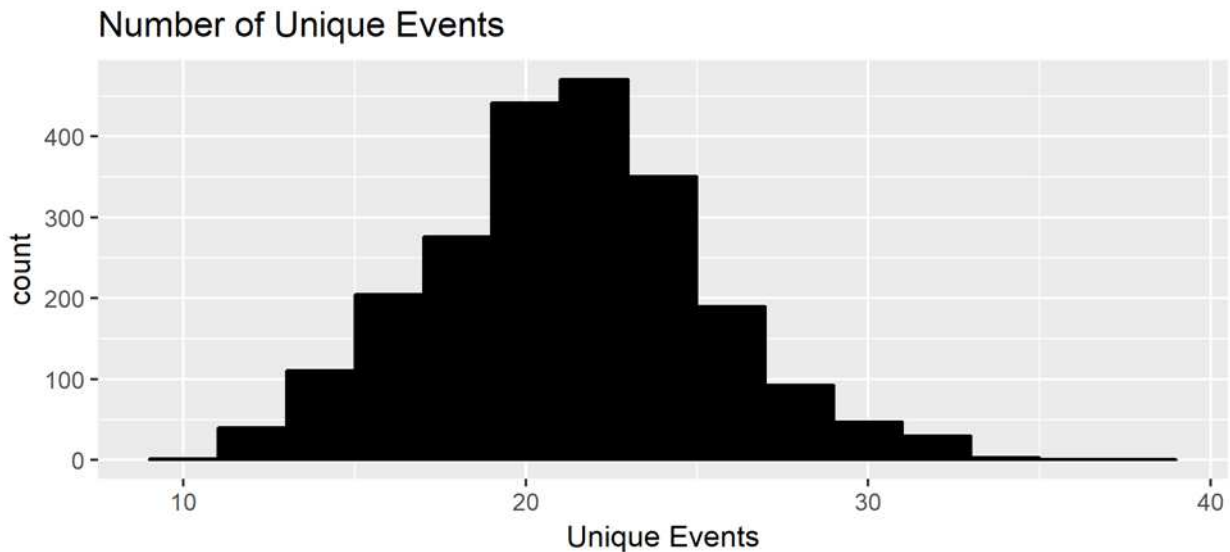


Figure 4-2 Histogram of unique events at all Colorado and Argentina gridpoints combined

4.2 Principal Component Analysis

Principal Component Analysis (PCA) is the technique used to objectively classify events. This analysis uses linear algebra to construct orthogonal vectors that best describe the dataset. The components that make up these vectors are referred to as loadings, and these are used to describe the relative importance of the variables in classifying the data. Each loading corresponds to a variable used to produce the analysis. In conjunction with these loadings, a series of numbers is produced, called PCs. The PCs indicate how well each time matches up with a particular pattern. They are used as a way to reduce the dimensionality of a problem, since the PCs represent all the variables input into the principal component algorithm returned as one number. Most often when PCA is used, these PCs are of the most interest, since they dramatically reduce the dimensionality of a problem. However, this study will focus more on the patterns themselves in an attempt to draw conclusions about the critical patterns in extreme precipitation.

Figure 4-3 illustrates this concept with a simple two variable example with synthetic data, variable a (x-axis) and variable b (y-axis). The two blue arrows represent PC1 (the loadings associated with the first principal component) and PC2 (the loadings associated with the second principal component). The arrow pointing down and left is PC1; up and left is PC2. It can be seen that PC1 explains most of the variance in this dataset, in fact around 94%. This is because for the most part, this data can be described as ‘when a is low, b is low’ and vice versa. The second principal component explains the remainder of the variance, which in this case is easily seen as the deviation from the major axis of this dataset; $y = x$. Within this secondary vector of variance, ‘when a is low, b is high’, is clearly counterintuitive and not descriptive of the dataset as a whole. This is a correct interpretation, since the variable a is merely a set randomly

generated from the normal distribution, and b is the variable a with a bit of noise added. It is equally as likely that the second set of PC loadings (PC2) would have resulted in ‘when a is low, b is high.’ Thus in this set the meaningful information is limited to PC1. With more variables this analysis gets more difficult to visualize but the principles remain the same. The PCs in this case would be positive for points in the lower left corner, near zero for points near the middle, and negative for points in the upper right corner. This is because those points in the lower left corner match the PC1 pattern (low a , low b) while the points in the upper right corner are the opposite of it (high a , high b). One PC value is associated with each individual point.

The advantage of this kind of pattern identification is that each principal component (PC1, PC2 etc.) is guaranteed to be orthogonal to all the others. This means that each principal component is completely independent of the others, meaning that they are certainly representing different patterns and variability in the data. For the results that will be presented here, only the first principal component will be retained due to most of the variability residing there.

For this study, principal component analysis will be performed using each of the 325 times above the threshold as inputs. This was done to retain a robust sample size, as well as to be able to track the nature of events throughout their duration. To test whether this method created problems by overly weighting the PCA toward one event, Monte Carlo simulations were performed. This was done by randomly selecting one time from each of the events for the Colorado gridpoints, performing PCA, and comparing the results to both the other Monte Carlo simulations as well as to the original PCA performed with data from each hour within the extreme event. Qualitatively the difference between the Monte Carlo produced analysis and analysis with all 325 points was minimal. This result is encouraging because it means that longer

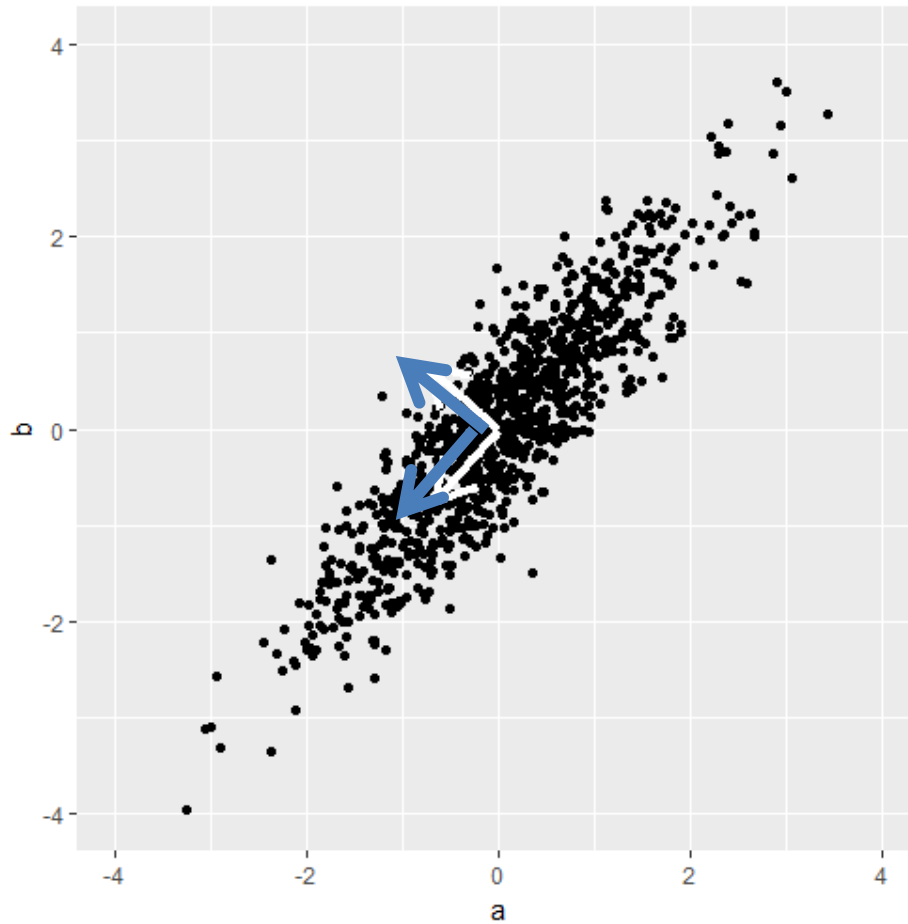


Figure 4-3 PCA Example. See Text.

events are not unduly influencing the PCA, and was expected because the meteorological variables in this space would not change much throughout an event. Rather events are clustered together at various places in the parameter space. PCA will create a vector that best defines the variability between these clusters, and whether there is 15 or 25 points in a given cluster will not significant impact on the results.

PCA was performed on two different sets of variables. The first incorporated standard atmospheric variables from MERRA-2 at hourly resolution such as wind (at 850 and 500hPa), tropopause and sea level pressure, cloud height, fraction of convective showers in gridpoint, precipitable water, length of event and the amount of precipitation for the hour. This PCA used

these variables at the gridpoint as well as each adjacent gridpoint, plus the length of the event, as input into the PCA for a total of 91 variables. The second used variables that are connected to lift in the atmosphere. These included Q-vector convergence at 700hPa with and without sigma (the static stability variable) constant, wind convergence at 10m, 850hPa, and the lowest model level above ground as well as wind dotted with terrain slope ($O = \vec{U} \cdot \nabla H$; where O is orographic lift, \vec{U} is the horizontal wind vector and ∇H is the gradient of the terrain) at those same levels, precipitable water and the precipitation. These variables are at 3-hourly resolution, so in this case all times within the 24-hour periods created from the one-hour precipitation were used for the analysis. Using both of these approaches allows for a finer analysis of how events are composed in the traditional meteorological sense (Chapter 7), as well as knowing what sources of lift are most important for producing extreme precipitation (Chapter 8).

4.3 ClickHist¹

ClickHist is software that allows the user to create clickable 2D histograms to explore a dataset. For example, the user can set one axis as precipitable water and the other as precipitation, then by clicking the points in the dataset create IDV bundles that allow the meteorological variables at the time of the event to be fully explored. It also allows for visualization of the covariance of two selected variables, and how events may occupy very different sectors of the parameter space. The user can click on these events, discover the date the event occurred, and examine a quickly produced meteorological summary to examine their similarities and differences on a large scale. This study will use this tool to select two case studies for comparison and an evaluation of the performance of MERRA-2 precipitation.

¹ Niznik, Matthew. 2016: ClickHist. 2018-03-29, <https://github.com/matthewniznik/ClickHist>

CHAPTER 5

TIMING AT SELECTED GRIDPOINTS

5.1 Introduction

This section will explore the timing of the extreme precipitation on yearly, monthly and hourly scales for selected gridpoints of interest in both Colorado and Argentina. The purpose of this is to ascertain what sort of decadal, annual and diurnal variability that the events identified in MERRA-2 possess. The selected gridpoints are near Northern Colorado, and near Mendoza and Córdoba in Argentina. Mendoza is located at the base of the Andes mountains, while Córdoba is farther east, at the base of the smaller Sierra de Córdoba mountain range. Both Córdoba and Mendoza have broadly similar climates to Northern Colorado, as they are semi-arid locations in the lee of a mountain range that experience summertime convective storms on a regular basis.

5.2 Córdoba, Argentina

Figure 5-1 presents the histogram of events per year at 31.5S 63.75W, the gridpoint closest to Córdoba. Each 24-hour period here counts as an event, so the histogram is partly influenced by the length of an event in any given year. The histogram here shows no obvious patterns, though there is perhaps some grouping of events into two and three year blocks. These blocks seem as though they may be correlated with ENSO, with blocks of events occurring mostly during El Niño years, the exception being the events in 2013 and 2014. However, the sample size is certainly not large enough to say anything with certainty regarding the correlation of MERRA-2 extreme precipitation to ENSO at decadal time scales in this dataset.

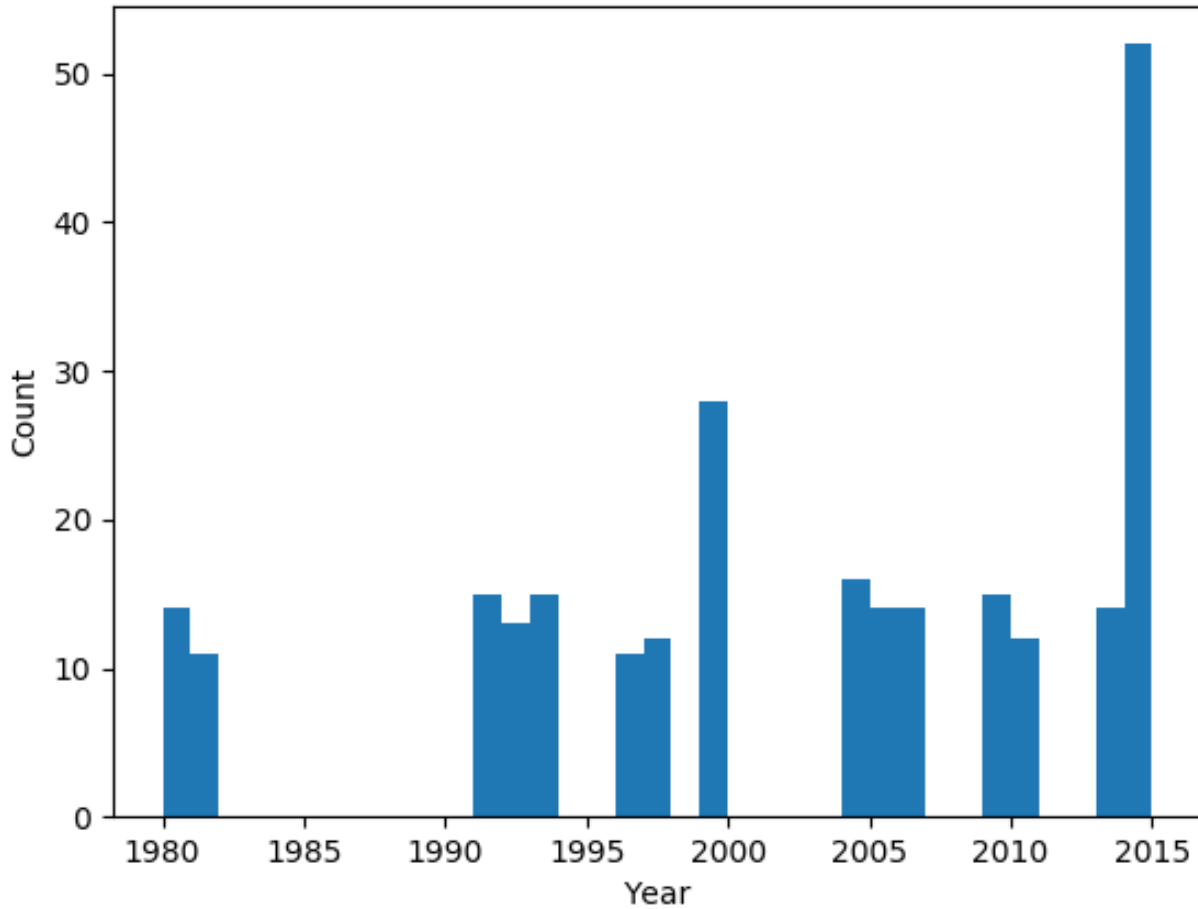


Figure 5-1 Histogram of number of events per year through the record at Córdoba.

Within the year there is also significant variability in months that can produce extreme precipitation at this gridpoint. Figure 5-2 shows the histogram of events by month. At the Córdoba gridpoint there is a clear preference for events to occur in the austral summer and transition seasons. Interestingly, from October through March the number of events increases each month until April, which experiences a sharp dropoff. Austral summer is when the low level jet and precipitable water, as well as frequency of MCS peak in the region, so this result agrees with previous research about the variability of precipitation in the area (Salio et al. 2007, Cavalcanti 2012, Rasmussen et al. 2016)

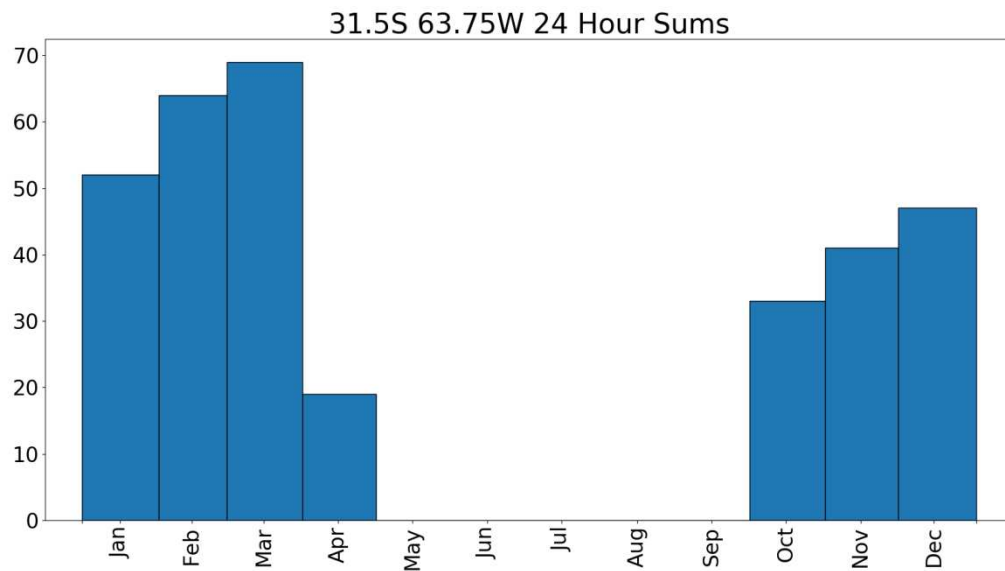


Figure 5-2 Histogram of number of events per month at Córdoba.

Plots of the time of day vs hourly precipitation were produced to investigate the character of diurnal precipitation at the gridpoint during extreme events. This plot is presented in Figure 5-3. Argentina's timezone is UTC - 3, so for example 12 UTC equates to 9am local time. There appears to be a subtle peak in the median hourly precipitation during events from the mid-morning into the afternoon, while the highest hourly amounts occur from mid-morning through evening. Relatively high amounts (>0.75 cm/hr) continue through the night showing the influence of the upscale growth of convection into an MCS with associated stratiform elements. This diurnal distribution is indicative of the primarily convective nature of the extreme precipitation at the gridpoint. This is further corroborated by the large amount of near zero hourly amounts present within the 24-hour periods, which means that the precipitation that adds to the 24 hour extreme is not spread out over the hour, but rather concentrated in a few certain hours of the day. The reader may note that the diurnal cycle at Mendoza is not as convective looking. This is due to a limitation in the MERRA-2 dataset and will be discussed in the following section.

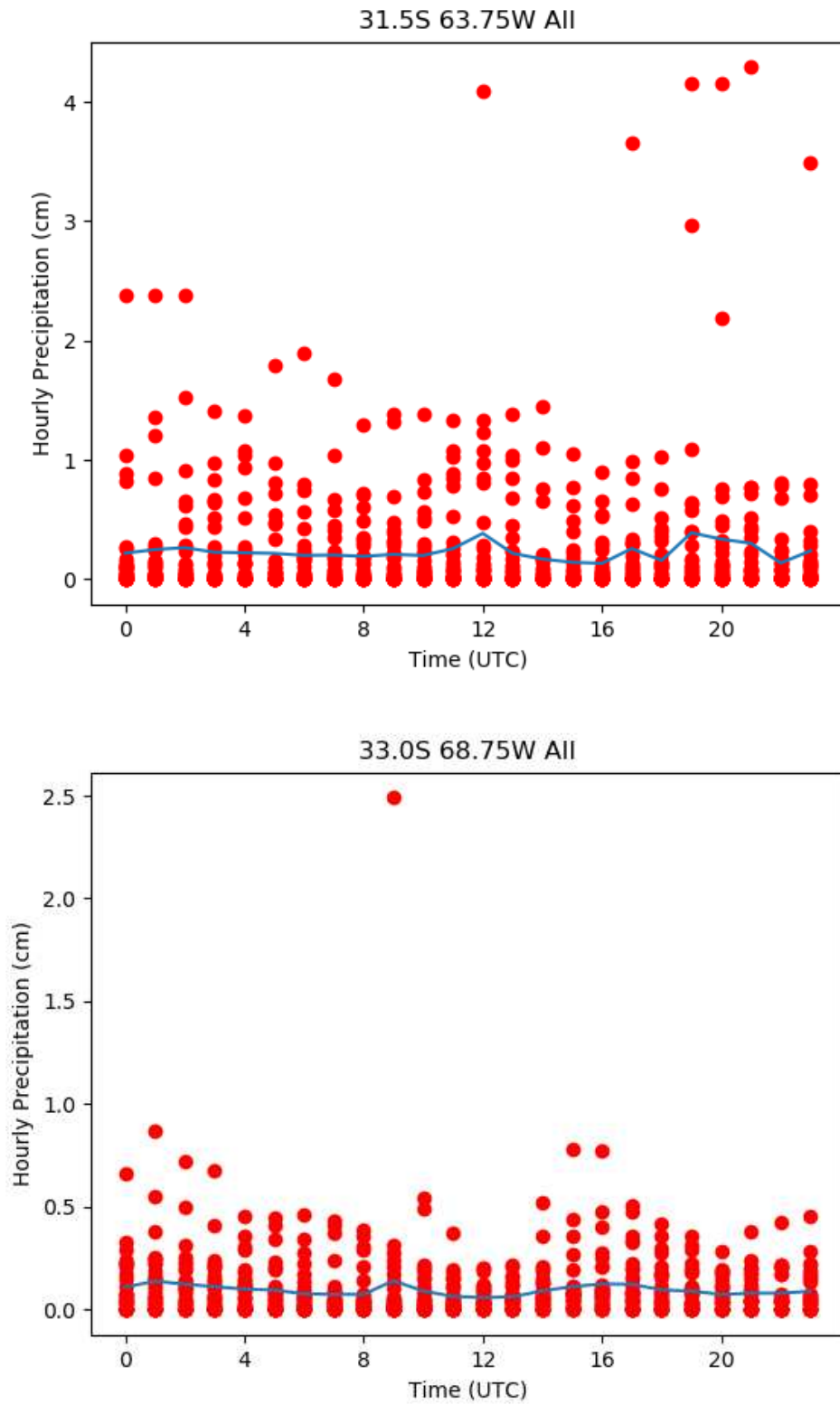


Figure 5-3 Plot of UTC time vs hourly precipitation during extreme events, Córdoba top and Mendoza bottom. The blue line shows the average of all hours at each time.

5.3 Mendoza, Argentina

The histogram of events per year for Mendoza (Figure 5-4; 33S 68.75W) at first glance looks similar to the corresponding histogram for Córdoba, which makes sense given the proximity of the two locations. There are important differences however, particularly in that events do not seem as grouped at this location, but rather are more like the events at the Colorado gridpoint, spread relatively evenly throughout the period of record, with perhaps a few clusters.

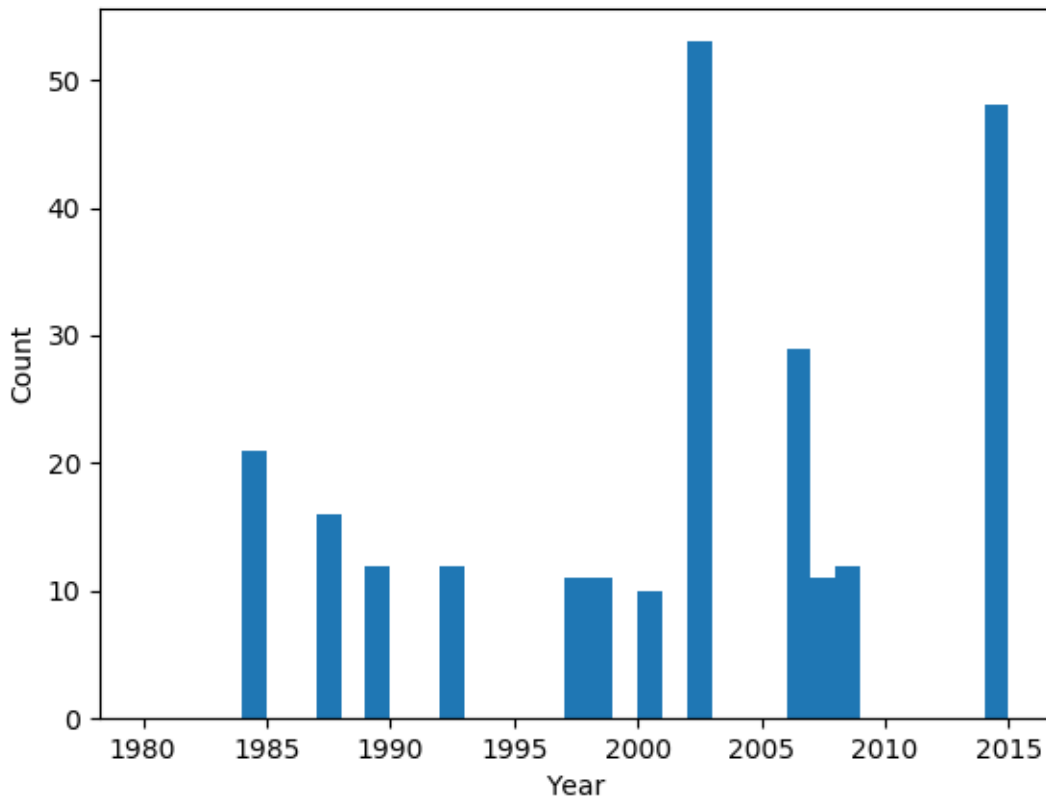


Figure 5-4 As in 5-1 but for Mendoza

Figure 5-5 represents the distribution of extreme precipitation throughout the year at Mendoza. The first thing the astute reader notices is that this makes absolutely no sense at all.

There are events (many of them!) in the austral winter. Austral winter is the driest time of the year at Mendoza, with the majority of precipitation in the region coming in the summer when moisture transport is most robust. Therefore, it is not logical that there would be extreme events in the winter months. These events are certainly spurious, but rest assured they are not the result of a bug in the code. Mendoza gets the vast majority of annual precipitation from deep convection in the summer months. What is happening here is due entirely to the resolution of MERRA-2, and in the model world it is real. Wintertime precipitation is very common during austral winter on the west side of the Andes, in much the same way the Cascades of the Pacific Northwest get blanketed in winter. Unfortunately, in MERRA-2, a this precipitation spreads too far onto the leeward side of the Andes. A map of what this looks like from a case that occurred on July 4, 1984 is presented in Figure 5-6. The steep gradient of precipitation amount is clearly visible from west to east on the lee side of the Andes. Unfortunately these amounts extend just far enough east to include the arid areas nestled against the foothills. It seems likely that since the model cannot accurately express just how steep the lee slopes of the Andes are, it considers Mendoza high enough to receive precipitation that blows over the mountain crest. If only hourly accumulations are considered, none of these wintertime events are above the 99.9th percentile threshold, but since the winter events are longer in duration the accumulation over 24 hours the amounts can reach above the 99.9th percentile for that duration. Because of these deficiencies, the Mendoza gridpoint is excluded from further analysis, as it would not be representative. The discussion here serves to present the challenges that still remain in using reanalysis data and objective methods. Córdoba does not suffer from effects such as this due to the Sierra de Córdoba being too low to intercept the mid-latitude westerlies which are providing the upslope

flow to the terrain to the west of Mendoza, and being far enough from the Andes that the coarse terrain resolution does not smooth the Andes into the area.

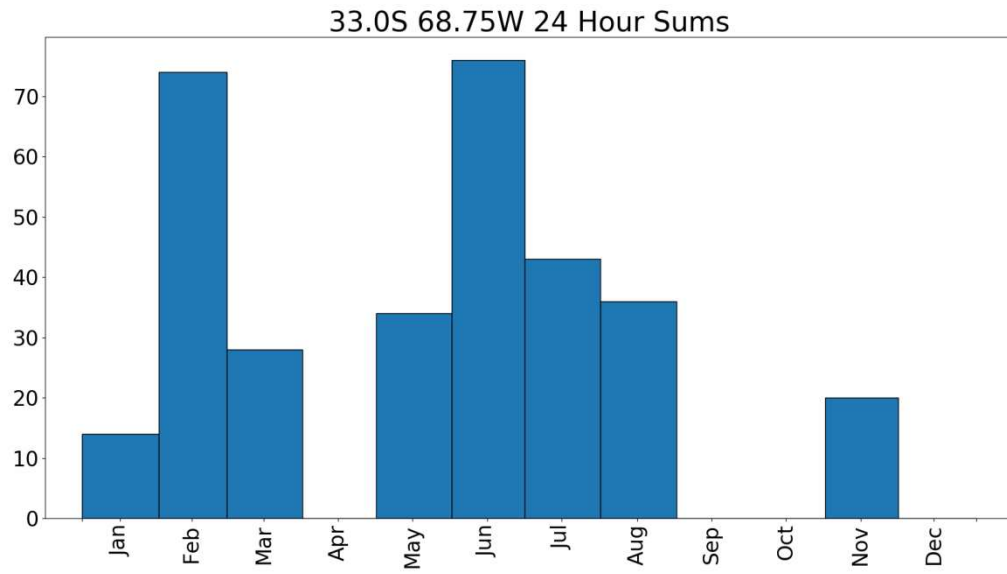


Figure 5-5 As in 5-2 but for Mendoza

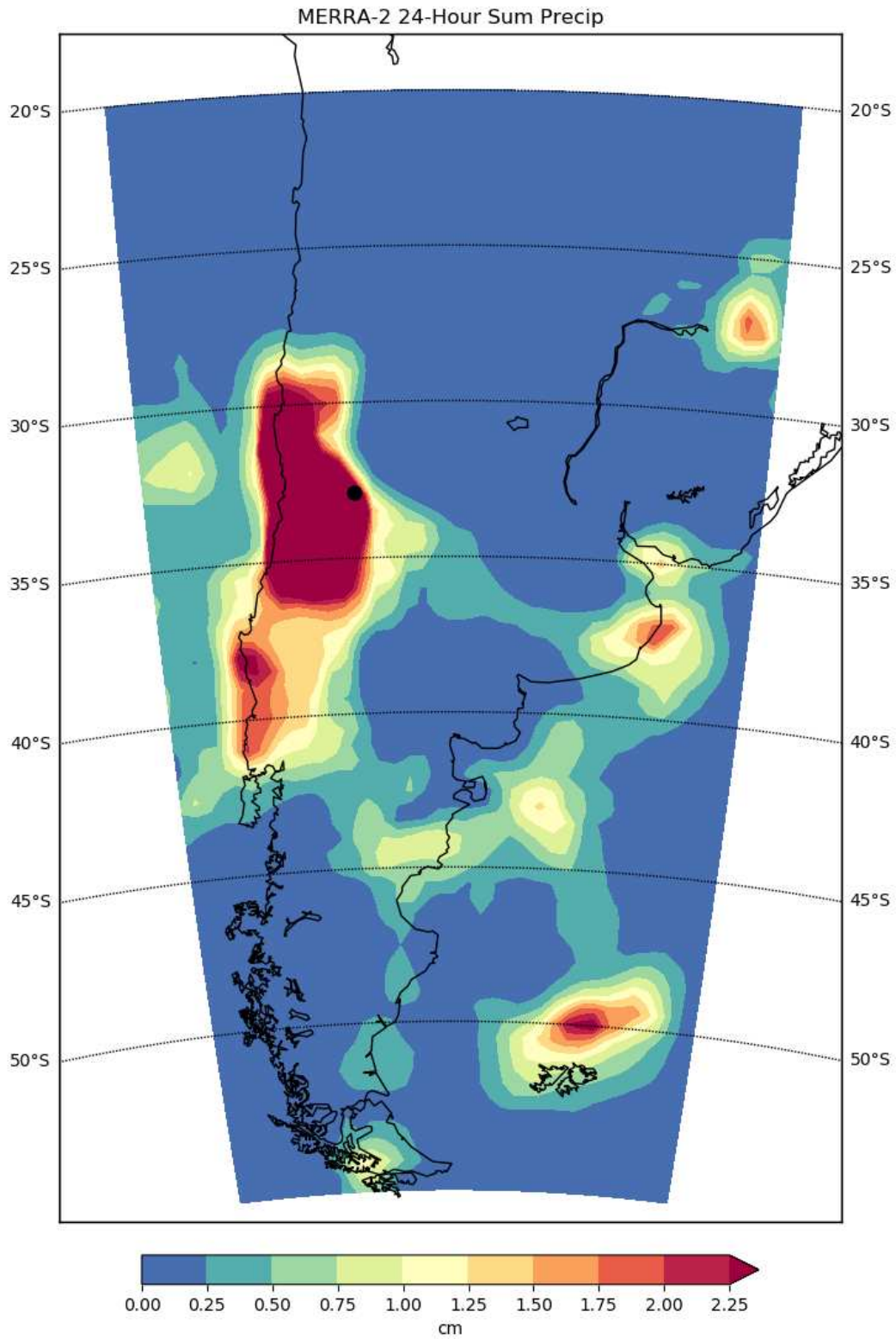


Figure 5-6 An “extreme event” during the austral winter at Mendoza. Mendoza is marked with the black dot.

5.4 Northern Colorado

Figure 5-7 shows the yearly histogram for Northern Colorado (40.5N 104.375W). Once again, no particular pattern stands out. Historic floods in 1997 and 2013 are represented, with the 1997 flood having a shorter number of 24 hour periods contained within it, as one would expect. Also, events here are far more spread out over the time period that at Córdoba, where they are more grouped. This could be a sign of a larger dependence of Córdoba on longer time scale ocean influences, or be an artifact of a small sample size for any sort of conclusions about a temporal cycle.

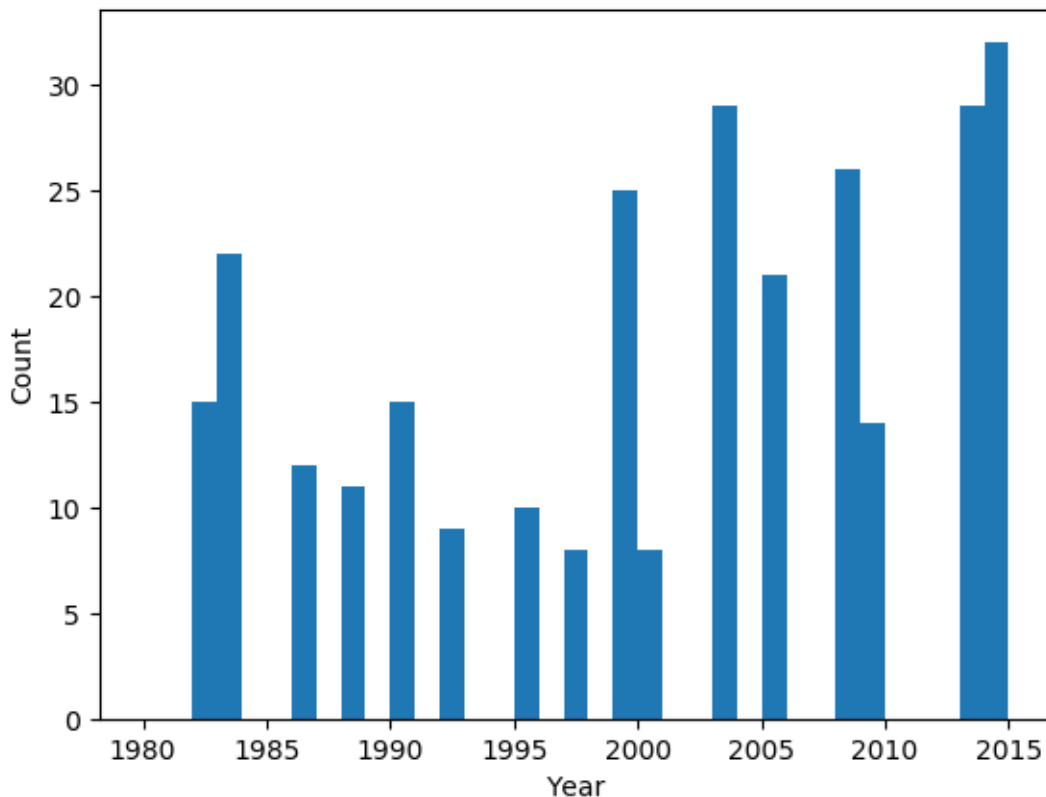


Figure 5-7 As in figure 5-1 but for Northern Colorado

Figure 5-8 illustrates the fact that events in northeast Colorado occur mostly in the spring months in the MERRA-2 dataset. There are a few events in July and August as well, which are known to be the peak months for flash flooding from convective storms in the region. March, April and May however are some of the wettest months of the year in the region as spring storms develop in the lee of the Rocky Mountains and create upslope flow into the region. This flow can lead to long lasting periods of precipitation that can turn extreme.

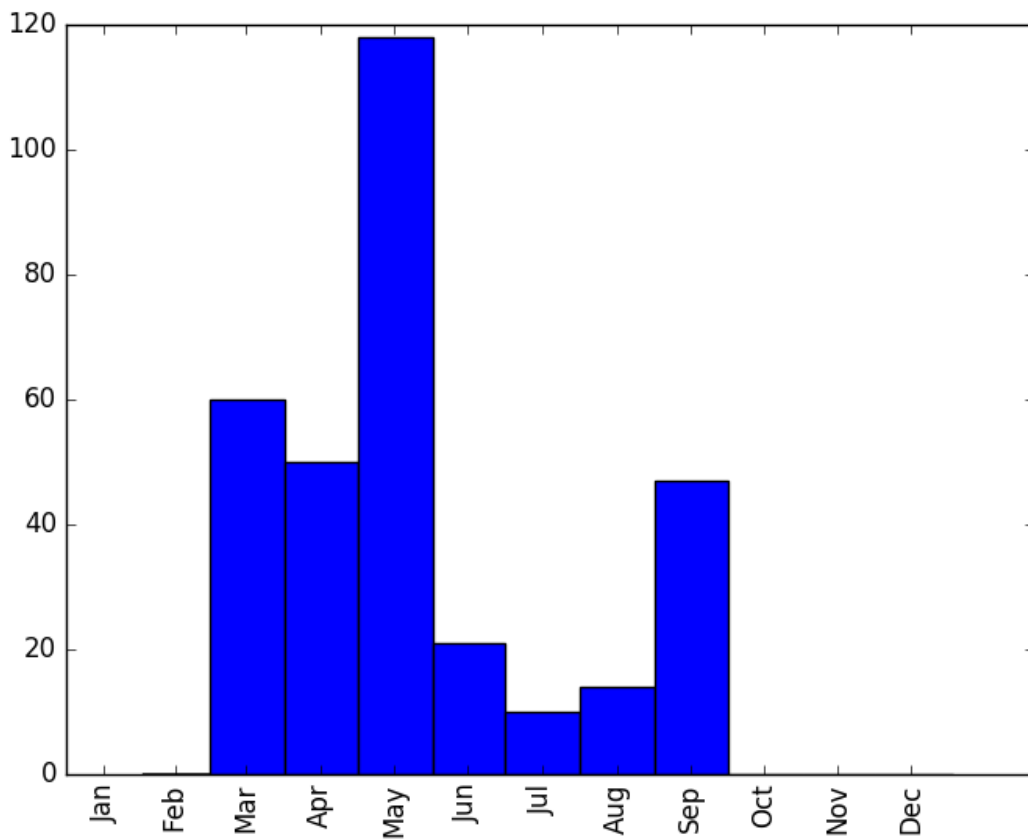


Figure 5-8 As in 5-2 but for Northern Colorado.

Figure 5-9 shows the diurnal distribution of precipitation during the extreme events at this gridpoint. It can be seen that relatively high values can be found at all times of the day, though there is a subtle minimum of the median in the early morning hours. The very highest

hourly precipitation amounts can be found during the late afternoon and evening, which correlates with the preferred times for convection to form. It should also be noted that the absolute amounts here and above are relatively low for an hourly amount due to the fact that the smaller scales where the highest rain rates happen are averaged throughout the gridbox.

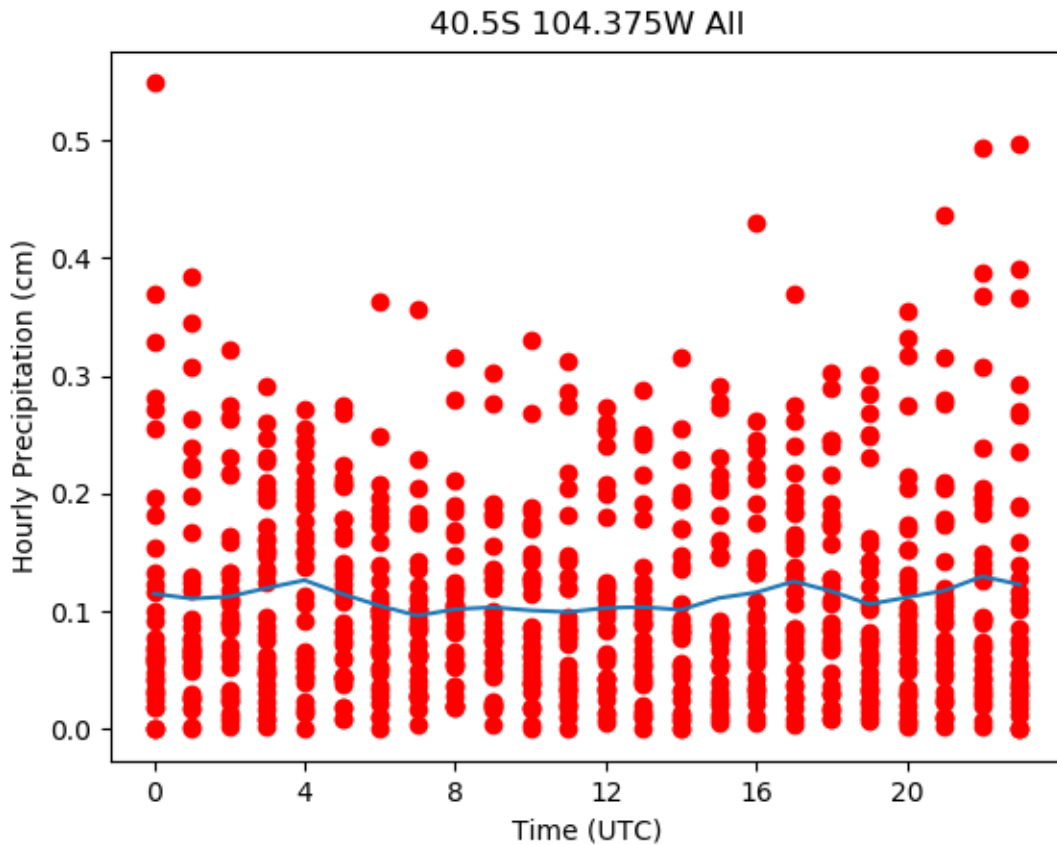


Figure 5-9 As in 5-3 but for Northern Colorado; timezone UTC-7 (0 UTC = 5pm local)

5.5 Conclusion

This section has explored the temporal characteristics of extreme precipitation at the selected gridpoints. No strong associations are noted in the distribution across years. The distribution across months gives an indication of the seasonality of the extreme precipitation. The

diurnal distribution gives clues as to whether the precipitation is convective or more synoptically forced, as synoptically forced precipitation would be spread evenly over the day while the highest rain rates associated with convective precipitation is primarily confined to the afternoon and evening. With upscale growth the convective precipitation and the associated stratiform rain region can last into the night and continue producing rainfall rates in excess of 0.75 cm/hr throughout the nighttime hours. This analysis also revealed the problem that occurs in this mode of analysis in the immediate shadow of the Andes, where erroneous precipitation is carried over the mountain crest into the gridpoint. This problem is not present at the Northern Colorado gridpoint because the wide longitudinal extent of the Rockies is well resolved by MERRA-2, and is not present at Córdoba because the point is far enough from the Andes to be free of the resolution caused smoothing of the terrain.

CHAPTER 6 ANALYSIS OF TWO EVENTS

6.1 Introduction

The following comparison of points was developed by utilizing ClickHist to pick two events from the parameter space of precipitation amount and precipitable water from a 3x3 block of gridpoints in northern Colorado, centered on 40.5N 104.375W. The full parameter space these events are picked from are shown in figure 6-1, with arrows labeling the position of each 24-hour period selected for analysis. This gridpoint is not at the epicenter of the 2013 event, but did receive significant precipitation. The events are chosen for having extreme (by the 99.9th percentile definition of this study) amounts of 24 hour precipitation in the MERRA-2 dataset despite widely varying precipitable water values. From the figure it can be seen that there is a high concentration of events in the MERRA-2 database of events with between 1 and 1.5cm of precipitable water occurring in situations that produced 2.5 to 3.5cm of rain in the model. ‘In the model’ is an important caveat as the seemingly low amount for an extreme event is related to the poor resolution of MERRA-2 compared to a convective resolution. This will be further discussed in this chapter. The events chosen are the famous September 2013 flood and an event from April 18, 2009. This latter event was centered in a more remote region, with a lower cumulative total, and therefore is not as famous as the September floods. It is a more ‘typical’ extreme event, rather than the extraordinarily exceptional circumstances that led to the September 2013 flood. Nonetheless these events provide a good look at events in varying environments, as well as the performance of MERRA-2 reanalysis at the extremes compared to stage IV.

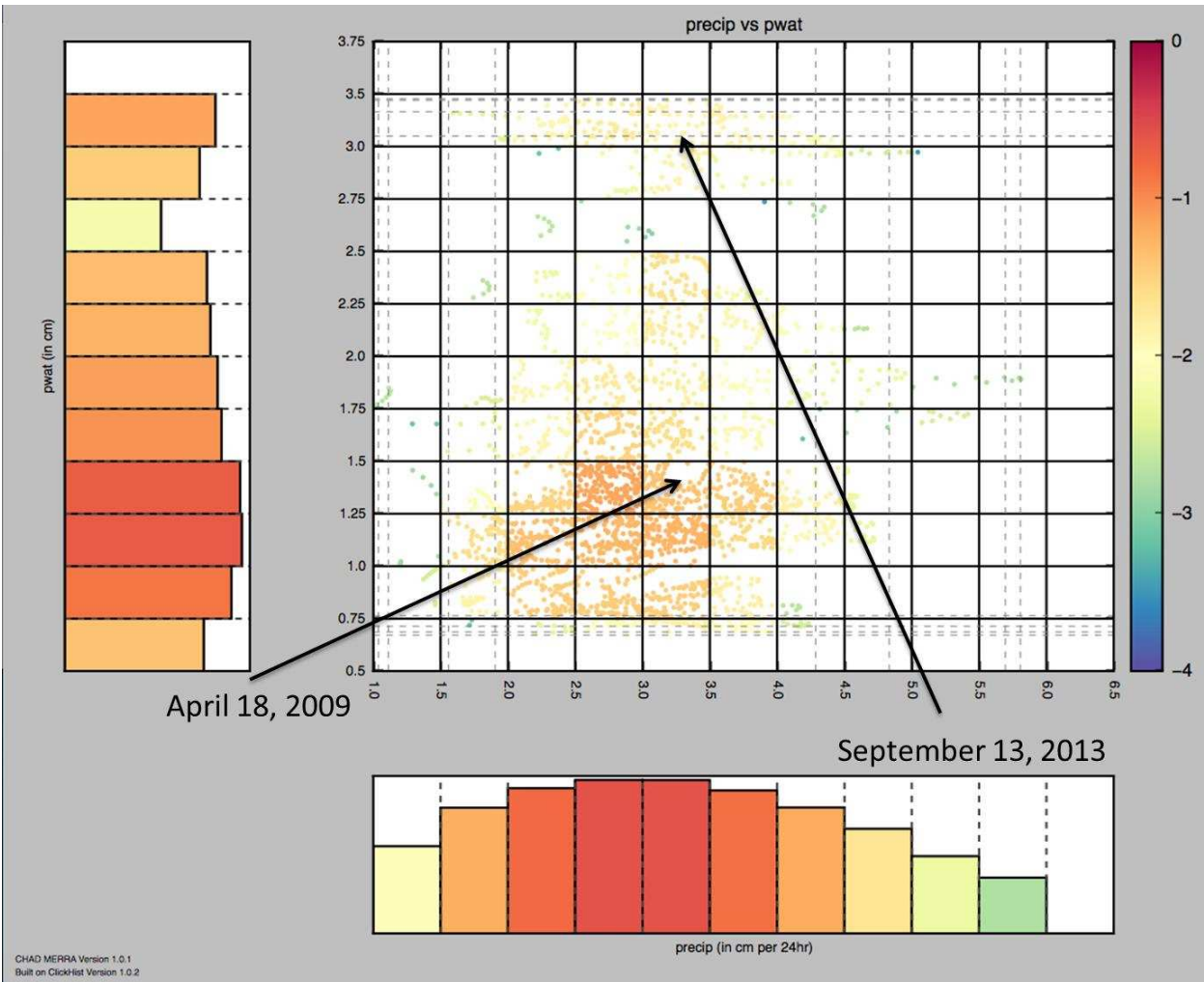


Figure 6-1 2D histogram of MERRA-2 precipitation vs precipitable water for all hours within 24-hour periods during extreme events. Dots are colored according to the density in the outlined gridboxes, according to the logarithmic scale at right. The general area in the parameter space of the two events discussed is indicated by the arrows.

6.2 Precipitable Water Scenario

Figure 6-2 shows the plot of precipitable water z-score (calculated by subtracting the monthly mean from the hourly observation and then dividing by the standard deviation) vs precipitation only for the center gridpoint. The z-score allows for characterization of how extreme the value of a parameter is at a given time compared to the normal value for that month. It can be seen that,

with one exception, extreme precipitation events occur when precipitable water is above average (a z-score greater than zero). This is not surprising. What may be more surprising is the wide range of z-scores that extreme events have occurred in. This accentuates the point that not only moisture, but lift also, is needed to produce extreme precipitation. In fact, despite having a much lower absolute amount (between 1 and 2cm for the April case, 3-4cm for the September case according to model initializations shown in Figures 6-3 and 6-4), the precipitable water in the April case is actually slightly more extreme for the month (higher z-score) than the September case. The figure also shows the evolution through time towards and back down from a peak of precipitation, with precipitable water remaining roughly constant through each event.

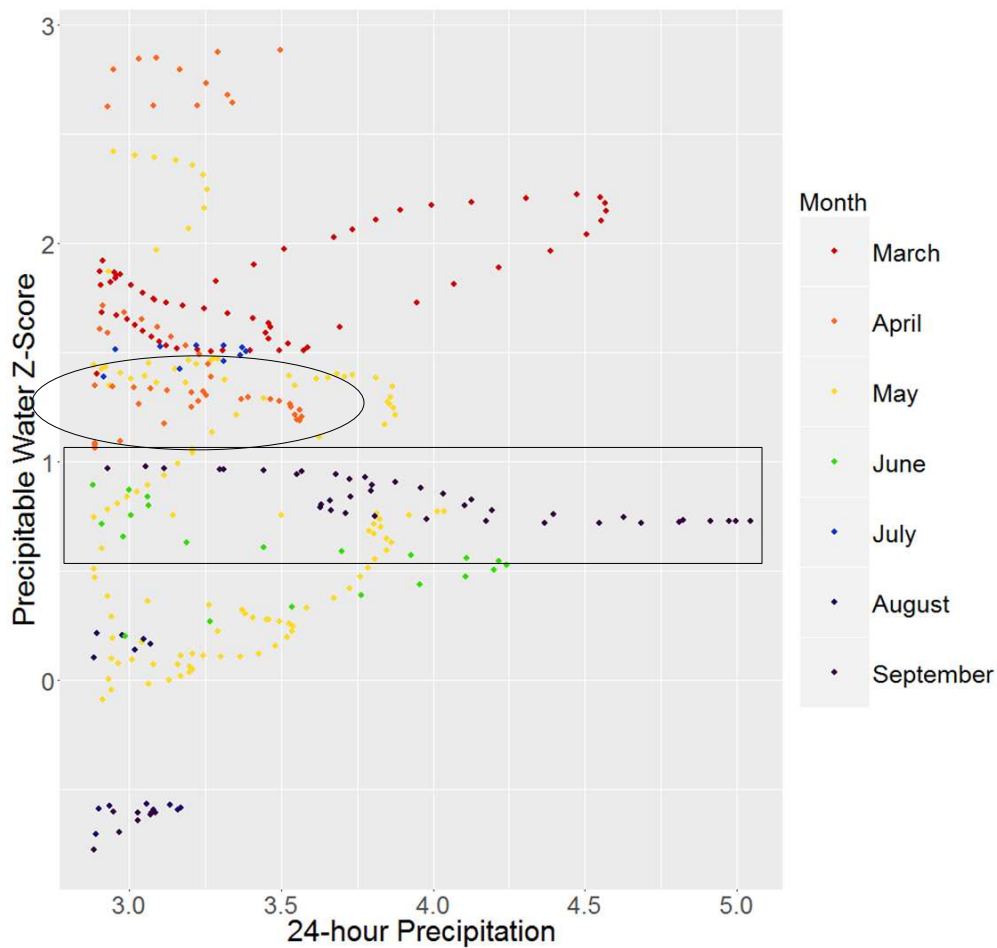


Figure 6-2 MERRA-2 99.9th percentile 24 hour precipitation in cm vs the Precipitable Water Z-Score for just the gridpoint 40.5N 104.375W. April event is circled, September event is boxed.

6.3 Synoptic Scenario

The central question is how the April event produced similar precipitation totals in a given 24 hours without the benefit of as high of a precipitable water total as the September event (overall totals in the September event were much larger, due to the event lasting longer, but individual 24 hour periods are comparable). Figure 6-3 shows the precipitable water, 850hPa height and wind for the September event. Much has been written of this event elsewhere, as noted in the literature review section, but it will suffice to say here that in this case relatively gentle upslope flow was driven by flow around the southern edge of a high pressure system, combined with the slow moving low over eastern Nevada. This flow was enough to trigger expansive areas of stratiform warm rain with embedded convection that led to the widespread flooding, despite a relatively benign synoptic situation.

The April event was much more driven by synoptic forcing. As can be seen in Figure 6-4, a vigorous cyclone was in place, driving upslope flow into northeast Colorado. With a clear cyclone in place, one can assume there was upper level support for lift beyond the orography as well. Indeed, this is borne out by plots of the QG-omega parameter proxies 850hPa temperature advection and 500hPa vorticity advection (not shown). Thus with a little more lift added to the environment, lower precipitable water scenarios can turn into extreme events.

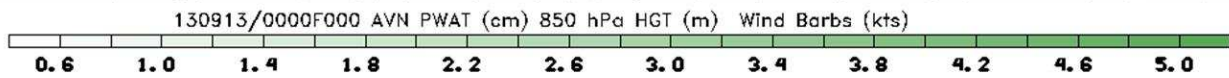
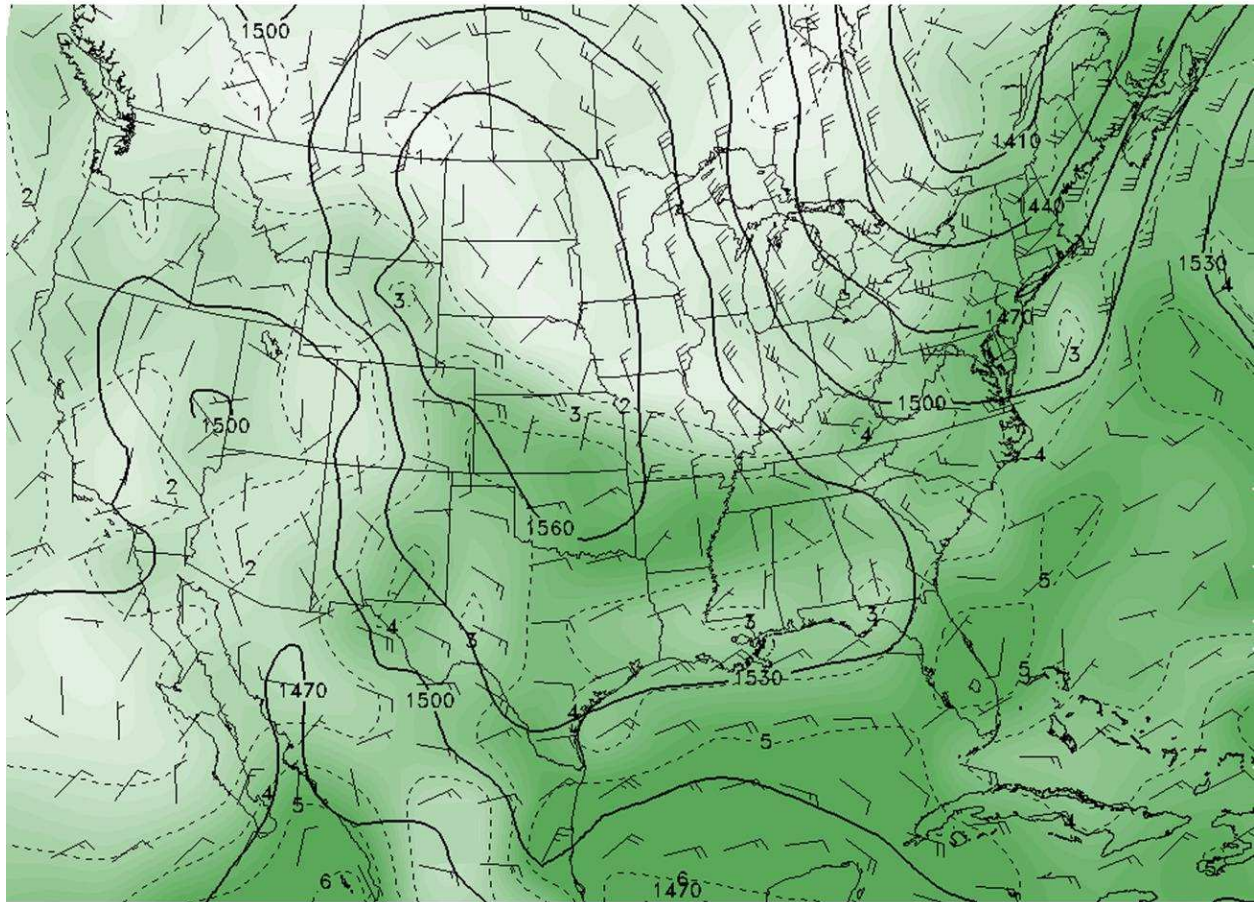


Figure 6-3 Precipitable Water, 850hPa heights and winds during the September flooding event

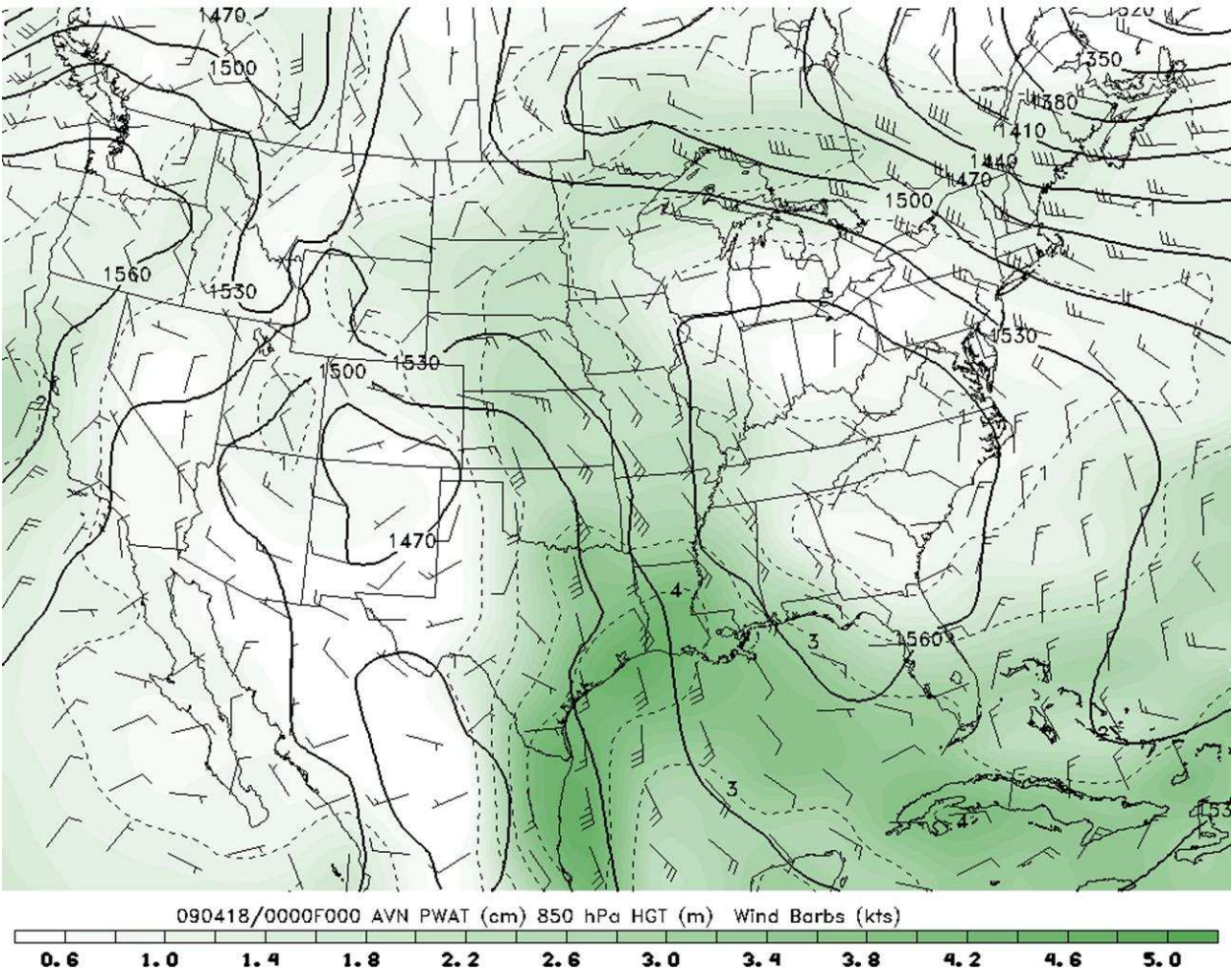


Figure 6-4 As in 6-3, but for the April event

6.4 Comparison of Quantitative Amounts

Perhaps the most interesting, and useful for the rest of this study, aspect of comparing these two events is in analysing the quantitative precipitation amounts in each case. Figures 6-5 and 6-6 show a contour fill of the events as represented in MERRA-2. Figures 6-7 and 6-8 show the same, but for stage IV analysis for comparison. A few things become apparent when undertaking this exercise. The first is that MERRA-2 is not adept at reproducing the location of localized maxima. Second, related to the first, is that MERRA-2 does not come close to being

able to reproduce the quantitative amounts of precipitation found in stage IV. This is because of the larger MERRA-2 grid size not adequately being able to resolve convection on these smaller scales. Broadly, the spatial patterns in MERRA-2 match those in stage IV. Additionally, where there are maxima in stage IV there are maxima in MERRA-2. Therefore, MERRA-2's quantitative precipitation is best taken for the broad spatial average that it is, while acknowledging that it is able to aptly identify precipitation maxima when there are precipitation maxima in the observed data. This fidelity to observations is greatly aided by the observation corrected nature of the MERRA-2 precipitation dataset used. Correct identification of extreme events is paramount to this research, and with the observation corrected dataset there is reasonable confidence that MERRA-2 identifies an extreme event when one actually occurred. The observation correction includes both satellite and gauge datasets, meaning that even data sparse areas experience some observation correction of the precipitation data.

24-hr Precipitation Ending 2009-04-18 12z

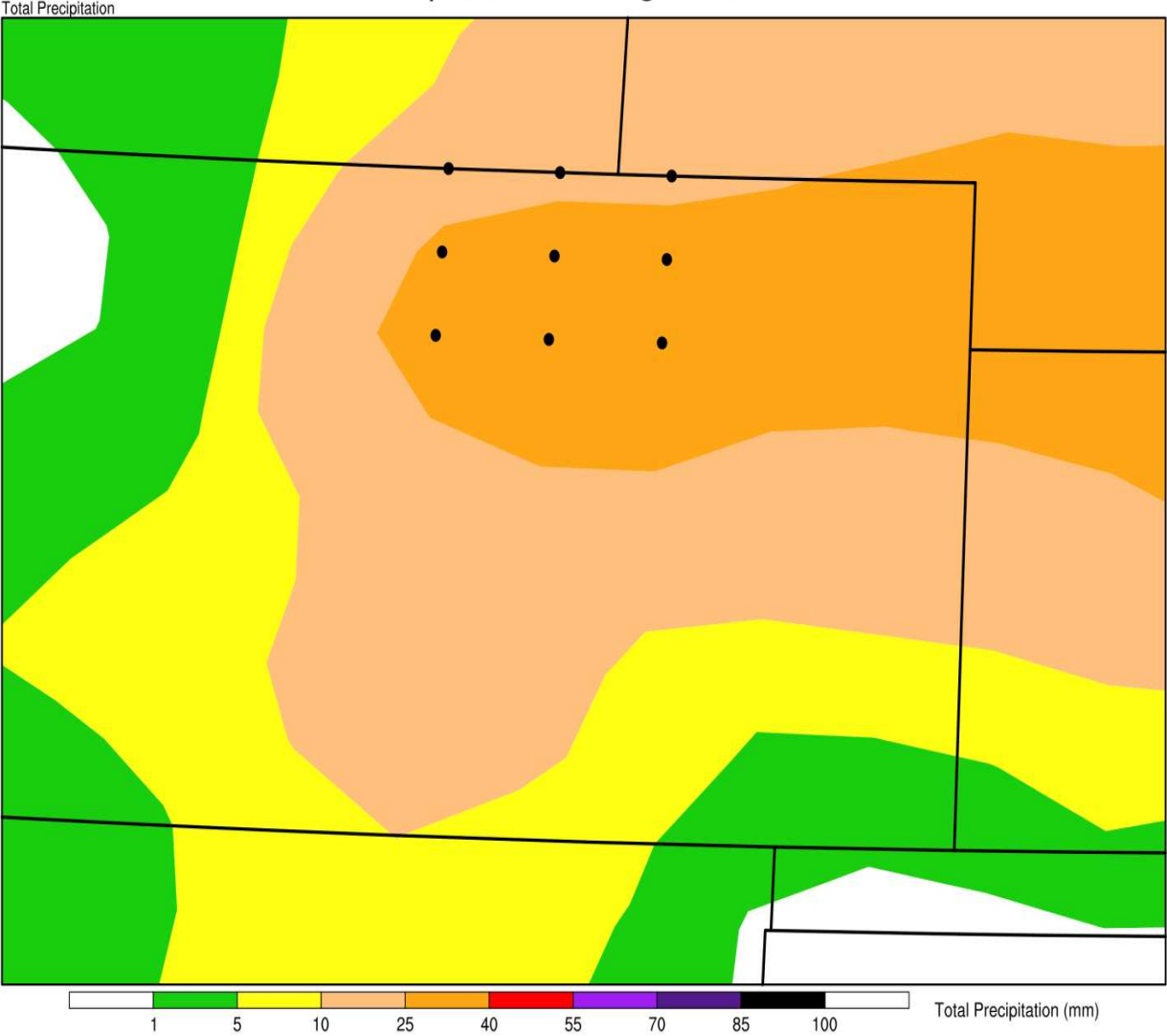


Figure 6-5 MERRA-2 precipitation; April 2009 event. Dots mark the location of the 3x3 block of points included in Figure 6-1. Color scale is the same for 6-5 to 6-9

24-hr Precipitation Ending 2013-09-13 12z

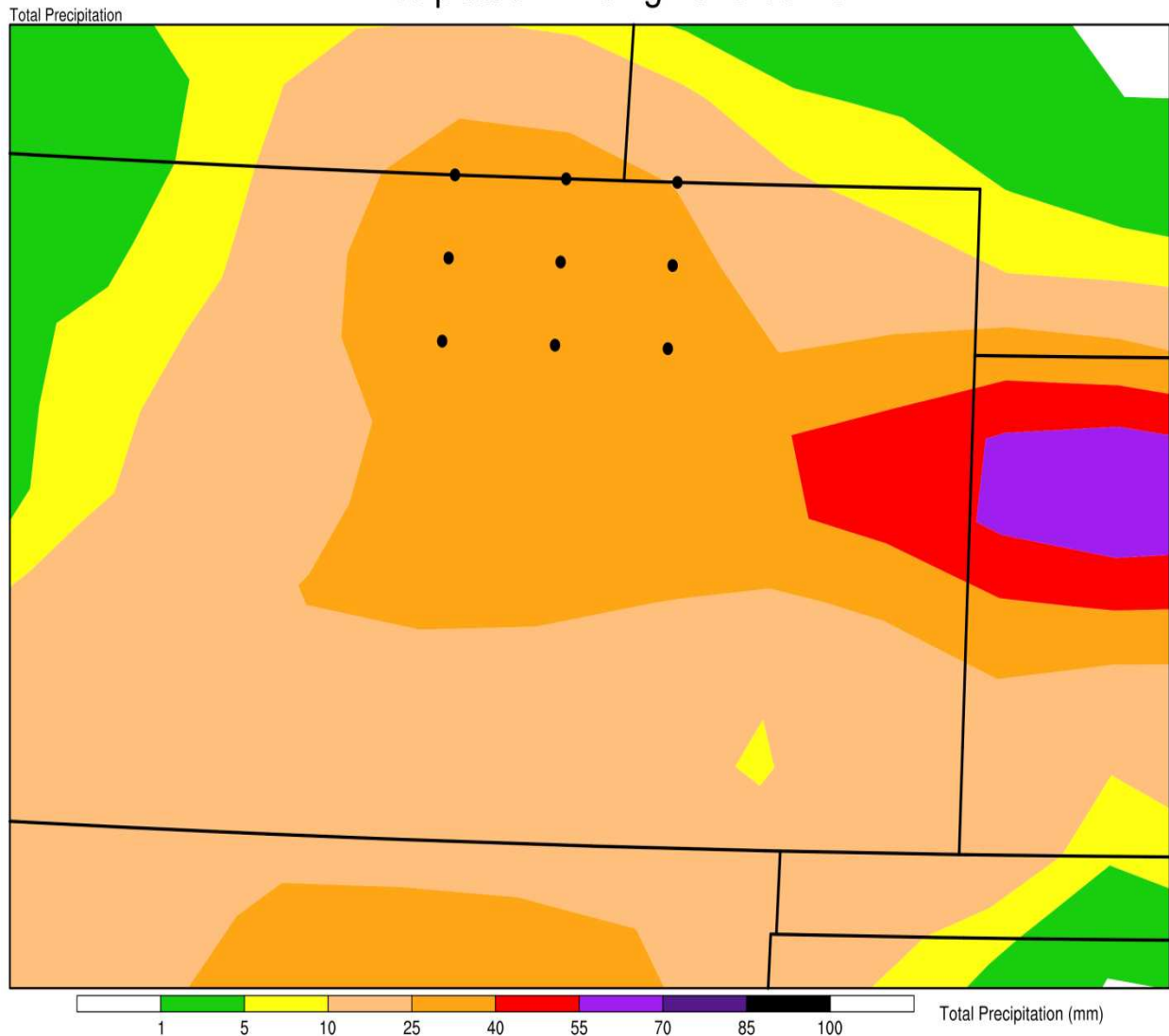


Figure 6-6 Same as 6-5, but for the September 2013 event, 24 hours ending September 13th 2013 at 12z

24-hr Precipitation Ending 2009-04-18 12z

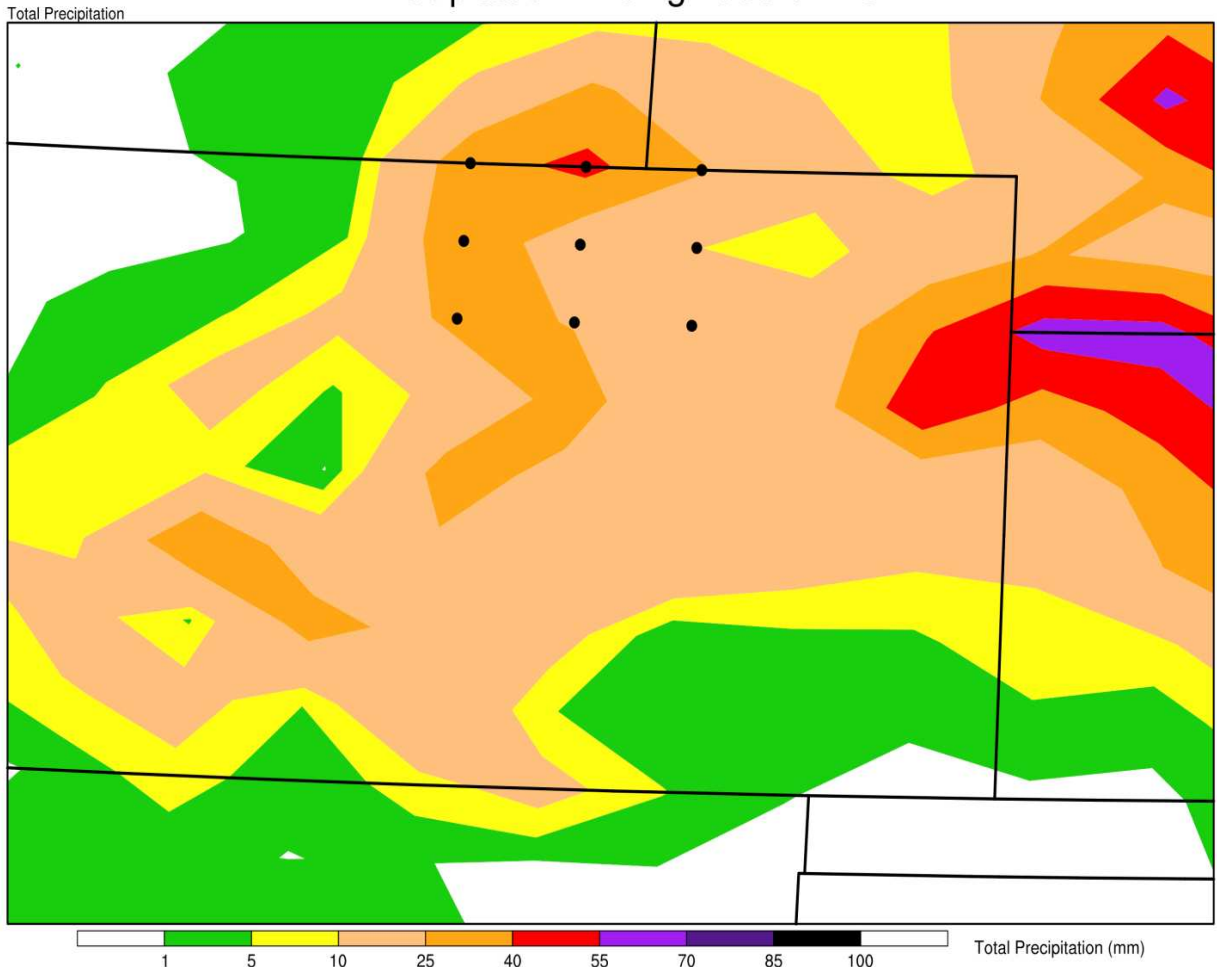


Figure 6-7 Stage IV 24 hour precipitation accumulation re-gridded to MERRA-2 grid for the 24 hours ending April 18th 2009 at 12z. Dots show the MERRA-2 grid spacing.

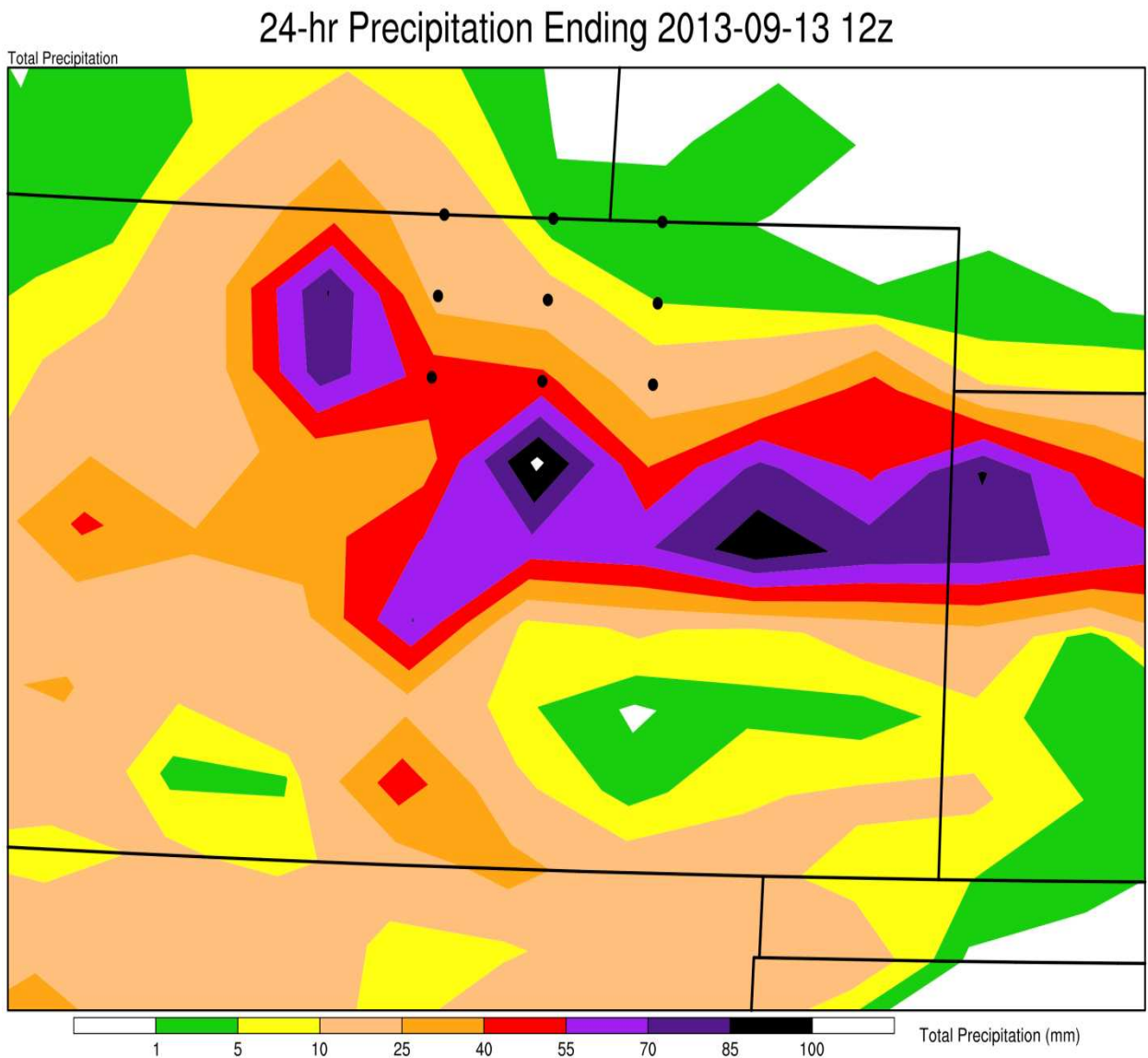


Figure 6-8 As in Figure 6-7 for the period ending 12z September 13 2013

6.5 Summary

This section shows the merits of using MERRA-2 for a widespread precipitation analysis. Despite a limited resolution, MERRA-2 is able to spatially locate relative maxima in the precipitation field. While comparison to stage IV reveals that it is unable to correctly identify the quantitative maxima, this limitation is mitigated because the main concerns are that relative maxima and spatial extent are well defined, which MERRA-2 is able to do. Thus confidence is

acceptably high that events defined as extreme in the MERRA-2 context are in fact extreme, and not unduly impacted by the resolution of the data product. In the same vein it can be said that it is unlikely that a significant number of extremes are missed because MERRA-2 does respond well to convective precipitation qualitatively though not quantitatively.

Comparing the two gridpoints also gives an opportunity to look at two very different regimes that each produced extreme precipitation. How different synoptic environments produce extreme precipitation is the focus of this project. In this case, despite being on different sections of the precipitable water and lift parameter space, as evidenced by the relatively low amount of forcing in the Colorado 2013 flood associated with a small shortwave moving around the ridge, with the stronger synoptic forcing for ascent in the April event associated with an upper level trough and clearly defined cyclone at 850hPa, these two events produced extreme precipitation. This result shows that extreme precipitation does not always come in one flavor for a given region. Describing these flavors will be the focus of the next chapter.

CHAPTER 7

PCA OF EXTREME EVENTS WITH COMMON METEOROLOGICAL VARIABLES

7.1 Introduction

This section discusses the use of standard atmospheric variables in a PCA analysis to describe modes of variability in the set of extreme precipitation events at each gridpoint. Eleven MERRA-2 variables are used. They are: 1) Sea level pressure 2) Fraction of gridpoint covered by convective showers 3) tropopause height 4 & 5) u and v 500hPa wind 6 & 7) u and v 850hPa wind 8) cloud top pressure 9) Precipitable water 10) length of event in number of 24 hour periods covered and 11) amount of precipitation in 24 hour period. Each of these variables was taken both from the central gridpoint that met the extreme criteria and each adjacent gridpoint for a total of 91 variables. All variables are 24 hour averages covering the same period as the 24hr accumulation, and were scaled before analysis. The loadings presented here are not rotated, so as to retain orthogonality for potential predictive power. These analyses help identify the biggest patterns of variability in the data, the ‘flavors’ that extreme precipitation occurs under. Throughout this section it is important to remember that a ‘low precipitable water’ is only low relative to the other extreme precipitation periods in the dataset, not in the absolute sense. While this analysis was done at every point in the domain, this chapter will focus on just the Northern Colorado (40.5N 104.375W) and Córdoba (31.5S 63.75W) gridpoints for the sake of brevity. These gridpoints were chosen for their local interest and the interest of the RELAMPAGO campaign in the Córdoba region.

7.2 Northern Colorado (40.5 North 104.375 West)

Figure 7-1 graphs the variable loadings of the PCA analysis at the titular gridpoint. The nine points of each variable, one for the center gridpoint that triggered the extreme designation and every surrounding gridpoint, read like a book. From left to right across the section of the plot corresponding to that variable are plotted the points to the northwest, north, northeast, east, center, west, southwest, south, southeast relative to the center gridpoint. The loadings in a PCA are interpreted relative to each other. It is important also to remember here that these PCs are only for the extreme event, so a low value of a variable in this context merely means low relative to the rest of the extreme events. Looking at the figure, it can be seen that precipitable water is anticorrelated with the pressure of the tropopause. This makes sense, as we would expect precipitable water to be lower in shoulder season events with a lower (higher pressure) tropopause. Further corroborating this view of the physical pattern this PCA represents is the fact that in the scenario with low precipitable water and a lower tropopause, the fraction of convective showers in the gridpoint is low and the pressure of the cloud heights is high (low clouds). The length of events is also slightly longer in this pattern. The opposite of this pattern would point to summertime pattern such as occurred in the September 2013 flood. This scenario involves higher amounts of precipitable water, a higher tropopause, and a higher fraction of convective showers than the other extreme events in the dataset. Thus the first PC consists of two opposing patterns, both of which are capable of producing extreme precipitation.

The first PC pattern at Northern Colorado is indeed significant according to the methodology of North et al. (1983). This is shown in Figure 7-2. When the confidence intervals of the eigenvalues from the PCA do not overlap, the PCA is considered significant. Therefore, in this case only the first PC is significant; explaining about 35% of the variance. The number of

observations for the calculation is considered to be the number of independent events that are in the dataset. If every point were used, the confidence interval would be falsely small. With PCA it is very easy to begin fitting noise, and so this check is an important step towards useful physical interpretation. If a PC is nearly significant with a discernable physical interpretation, this can be considered acceptable for the purposes of this study as well.

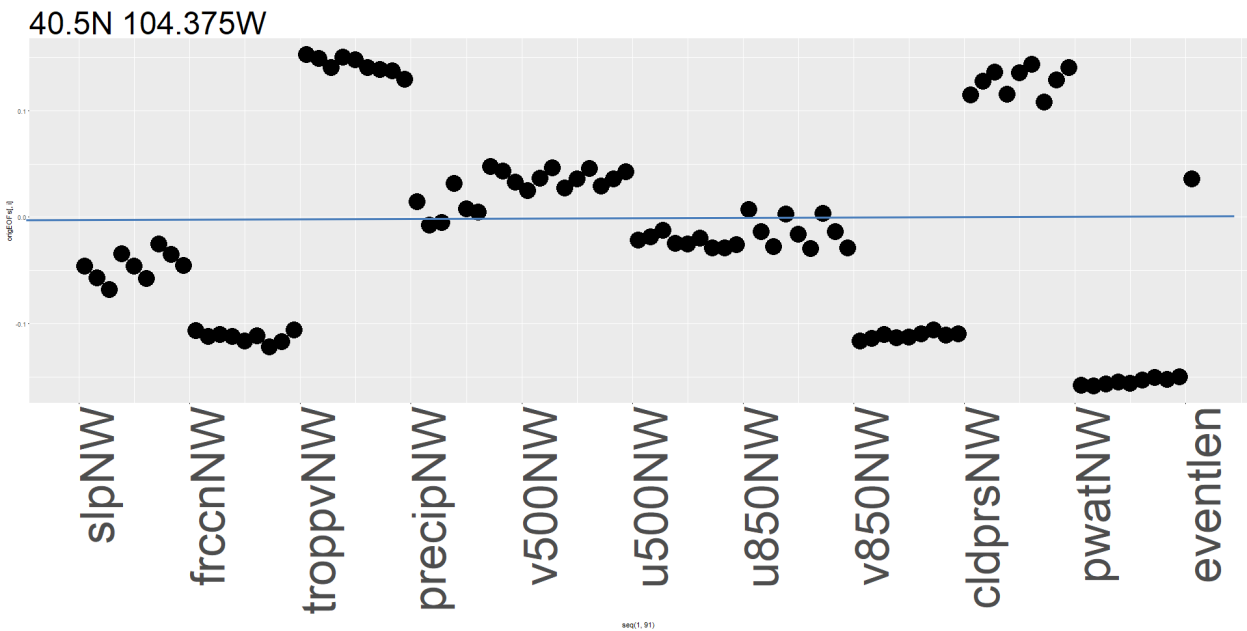


Figure 7-1 Plot of PC1 loadings. Variables are as follows: slp – sea level pressure; frccn – fraction convective showers; troppv – pressure of 2PVU tropopause; precip – the 24 hour precip at the gridpoint; v500 – v wind at 500hPa; u500 – u wind at 500hPa; u850 – u wind at 850hPa; v850 – v wind at 850hPa; cldprs – cloud top pressure; pwat – precipitable water; eventlen – number of 24 hour periods during the event. NW at the end of all the variables refers to the fact that the variable label is aligned with the northwest gridpoint on the far left of the set for the variable. Y-axis labels are small because the relative amount is more important than absolute magnitude, zero is marked with a blue line.

It is useful to produce plots of meaningful atmospheric parameters in conjunction with the PC1 analysis to investigate how the pattern looks in the more familiar context of weather maps. Figure 7-3 shows the composite of 500 hPa height associated with the bottom 25% of PCs (in other words, the events most opposite of the pattern shown in PC1). This composite is created

by averaging the 500hPa heights at all times associated with PCs in the bottom 25%. The pattern shows a large ridge over the area. Figure 7-4 is the 500hPa composite associated with the top 25%

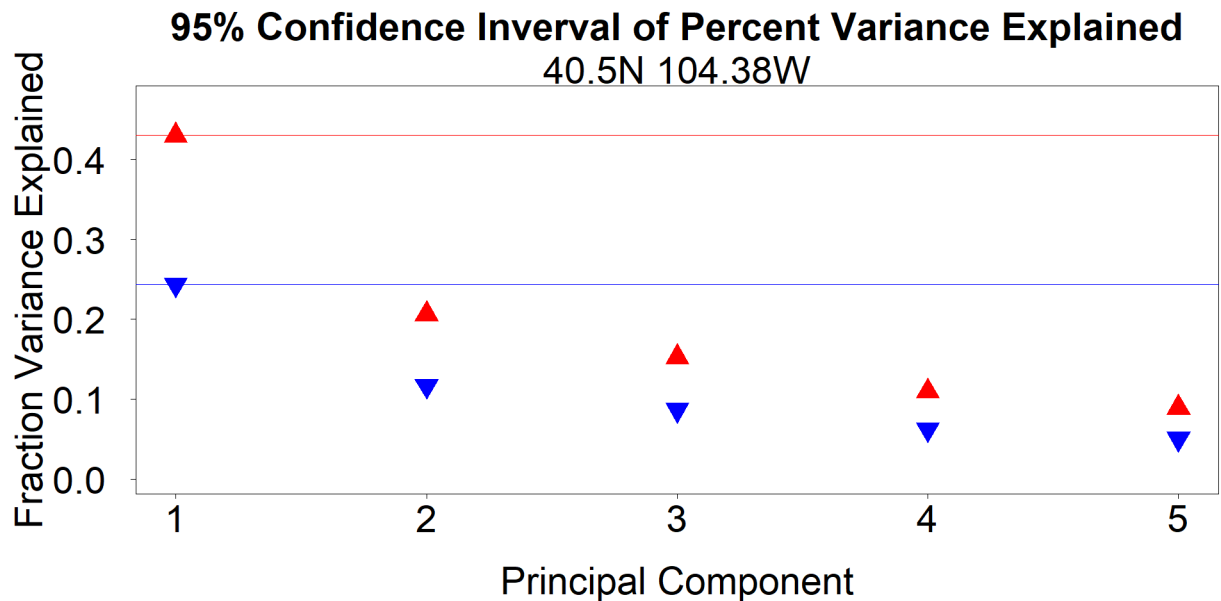
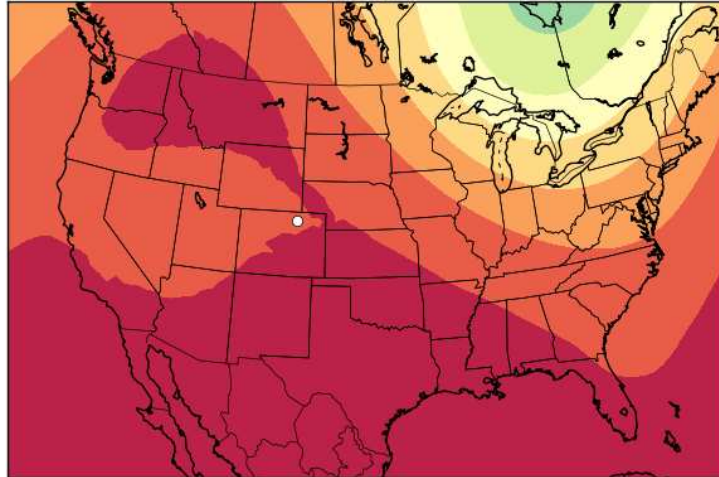
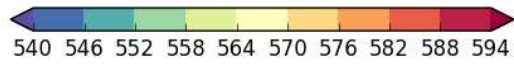


Figure 7-2 Plot of confidence intervals (denoted by red and blue triangle) for each principal component. Horizontal lines are provided for ease of interpretation of the North et al. methodology for significance, where a PC is significant if there is no overlap with the next PC. PC1 is the only one that is significant according the methodology of North et al., explaining ~35% of variance

of PCs, the events that look most like the pattern in Figure 7-1. Here a cutoff low is observed, in a location that promotes favorable upslope flow. Similarly, figures 7-5 and 7-6 show the pattern for the top and bottom 25% of PCs but for precipitable water. The differences are slightly less notable here, but the composite of the top 25% clearly shows a long trail of moisture wrapping into a cyclone. The bottom 25% shows a more amorphous blob of moisture over Texas feeding into Colorado, with much higher absolute amounts of water due to the summer season.

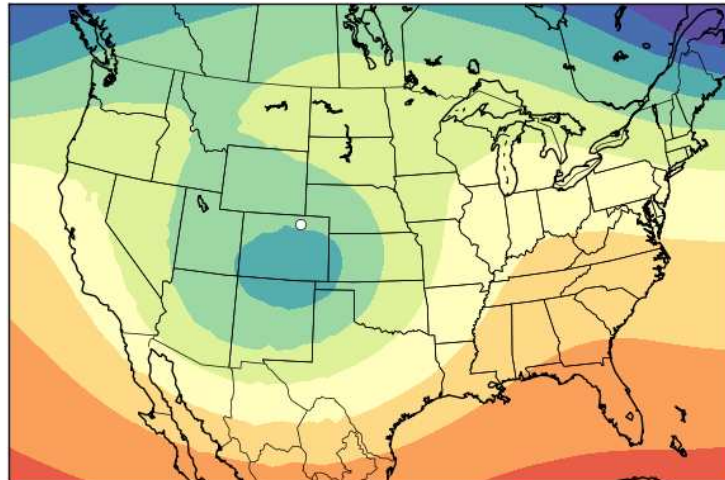


Start:2013-09-13 03:00Z
 End: 2014-08-01 22:59Z

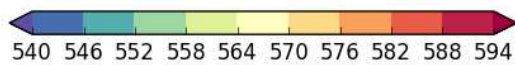


500hPa Height (dm)

Figure 7-3 Composite of 500hPa height associated with the bottom 25% of PCs. Start and end times refer to the start of the first event used in the composite and end of the last event



Start:1983-03-06 19:59Z
 End: 2003-03-21 13:00Z



500hPa Height (dm)

Figure 7-4 As in 7-3 but for the top 25% of PCs

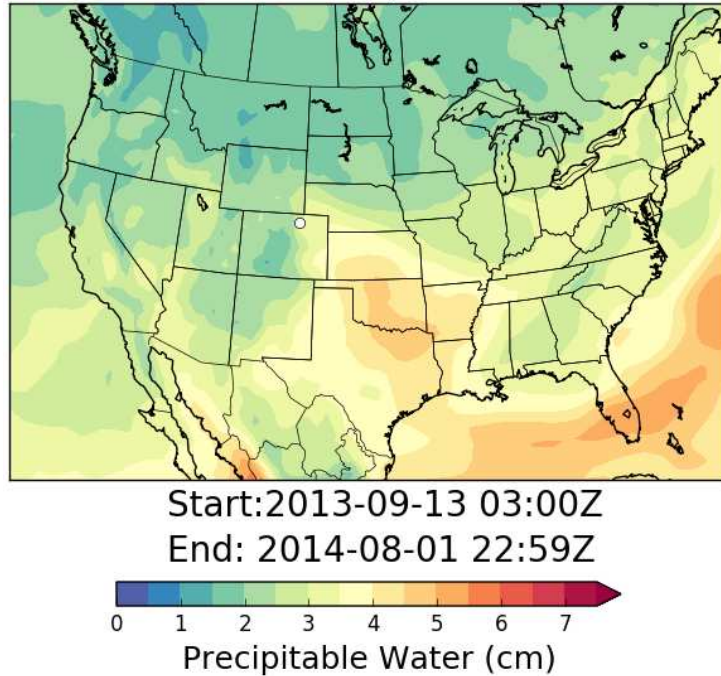


Figure 7-5 Composite of the precipitable water associated with the bottom 25% of PCs

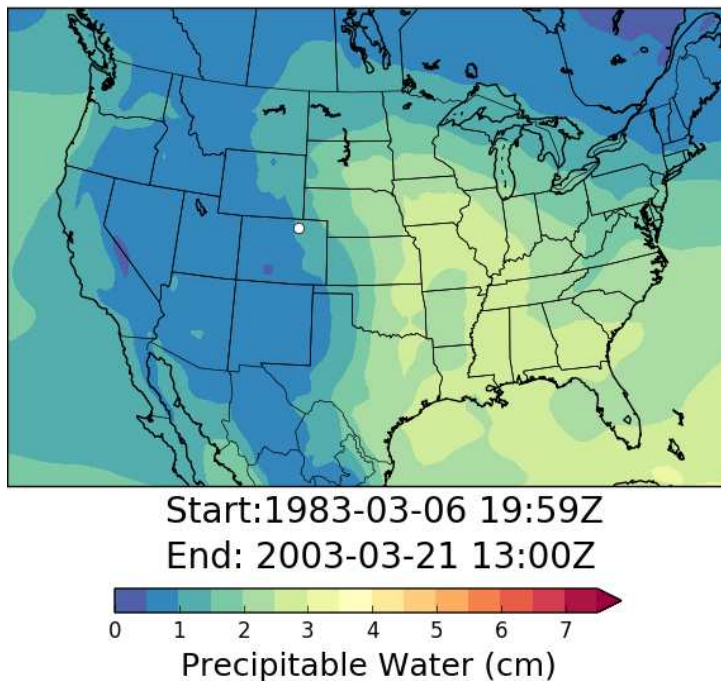


Figure 7-6 As in 7-5 but for the top 25% of PCs

Thus we see that in Colorado there are two very distinct regimes of atmospheric conditions that can result in extreme precipitation. One of these conditions relies more on a high

precipitable water, while the other relies more on synoptic lift. The high precipitable water regime is more common in the late summer, while the synoptic regime holds more sway in the shoulder seasons when baroclinic energy is stronger.

7.3 Córdoba, Argentina (31.5S 63.75W)

Figure 7-7 shows the loadings pattern for Córdoba. In many facets, this plot is very similar to the analogous plot for Colorado. There are key differences, however. Like in the Colorado case, precipitable water is a key distinguishing characteristic for extreme events. Clearly, some extreme events have more precipitable water than others, providing a significant source of variability in the parameter space of extreme events. A major difference, however is that here tropopause height is not as important of a factor as it is in Colorado. Instead, sea level pressure is as important as precipitable water. Another key association is that the u wind at 850hPa being more easterly than the mean correlates with lower precipitable water. This indicates that for Córdoba, upslope flow from the east is an important compensation if very large amounts of precipitable water are unavailable. Figure 7-8 is the significance plot for this gridpoint, again indicating that the first PC is the only one that is significant, while the other PCs are likely fitting noise. This first PC explains around 30% of the variance.

As in Colorado, composite plots were made as well. Presented here are composite plots for sea level pressure and precipitable water. Sea level pressure was chosen for presentation here because it has a high loading, while tropopause pressure (which correlates with 500hPa height) and 500hPa winds have lower loadings. Figures 7-9 and 7-10 show the top and bottom 25% composites for sea level pressure, while 7-11 and 7-12 do the same for precipitable water.

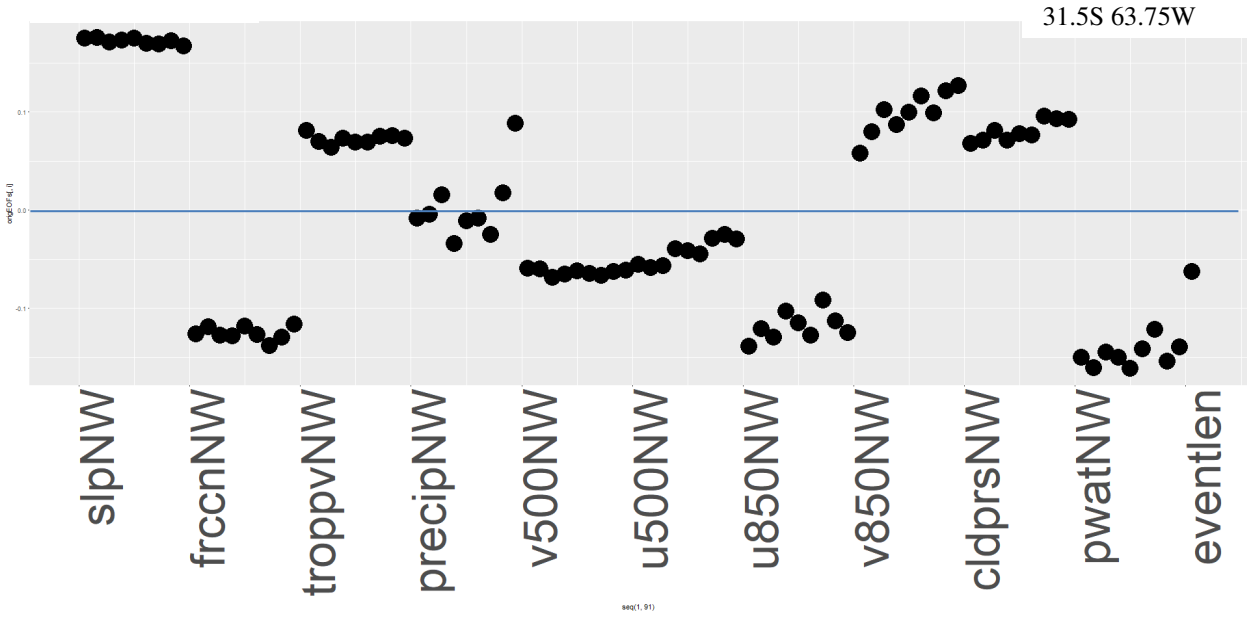


Figure 7-7 Loadings for PC1 for the Córdoba gridpoint, in the same format as Colorado

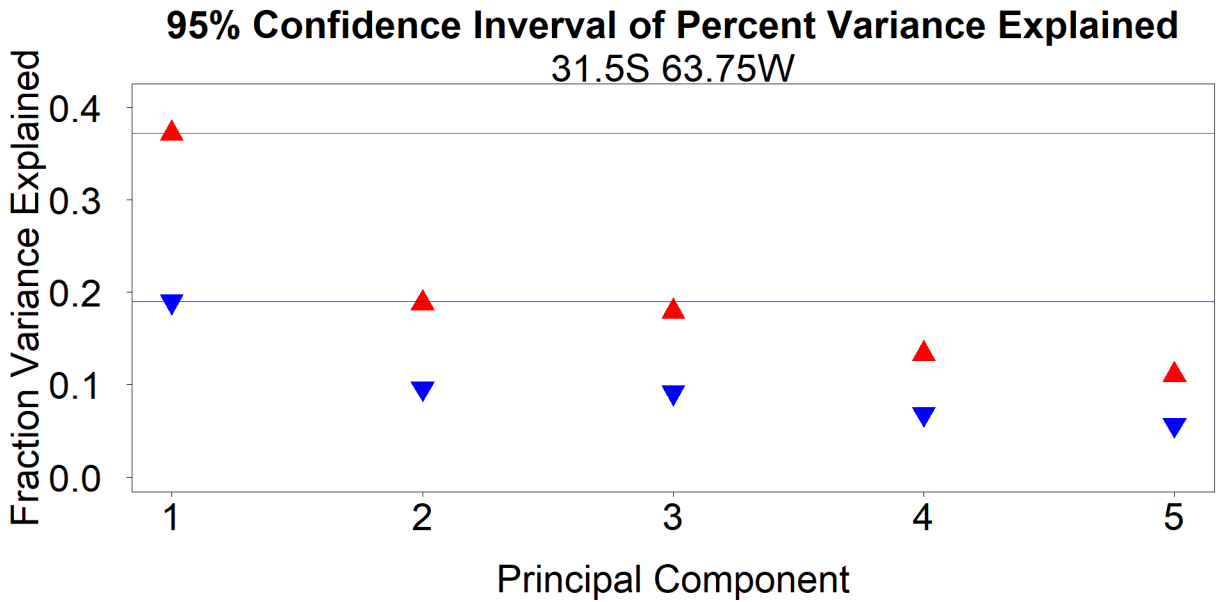


Figure 7-8 Significance plot for the Córdoba PCA

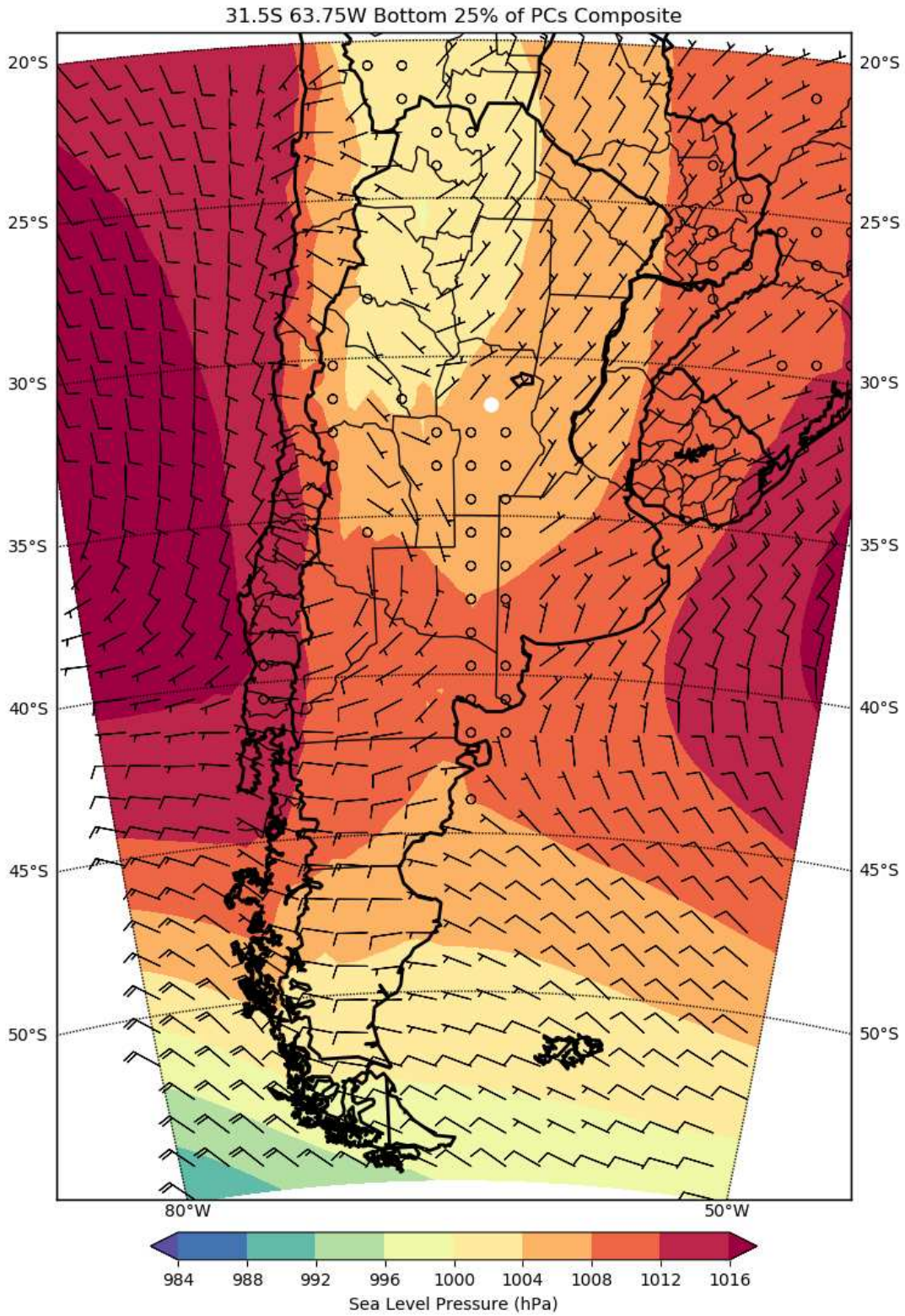


Figure 7-9 Composite of sea level pressure and 10m wind associated with the bottom 25% PCs. Wind barbs are shown in the standard way: long tail = 10kts, short tail = 5 kts, flag = 50kts. Location of the gridpoint is shown by the white dot.

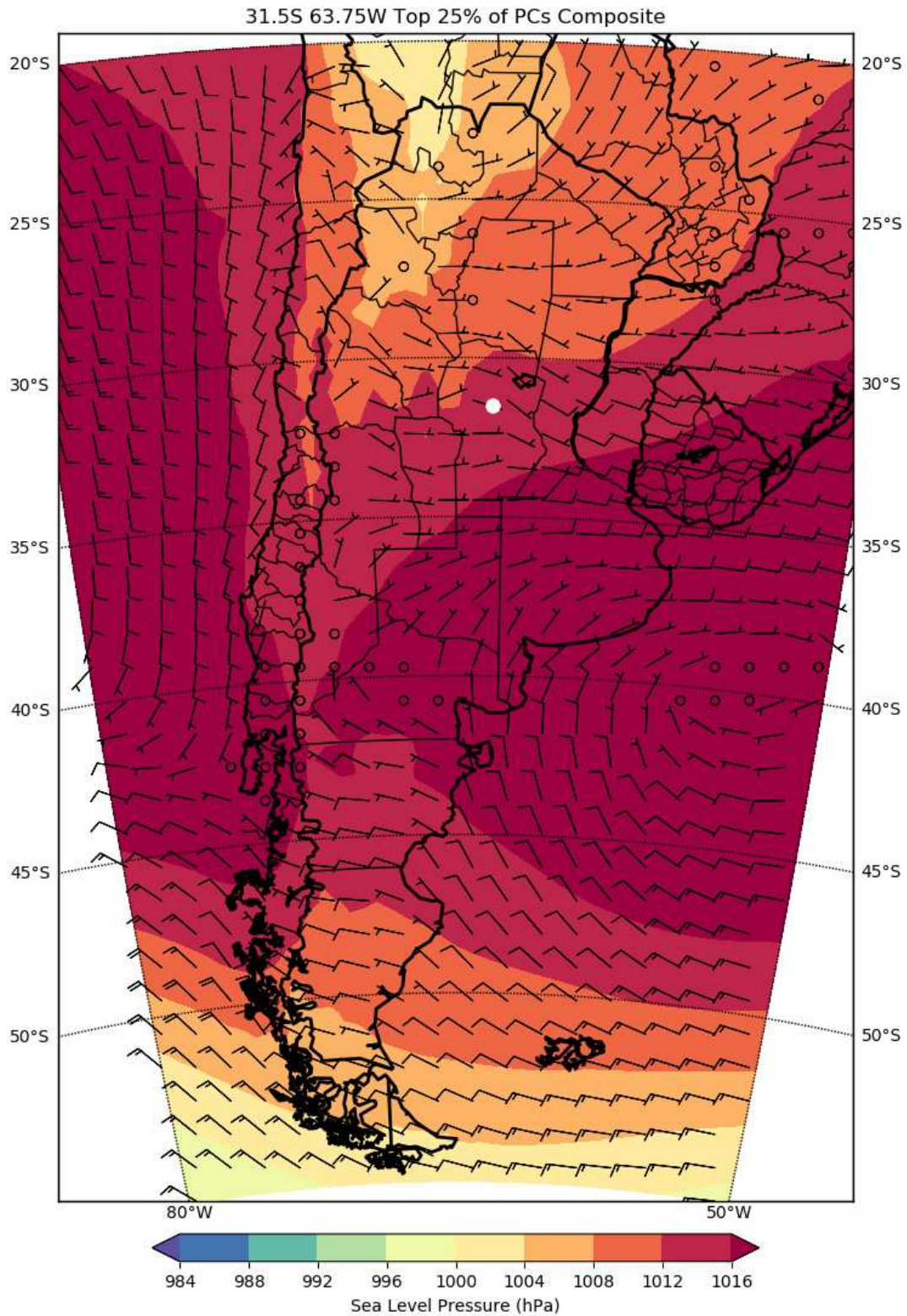


Figure 7-10 Composite of sea level pressure and 10m wind associated with the top 25% PCs. Wind bars are shown in the standard way, long tail = 10kts, short tail = 5 kts, flag = 50kts. Location of the gridpoint is shown by the white dot.

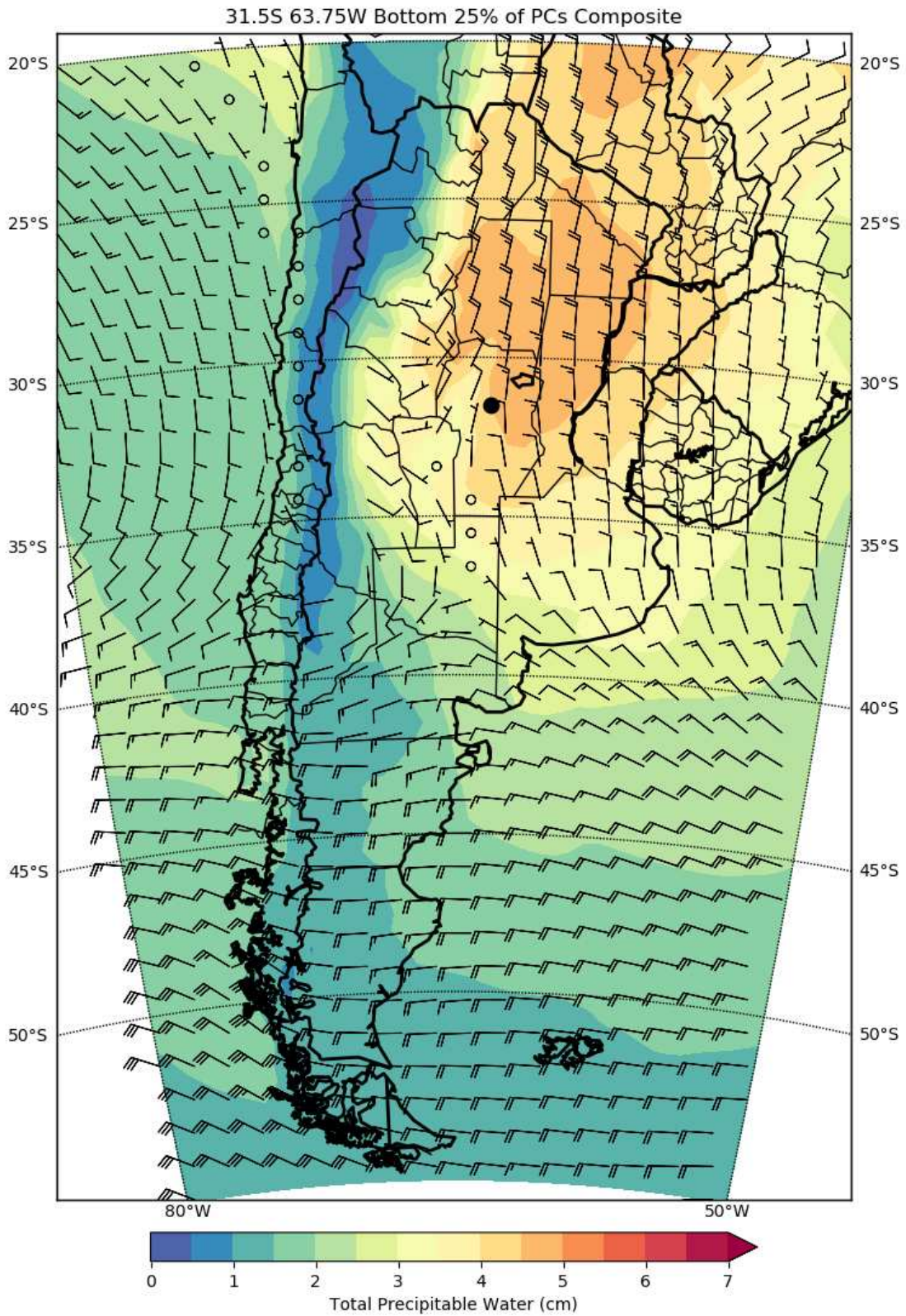


Figure 7-11 Composite of precipitable water associated with the bottom 25% PCs. Wind barbs are composite 850hPa wind. Gridpoint marked the black dot

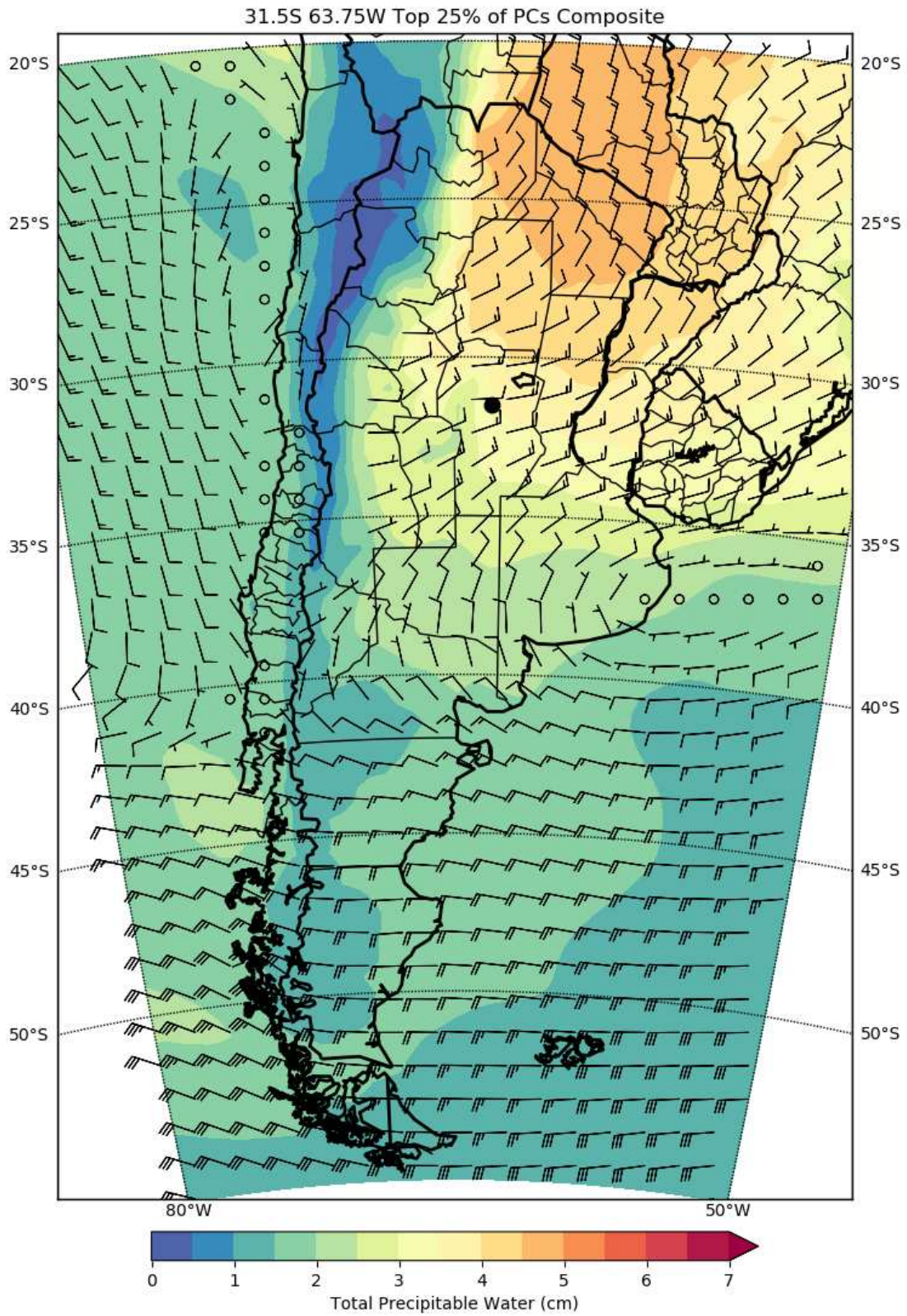


Figure 7-12 Composite of precipitable water associated with the top 25% PCs. Wind bars are the composite 850hPa wind. Gridpoint marked with black dot

These plots show that unlike Colorado, where there are clearly two distinct regimes that can produce extreme precipitation, the pattern at Córdoba appears to be variation on a theme. That theme is a surface lee trough to the north of the location, and a tongue of moisture likely associated with a low level jet descending from the north. The variation in this scenario is how strong the lee trough is coupled with how far south the main stem of moisture reaches. In the top 25% of PCs the gradient of sea level pressure is such that the surface wind vector would be more directly upslope into the Sierra de Córdoba. The bottom 25% of PCs show a stronger lee trough that is able to pull more moisture southward, but the wind vectors that would result from this surface pressure pattern would not be as favorable for upslope flow. However, with more local forcing from pressure falls with the lee trough and more moisture, storms are still able to produce extreme precipitation.

7.4 Conclusion

From these PC analyses, the variability within extreme scenarios was explored. At Northern Colorado two very distinct regimes were described. The first involved a large ridge under which moist air could be brought upslope into convection. The September 2013 flood is the archetype of this regime. The second was a cutoff low over Colorado driving upslope flow into the foothills. This type of pattern is best known for producing prodigious snowfall, but when it occurs even later in the season with more access to moisture these scenarios can result in extreme events. At Córdoba the situation is different. Here instead of two very different regimes, the PCA identifies variability along what can be thought of as a single axis where the strength of the lee trough is varied. The strength of the lee trough controls the amount of upslope flow as well as how far south the Amazonian plume of moisture is able to progress.

CHAPTER 8

PCA OF METEOROLOGICAL VARIABLES DIRECTLY CORRELATED WITH LIFT

8.1 Introduction

In addition to the more standard atmospheric variables, variables known to directly relate to lift were also calculated. This was done to further corroborate the conclusions from the set of PCs using more standard data, as well as potentially provide a deeper insight into these events. The variables selected were: Q-vectors, precipitable water, lapse rate in the lowest three model levels, divergence at low levels, and orographic lift (wind dotted with slope of terrain). Each plot contains two sets of Q-Vectors, one with the calculation of static stability included and one without. As before the loadings of the PCs of these variables will be presented and discussed. The locations of the gridpoints remain the same. Because the neighboring gridpoints were not noted to provide any further useful insight, for this analysis only the variables at the gridpoint are considered. Statistical significance plots will not be shown here because of the severely dependent variables (the two q-vector versions, two versions of convergence at low levels, two versions of upslope flow at low levels) used in the analysis reducing their utility as an objective measure of significance. The algorithm explaining how these dependent variables vary together is simply teasing noise out of an overall good correlation. The analysis is still useful in terms of how the variables relate to each other in their groups, but since we are here violating the practice that all the variables input into the algorithm be independent, the techniques for statistical significance will not hold.

8.2 Northern Colorado

Figure 8-1 presents the first PC of the PCA analysis with the lift variables. It can be seen that this lower precipitable water scenario is associated with more low level convergence, but also less upslope flow and q-vector convergence. Also in this scenario, lapse rates are steeper in the lowest levels. Precipitation falls right on the zero line, indicated that neither the positive nor the negative pattern produces more precipitation than the other. The scenario depicted below seems to be that of a frontally forced system, one with relatively high convergence compared to the more benign patterns that can still cause extreme precipitation. The opposite of this pattern is more like that more benign larger scale pattern, with less dynamically forced convergence but more precipitable water, combined with upslope flow. The most important factors (with the highest loadings) in distinguishing events are the orographic lift terms. This indicates that in some situations of extreme precipitation, orographic lift is much more important than in others.

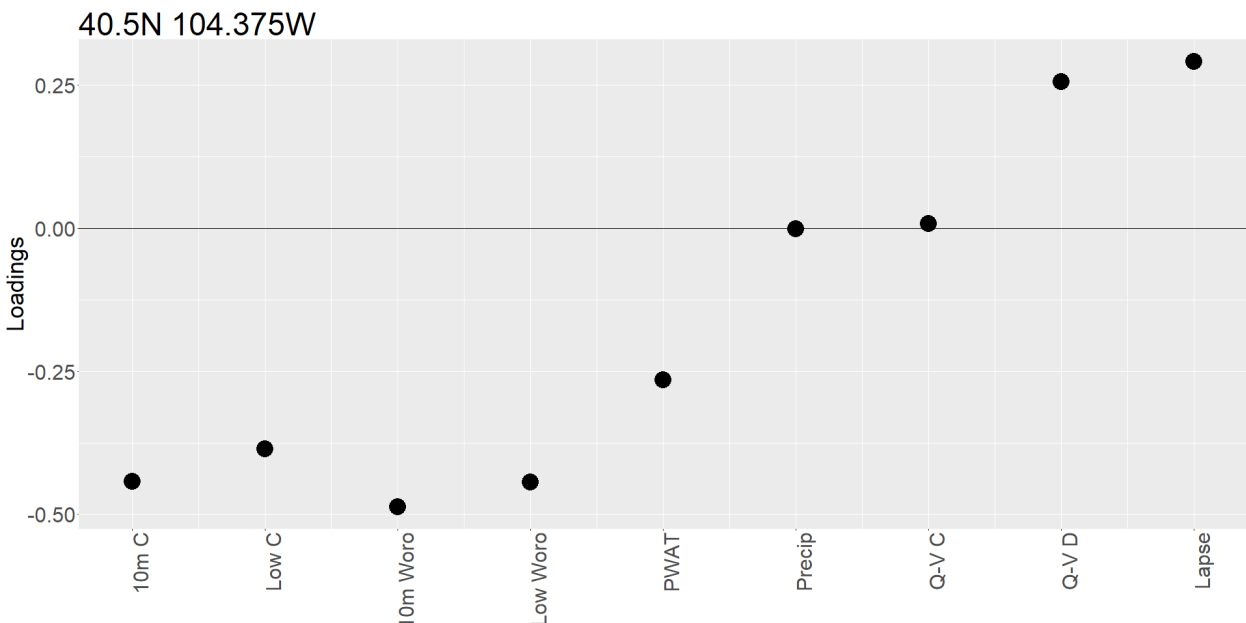


Figure 8-1 Plot of the loadings for the PCA of lift variables. From left to right are 10m convergence, convergence in the lowest above ground model level (25mp increments), 10m orographic lift, orographic lift in lowest model level, precipitation, Q-vectors with the stability parameter held constant, Q-vectors with the stability parameter dynamic, and lapse rate.

8.3 Córdoba, Argentina

Figure 8-2 is the lift variables loadings for Córdoba. In this pattern it at first glance it appears that the negative index of the pattern is the only one remotely supportive of precipitation. The positive version of the pattern has: less convergence at the surface, low relative precipitable water, shallower lapse rates and less q-vector convergence. Indeed it is observed that less precipitation falls in this positive pattern than in the negative pattern. However, there are a few things about the positive pattern that do support precipitation, namely the relatively higher upslope flow. It seems that in scenarios where the other factors are not as favorable as they are in other extreme weather scenarios (it is important to remember here that less convergence certainly does not mean no convergence or divergence) upslope flow can provide compensation. This is able to turn somewhat less favorable scenarios into extreme precipitation events. It is also worth noting that in the PC's most of the values fall around -2 to 2, but where there are large outliers they are on the negative side. This is possibly indicative of the fact that when it rains it pours in terms of the combination of q-vector convergence more precipitable water, and steeper lapse rates. This combination of variables is indicative of exceptionally strong synoptic systems sweeping through the area.

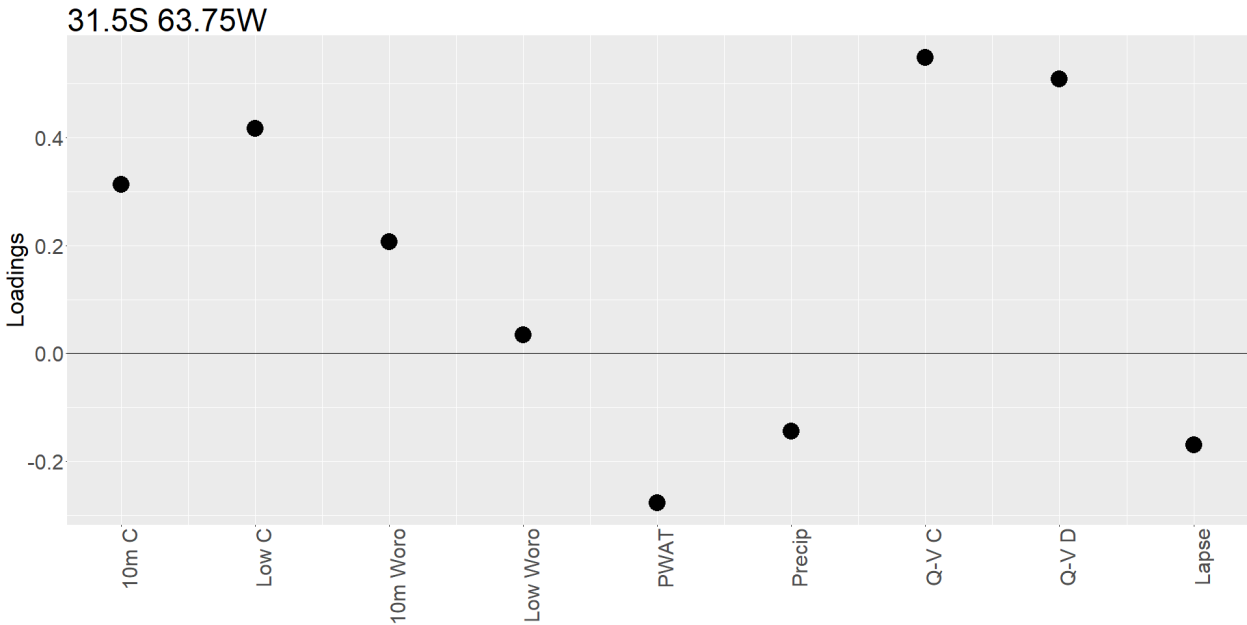


Figure 8-2 Lift variable loadings at Córdoba

8.4 Summary

Other variables have been put through the PCA algorithm, and they show corroborating results with the more standard atmospheric variables. Both locations show strong evidence that amount of upslope flow is a distinguishing characteristic between extreme events. At Northern Colorado the dichotomy between high convergence low precipitable water vs high precipitable water low convergence scenarios is again noted as it was in the standard variable PCA. Córdoba shows less precipitable water correlating with less q-vector convergence. This makes sense with the earlier observation that the in the low precipitable water case the lee trough does not extend as far south. Overall these different sets of variables allow for a new perspective to look at these extreme events.

CHAPTER 9 EVENTS IN CONTEXT

9.1 Introduction

So far this work has only discussed extreme events relative to each other. But what about comparing extreme events to the day to day weather? This is an important task, since as mentioned earlier; ‘low precipitable water’ could still mean an extreme value for that day or time of year, but less than all the other extreme events. Therefore the plots presented in this section were created. They illustrate the 24 hour running mean of the hourly z-score through the year, with the hourly z-scores of the events plotted as black dots. The shaded area represents the 24 hour running mean of plus and minus one standard deviation.

9.2 Precipitable Water

Plots of the precipitable water through the year are presented for both the Northern Colorado and Córdoba gridpoints in figures 9-1 and 9-2 respectively. There are important things to take away from these plots. There is a bit less interannual variability in precipitable water at Córdoba than at Northern Colorado, as one might expect for a subtropical vs mid-latitude location. At Northern Colorado, the air is simply too cold in the winter to hold enough moisture for an extreme event. While Córdoba has less seasonal variation, it does have far more day to day variation throughout the year, even in the winter, which is another indication of its subtropical location. It should be noted that many of these extreme events span the -1 to +1 standard deviation range. Since the individual points here are merely within the 24 hours that the extreme precipitation fell in, and not necessarily indicative of conditions while rain was falling,

this may not be surprising. It does indicate that many of these events have a ‘ramp up’ phase as moisture enters the area. Other events clearly indicate the sustained presence of strongly anomalous values. These tend to occur in the summer at both locations, where perhaps the amount of water in the air was the primary driver of extreme precipitation. Both of the points also have at least one event whose points are all near average precipitable water for the time of year. At Northern Colorado, this is an August event, while at Córdoba this occurs in January. These are similar in that they occur at similar points in the seasonal cycle, one or two months past the summer solstice. These types of events show that strongly anomalous precipitable water is not a requirement for extreme precipitation in these regions.

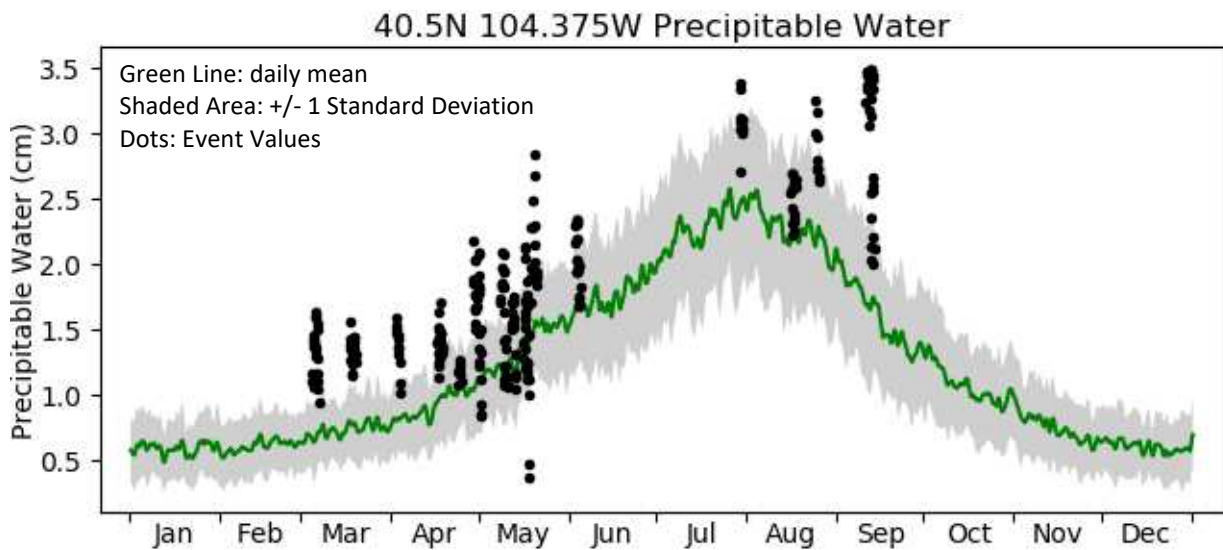


Figure 9-1 Plot of the 24 hour running mean of precipitable water z-scores through the year near Northern Colorado. The z-score for any time during an extreme event is plotted as a black dot.

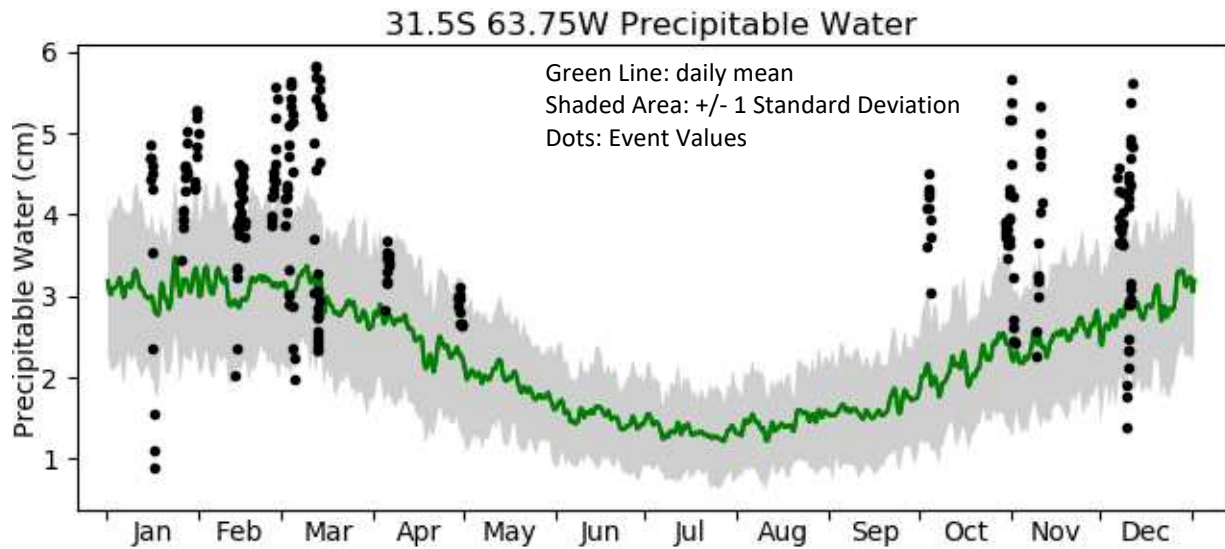


Figure 9-2: Same as Figure 9-1 but for Córdoba

9.3 Low Level Divergence

The same types of plots were produced for divergence of the 10m wind, and are presented as figures 9-3 and 9-4 for Northern Colorado and Argentina respectively. The pattern of seasonal variability in each location is very interesting. Northern Colorado clearly has a minimum of divergence (maximum of convergence) in the summer months, and a relatively steady spread between plus and minus one standard deviation throughout the year. Córdoba has no definitive seasonal cycle in the mean value, but clearly has a seasonal cycle in the spread between plus and minus one standard deviation. Regarding the values during events, it is clear that convergence at low levels is far more important in Colorado than in Córdoba. Most Colorado events have at least one point below the minus one standard deviation range. Meanwhile, Córdoba events, while certainly containing some events for which convergence was important, do not contain the same number or magnitude as in Colorado. This is indicative of a

major source of ascent in Colorado events being low level convergence, while in Córdoba events this factor is not as important to the lifting of air.

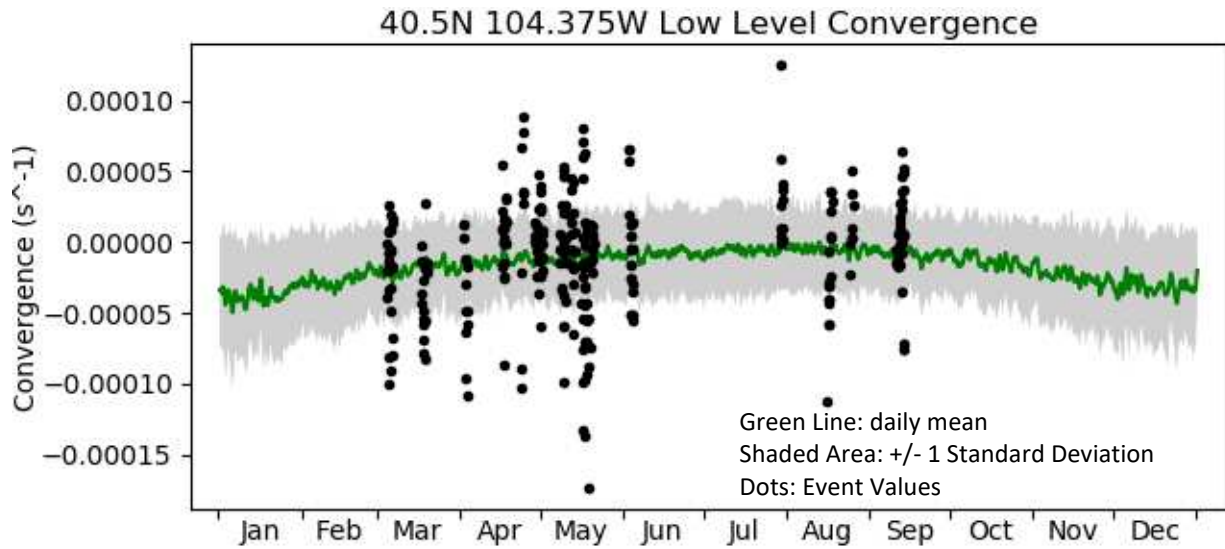


Figure 9-3 10m wind divergence (more negative is more convergence) for Northern Colorado. Shading and lines as in the previous two figures.

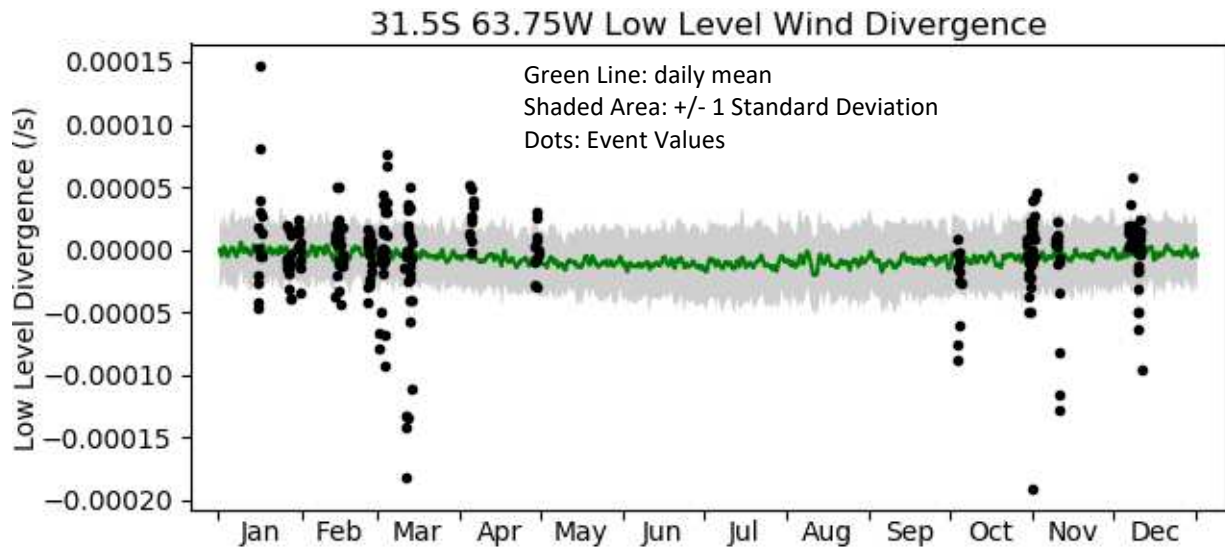


Figure 9-4 Same as 9-3 but for Córdoba

9.4 Conclusion

These plots illustrate that atmospheric variables can have a wide range of values compared to the background climatology. The two variables selected here, precipitable water and low level convergence, are chosen to highlight the differences between the two gridpoints at different latitudes in opposite hemispheres. These points show differences in seasonal cycle as well as differences and similarities in the importance of each variable to extreme precipitation. The differences in seasonal cycle are likely due to the nine degree difference in magnitude of latitude between the two points, which is enough to put Northern Colorado definitively in the mid-latitudes and Córdoba in the sub-tropics. Unlike at Northern Colorado, 10m convergence does not seem to be as reliable indicator of extreme potential for Córdoba, especially for events that occur during the springtime. Precipitable water profiles during extreme events look broadly similar however. These plots provide important context for the extreme events against the backdrop of climatological seasonal variability

CHAPTER 10

ANALYSES OF 1-HR AND 24-HR OVERLAP

10.1 Introduction

This section will explore the contribution of one-hour extremes to 24 hour extremes in Argentina. This analysis provides a way to look at both the likelihood that convection is involved in all or most extreme values at a point or whether the precipitation falls more gradually over time. The overlap (and lack thereof) between extreme instances at these two temporal scales, as well as the environments these events occur in, allows for insight into the processes that factor most into such events. Rising amounts of water in the air would seem likely to provide a boost to one-hour intensities due to increased efficiency. But over a 24-hour period, only a few hours will not create an extreme event for most locations. This chapter will zoom back out to all of Argentina to answer how much overlap there is between these temporal timescales throughout the country.

10.2 Results

Figure 10-1 shows the percentage of all precipitation in the 24-hour events that comes from the total of the precipitation in the 1-hour events. Illustrated in this map is the fact that extreme 1-hour precipitation is a higher percentage of 24-hour extreme precipitation along the east slopes of the Andes, where convection initiates and very strong thunderstorms have been observed by TRMM. This indicates that in these regions, convective processes have a larger influence on extreme events. The other region that stands out is the Atacama Desert, where almost any rain at all is both a 1-hour and 24-hour extreme event. Figure 10-2 shows the

percentage of 24-hour extreme events that do not contain a 1-hour extreme event. The regions highlighted here include the western slopes of the Andes and the plains to the west of the Andes. These areas are those that are more likely to experience extreme precipitation in a steady rain that persists for most or all of the 24-hour period, from westerly winds interacting with the Andes and large mesoscale convective systems respectively.

Figure 10-3 shows cumulative precipitation during 24-hour extreme events from the gridpoint nearest Córdoba, the city that will serve as the center of operations for RELAMPAGO. At this gridpoint there were no 24-hour events that did not include an extreme 1-hr event, which is not surprising given the propensity of convection in the area. This data shows that the 24-hour sums at this convectively influenced gridpoint consist of a few groups of jumps of an hour or two of precipitation. The cluster around 24 hours occurs because when plotting cumulatively across the entire event, and not just one 24 hour period, the first running 24 hour sum that triggers the threshold is likely to have just barely cleared the threshold, and some events continue rising from there. Figure 10-4 shows the same but for 35.5S 64.375W, an area that had about a third of 24-hour events marked as 24 only. For the events that contain intersections with extreme 1-hour precipitation, the traces look much as they do near Córdoba. The 24-hour traces for the 24-hour only events show much steadier precipitation over the period, indicating that these periods are indeed different meteorologically and not merely instances analogous to the intersection periods but with slightly less one hour precipitation.

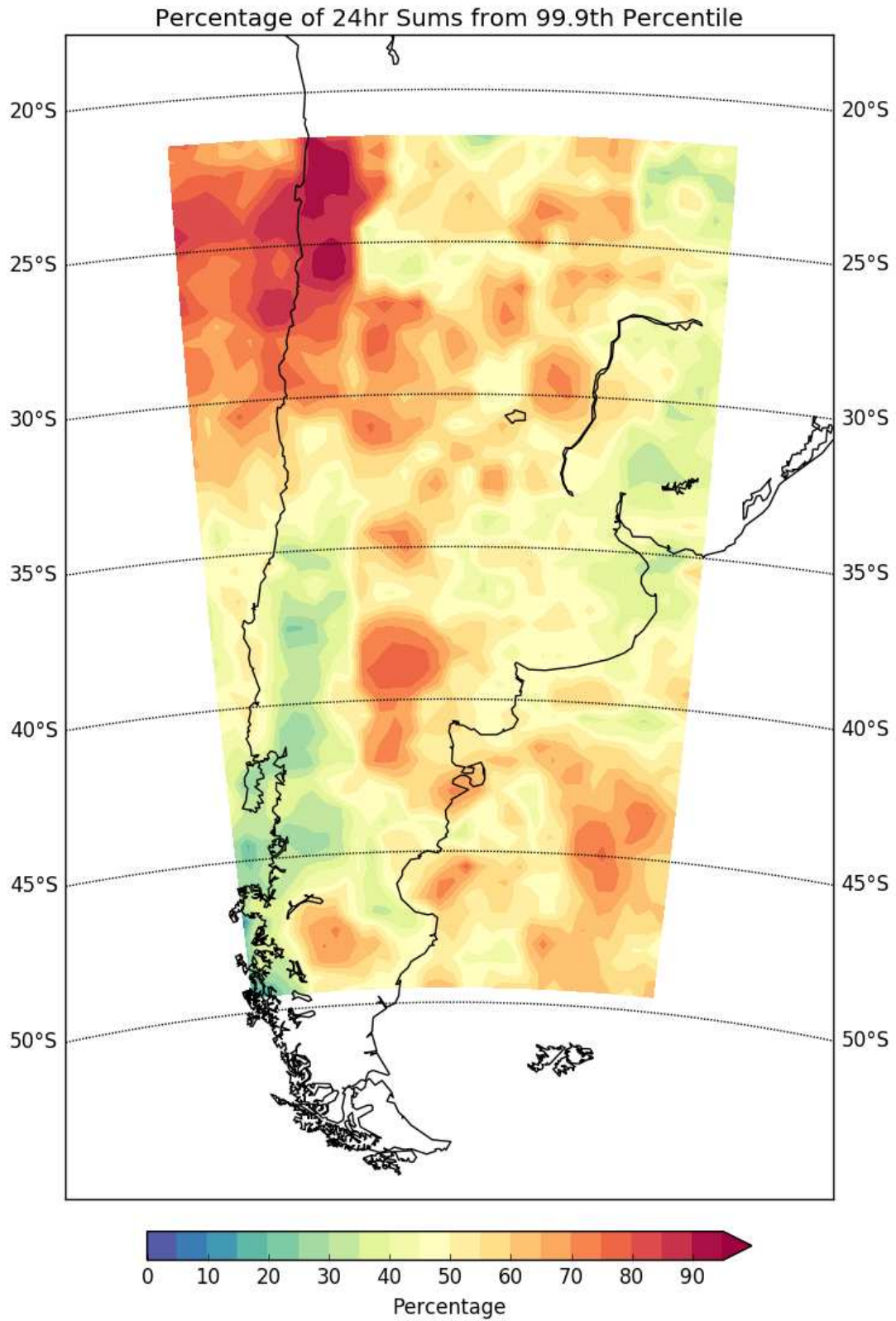


Figure 10-1: Percentage of total amount of 99.9th 24-hour precipitation at each gridpoint that comes from the 1-hour precipitation above the 99.9th percentile

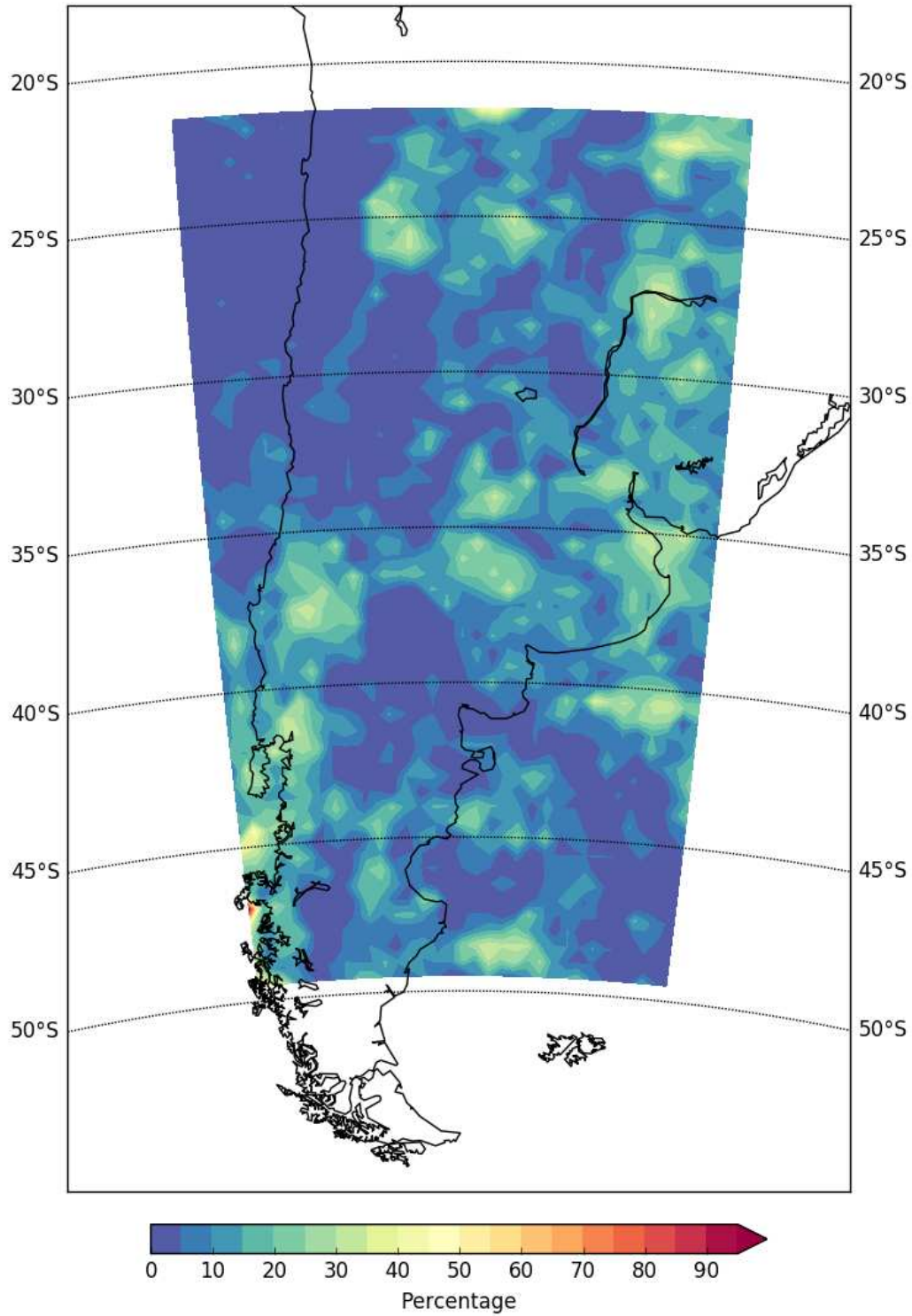


Figure 10-2: The percentage of the amalgamated 24hr periods that do NOT contain a 1-hour extreme event at each gridpoint

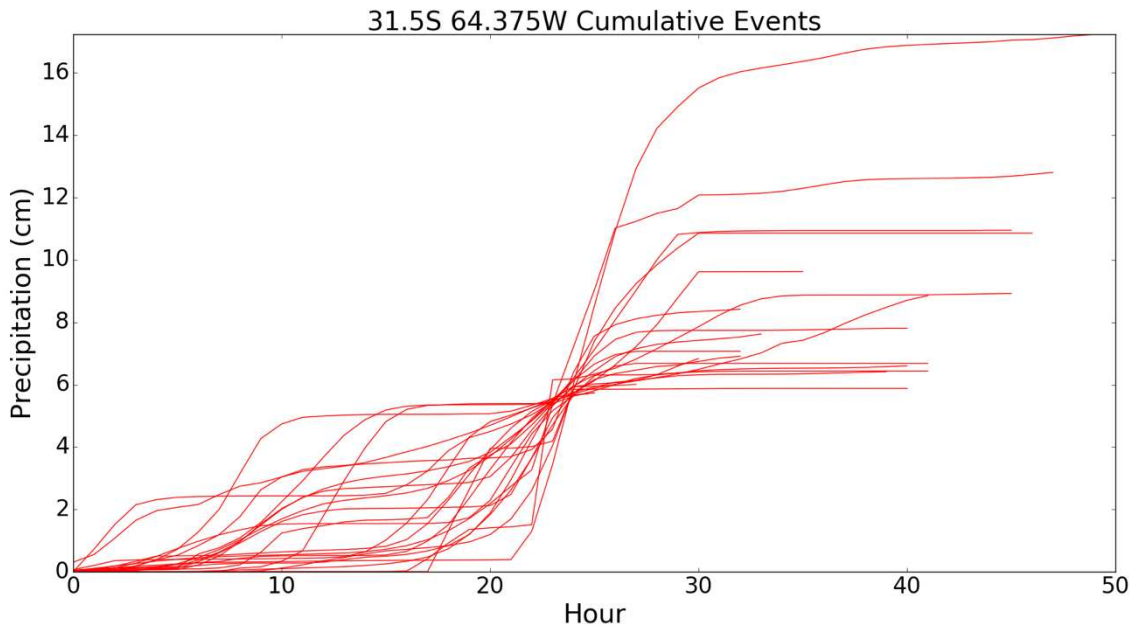


Figure 10-3 Cumulative precipitation from Córdoba during each of the unique events. The value plotted at each hour is the sum of that hour and all previous hours.

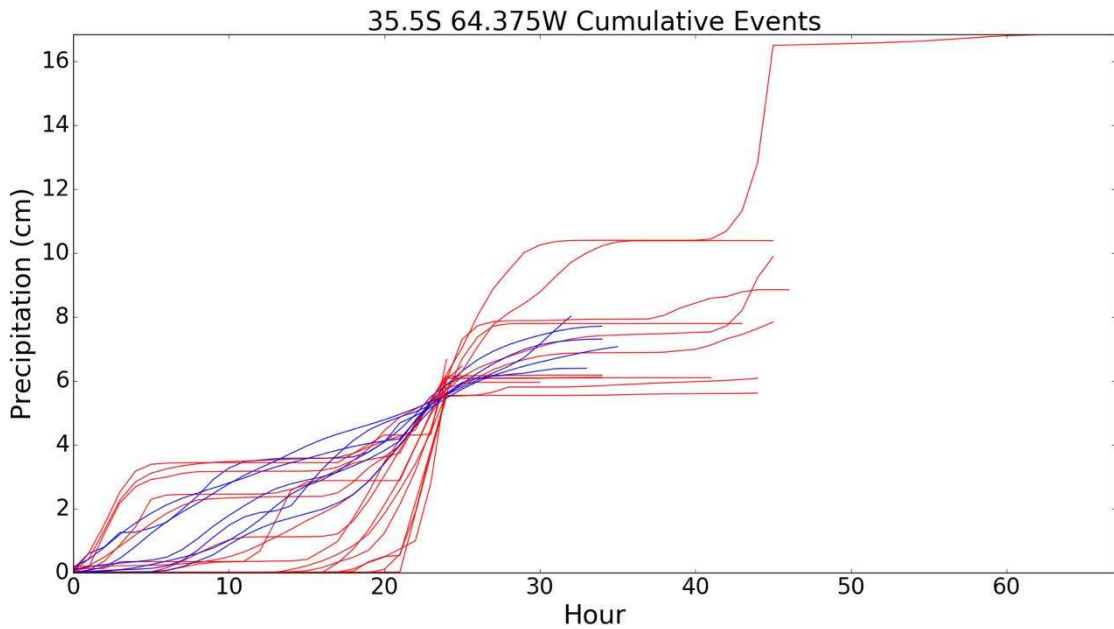


Figure 10-4 35.5S 64.375W, below, which is 4 degrees south of Córdoba

Figures 10-5 and 10-6 show the composite 500hPa height for each category at the respective gridpoints. It is clear from these plots that there are distinct differences between the

categories in the upper level pattern and consequently forcing. At both gridpoints instantaneous only shows the least pronounced upper level pattern, with intersect showing a more meridional pattern. This is less obvious at the Córdoba gridpoint, but the instantaneous pattern shows contours that are farther apart and more parallel to each other as opposed to the intersect pattern that shows tighter contours narrowing towards the east. At 35.5S 64.375W the 24-only composite shows a strongly pronounced upper level pattern leading into a jet streak that the gridpoint is in the (favored for lift) equatorward entrance region. Figures 10-7 and 10-8 show the same as 10-5 and 10-6 but for precipitable water, and here the differences are apparent. Both intersect and 24-hour only periods show more precipitable water than the instantaneous only periods, with 24-hour only showing slightly more than intersect.

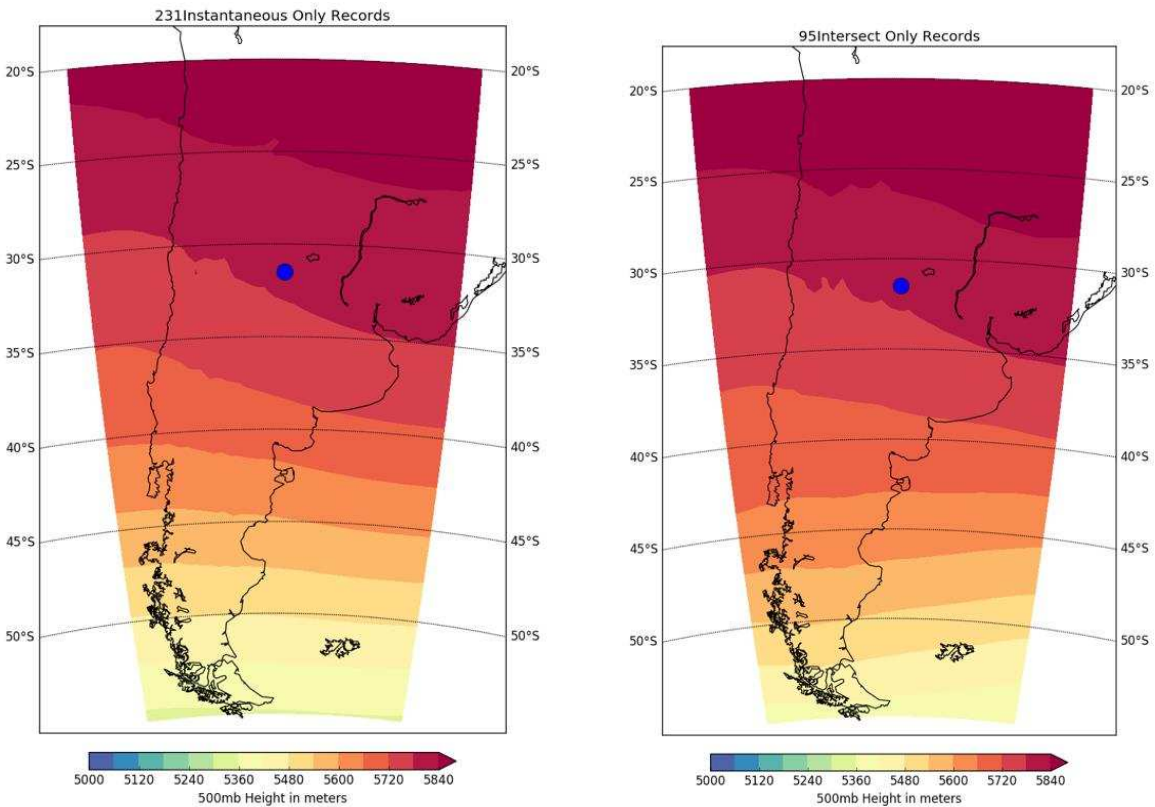


Figure 10-5 On the left is the average of 500hPa heights for instantaneous events above the 99.9th percentile not in a 24 hour event at Córdoba; on the right is the same for instantaneous events above the 99.9th percentile in a 24-hour event. Córdoba is noted by blue dot.

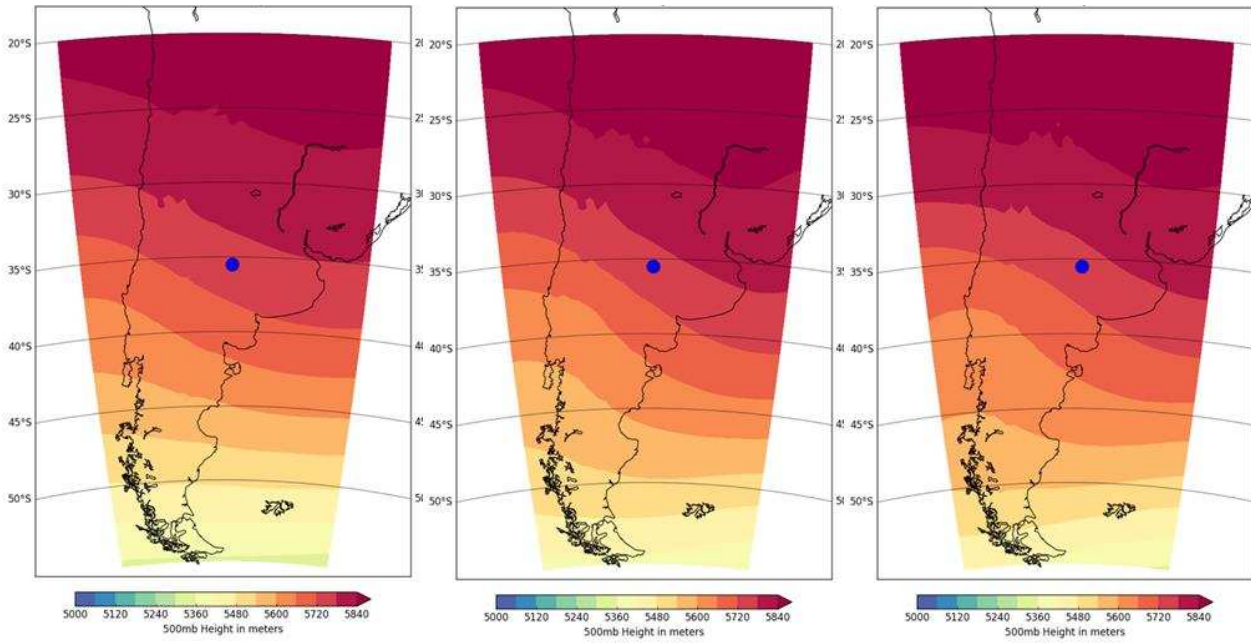


Figure 10-6 On the left is average 500hPa height for instantaneous events not in a 24 hour event, in the middle is the average for instantaneous events in a 24-hour event and on the right is the average during 24-hour events that did not contain an instantaneous event. For the gridpoint 35.5S 64.375W, which is noted by the blue dot

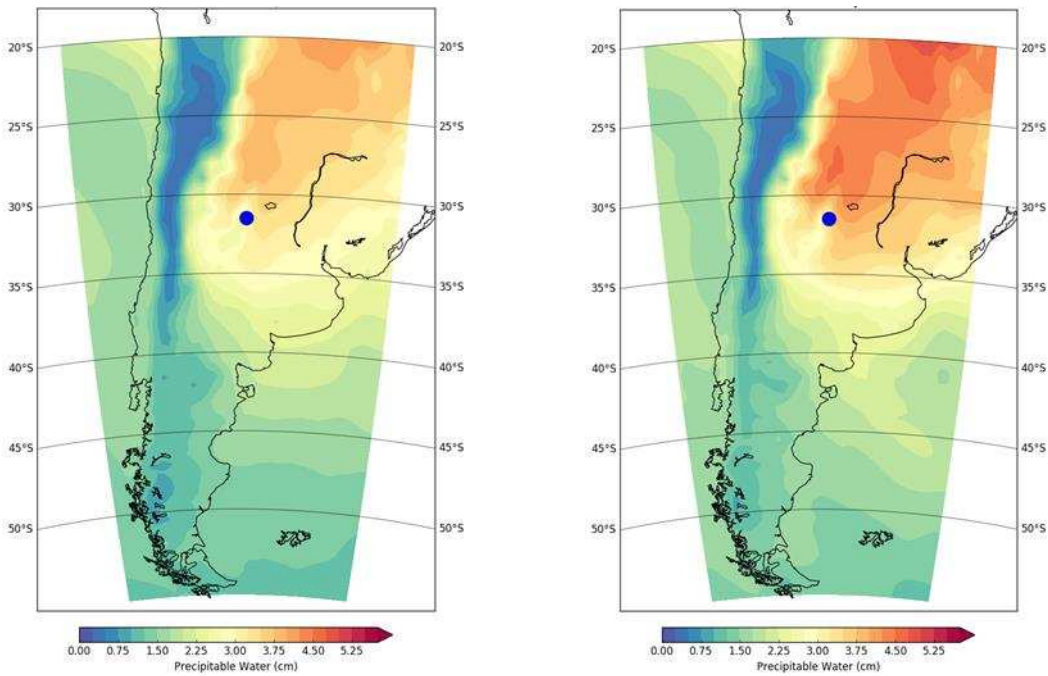


Figure 10-7 The same as Figure 10-5 but for precipitable water.

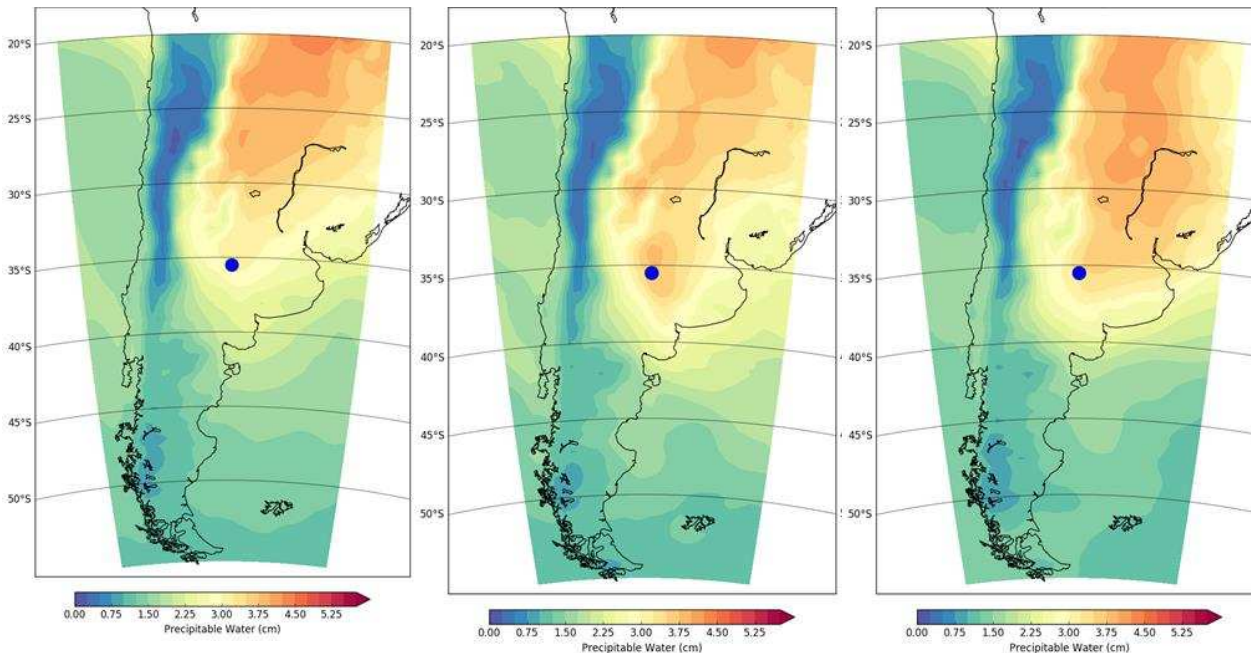


Figure 10-8 Same as figure 10-6 but for precipitable water.

10.3 Conclusions

These results point towards the fact that precipitation, especially sustained precipitation, requires both moisture and lift. At both the analyzed gridpoints, instantaneous precipitation outside of the 24-hour periods was associated with lower values of precipitable water and qualitatively weaker forcing at upper levels. Sustaining the pulses of convection in the cumulative plots requires the influence of factors outside simply more water, pointing to the role of the upper level forcing. The highest 24-hour totals occur when heightened forcing is able to take advantage of heightened water. It can be said that in the cases of these gridpoints the higher precipitable water is the result of dynamics such as lee cyclone development east of the Andes due to the upper level forcing. These lee cyclones are able to pull moist air from the Amazon into Argentina while also providing lift. The 1-hour cases however, rely more heavily on smaller scale processes such as surface heating for lift and therefore do not require as strong upper level

forcing. These events also do not need as high of atmospheric water content because they are composed largely of single or groups of thunderstorms that can grow and die without a constant source of moisture. Therefore, it is clear that extreme events at short timescales can occur without extreme moisture values, and it remains unclear how these events may be affected by the overall trend of rising atmospheric water vapor. Similarly, it can be seen that 24-hour events require aid from upper level forcing, something that is unaffected by atmospheric water vapor. Thus the uncertainty with regard to these events in the future is also quite large, since there are currently competing ideas as to what effect arctic amplification of warming may have on the jet stream.

CHAPTER 11 SUMMARY AND CONCLUSIONS

11.1 Summary

This thesis has explored the characteristics of extreme precipitation in Colorado and Argentina. Two gridpoints, near Northern Colorado and Córdoba, Argentina, were chosen as a focus to allow detail to be shown without undue length. These specific gridpoints were selected for local interest and as the center of the RELAMPAGO campaign, respectively. The temporal characteristics of these events were investigated, revealing strong seasonal dependence of the events on yearly timescales. No significant grouping was noted on decadal timescales, but it is possible that the Córdoba gridpoint is affected by ENSO. Two events were compared at the Northern Colorado gridpoint to gain an understanding of the synoptic forcings that can produce extreme precipitation amount of precipitation for widely varying amounts of precipitable water. This portion of the study also compared MERRA-2 data to stage IV data interpolated to the MERRA-2 grid in order to understand the effect that the coarseness of the MERRA-2 grid has on the quantitative amounts of precipitation. This effect was found to be a significant underestimation, but the spatial characteristics of the events were reasonably well captured. Two different sets of PCA were calculated. These PCA illustrated the different regimes of precipitation extremes that can occur. Colorado was distinctly split into summertime (high ridge, lots of precipitable water) and shoulder season regimes. The classification of Córdoba events primarily defined variability in the lee trough as the main factor that distinguishes between extreme precipitation events. PCA analysis using only the extreme events only describes variability within those events, so plots comparing a few of the variables used in the PCA to

climatological variables were computed. These plots confirmed that the PCA was indeed producing a good analysis of distinct events, rather than teasing out noise amid tightly clustered events. This interpretation is further corroborated by the plots of the significance of the eigenvectors, which show that the PC1 in both cases is significant and explains ~30-35% of variability. Finally, instantaneous extremes were compared to the 24 hour events. It was found that extreme events in the Córdoba region contribute a large amount to total precipitation, further confirming the results presented in this study's literature review. Moving forward knowledge of what extreme events have looked like in the past 36 years is important to attempting to project what these events might look like in the future. This study has taken a step toward that goal.

REFERENCES

- Agosta, E.A. and R.H. Compagnucci, 2012: Central-West Argentina Summer Precipitation Variability and Atmospheric Teleconnections. *J. Climate*, **25**, 1657–1677
- Allen, J.T., D.J. Karoly, and K.J. Walsh, 2014: Future Australian Severe Thunderstorm Environments. Part II: The Influence of a Strongly Warming Climate on Convective Environments. *J. Climate*, **27**, 3848–3868
- Barnes, E.A. and L. Polvani, 2013: Response of the Midlatitude Jets, and of Their Variability, to Increased Greenhouse Gases in the CMIP5 Models. *J. Climate*, **26**, 7117–7135
- Bosilovich, M. G., and Coauthors, 2015: MERRA-2: Initial evaluation of the climate. NASA/TM-2015-104606, Vol. 43, 139 pp. [Available online at <https://gmao.gsfc.nasa.gov/pubs/tm/docs/Bosilovich803.pdf>.]
- Brandenburg, F. H., 1900: Seasonal Forecasts in Colorado. *Mon. Wea. Rev.*, **28**, 206-207
- , 1911: Floods in Colorado and North-Western New Mexico. *Mon. Wea. Rev.*, **39**, 1570-1579
- C. A., 1902: Meteorology in Argentina. *Mon. Wea. Rev.*, **30**, 316-316
- Clayton, H. H., 1917: Atmospheric Circulation and the Weather in Argentina. *Mon. Wea. Rev.*, **45**, 60
- Cavalcanti, I. F. A., 2012: Large scale and synoptic features associated with extreme precipitation over South America: A review and case studies for the first decade of the 21st century. *Atmos. Res.*, **45**, 60
- Diffenbaugh, N., M. Scherer, and R. Trapp, 2013: Robust increases in severe thunderstorm environments in response to greenhouse forcing. *Proc. Natl. Acad. Sci. USA*, **110**, 16 361–16 366,
- Doswell, C.A., H.E. Brooks, and R.A. Maddox, 1996: Flash Flood Forecasting: An Ingredients-Based Methodology. *Wea. Forecasting*, **11**, 560–581
- Durango Herald, 2011: Durango’s Worst Flood. Accessed 8 March 2018, <https://durangoherald.com/articles/9779#slide=0>
- Durkee, J. D., T.L. Mote, and J. M. Shepherd, 2009: The Contribution of Mesoscale Convective Complexes to Precipitation across Subtropical South America. *J. Climate.*, **22**, 4590-4605
- Flohn, H., A. Kapala, H. R. Knoche, H. Mächel, 1990: Recent Changes of the Tropical Water and Energy Budget and of Midlatitude Circulations. *Climate Dyn.*, **4**, 237-252

- Francis, J.A., 2017: Why Are Arctic Linkages to Extreme Weather Still up in the Air?. *Bull. Amer. Meteor. Soc.*, **98**, 2551–2557
- Garavaglia, C. R., M. E. Doyle and ,V. R. Barros, 2014: Statistical Relationship Between Atmospheric Circulation and Extreme Precipitation in La Plata Basin. *Meteorol. Appl.* **21**, 553-562
- Gelaro, R., W. McCarty, M.J. Suárez, R. Todling, A. Molod, L. Takacs, C.A. Randles, A. Darmenov, M.G. Bosilovich, R. Reichle, K. Wargan, L. Coy, R. Cullather, C. Draper, S. Akella, V. Buchard, A. Conaty, A.M. da Silva, W. Gu, G. Kim, R. Koster, R. Lucchesi, D. Merkova, J.E. Nielsen, G. Partyka, S. Pawson, W. Putman, M. Rienecker, S.D. Schubert, M. Sienkiewicz, and B. Zhao, 2017: The Modern-Era Retrospective Analysis for Research and Applications, Version 2 (MERRA-2). *J. Climate*, **30**, 5419–5454
- Grimm, A.M. and R.G. Tedeschi, 2009: ENSO and Extreme Precipitation Events in South America. *J. Climate*, **22**, 1589–1609
- Groisman, P.Y., R.W. Knight, T.R. Karl, D.R. Easterling, B. Sun, and J.H. Lawrimore, 2004: Contemporary Changes of the Hydrological Cycle over the Contiguous United States: Trends Derived from In Situ Observations. *J. Hydrometeor.*, **5**, 64–85.
- Hoffman, R.N., N. Privé, and M. Bourassa, 2017: Comments on “Reanalyses and Observations: What’s the Difference?”. *Bull. Amer. Meteor. Soc.*, **98**, 2455–2459
- Jiang, P., Z. Yu, M. R. Gautam, K. Acharaya, 2016: The Spatiotemporal Characteristics of Extreme Precipitation Events in the Western United States. *Water Resour. Manage.* **30**, 4807–4821.
- Junker, N.W., R.S. Schneider, and S.L. Fauver, 1999: A Study of Heavy Rainfall Events during the Great Midwest Flood of 1993. *Wea. Forecasting*, **14**, 701–712
- Lin, Y., and K. E. Mitchell, 2005: The NCEP stage II/ IV hourly precipitation analyses: Development and applications. Preprints, 19th Conf. on Hydrology, San Diego, CA, Amer. Meteor. Soc., 1.2. [Available online at <http://ams.confex.com/ams/pdfpapers/83847.pdf>.]
- Maddox, R. A., C. F. Chappell, and L. R. Hoxit, 1979: Synoptic and mesoscale aspects of flash flood events. *Bull. Amer. Meteor. Soc.*, **60**, 115–123.
- , F. Canova, and L.R. Hoxit, 1980: Meteorological Characteristics of Flash Flood Events over the Western United States. *Mon. Wea. Rev.*, **108**, 1866–1877
- , R. A., F. Caracean, L. R. Hoxit, and C. F. Chappell, 1977: Meteorological aspects of the Big Thompson flash flood of 31 July 1976. NOAA Tech. Rep. NOAA-TR-ERL 388 APCL 41, 87 pp

- Mahoney, K., F.M. Ralph, K. Wolter, N. Doesken, M. Dettinger, D. Gattas, T. Coleman, and A. White, 2015: Climatology of Extreme Daily Precipitation in Colorado and Its Diverse Spatial and Seasonal Variability. *J. Hydrometeor.*, **16**, 781–792.
- Nelson, B.R., O.P. Prat, D. Seo, and E. Habib, 2016: Assessment and Implications of NCEP Stage IV Quantitative Precipitation Estimates for Product Intercomparisons. *Wea. Forecasting*, **31**, 371–394.
- Niznik, Matthew. 2016: ClickHist. 2018-03-29, <https://github.com/matthewniznik/ClickHist>
- Ohmura, A. and M. Wild, 2002: Is the Hydrologic Cycle Accelerating? *Science*, **298**, 1345–1346.
- Parker, W.S., 2016: Reanalyses and Observations: What’s the Difference?. *Bull. Amer. Meteor. Soc.*, **97**, 1565–1572
- , 2017: Reply to “Comments on ‘Reanalyses and Observations: What’s the Difference?’”. *Bull. Amer. Meteor. Soc.*, **98**, 2461–2461
- Penabla, O. P., and W. M Vargas, 2004: Interdecadal And Interannual Variations of Annual and Extreme Precipitation Over Central-Northeastern Argentina. *Int. J. Climatol.* **24**: 1565–1580
- Petersen, W.A., L.D. Carey, S.A. Rutledge, J.C. Knievel, N.J. Doesken, R.H. Johnson, T.B. McKee, T.V. Haar, and J.F. Weaver, 1999: Mesoscale and Radar Observations of the Northern Colorado Flash Flood of 28 July 1997. *Bull. Amer. Meteor. Soc.*, **80**, 191–216
- Púčik, T., P. Groenemeijer, A.T. Rädler, L. Tijssen, G. Nikulin, A.F. Prein, E. van Meijgaard, R. Fealy, D. Jacob, and C. Teichmann, 2017: Future Changes in European Severe Convection Environments in a Regional Climate Model Ensemble. *J. Climate*, **30**, 6771–6794
- Randles, C.A., A.M. da Silva, V. Buchard, P.R. Colarco, A. Darmenov, R. Govindaraju, A. Smirnov, B. Holben, R. Ferrare, J. Hair, Y. Shinozuka, and C.J. Flynn, 2017: The MERRA-2 Aerosol Reanalysis, 1980 Onward. Part I: System Description and Data Assimilation Evaluation. *J. Climate*, **30**, 6823–6850
- Rasmussen, K.L. and R.A. Houze, 2011: Orographic Convection in Subtropical South America as Seen by the TRMM Satellite. *Mon. Wea. Rev.*, **139**, 2399–2420
- , M.M. Chaplin, M.D. Zuluaga, and R.A. Houze, 2016: Contribution of Extreme Convective Storms to Precipitation in South America. *J. Hydrometeor.*, **17**, 353–367.
- , and R.A. Houze, 2016: Convective Initiation near the Andes in Subtropical South America. *Mon. Wea. Rev.*, **144**, 2351–2374

- Rose, B.E. and M.C. Rencurrel, 2016: The Vertical Structure of Tropospheric Water Vapor: Comparing Radiative and Ocean-Driven Climate Changes. *J. Climate*, **29**, 4251–4268
- Salio, P., M. Nicolini, and E.J. Zipser, 2007: Mesoscale Convective Systems over Southeastern South America and Their Relationship with the South American Low-Level Jet. *Mon. Wea. Rev.*, **135**, 1290–1309
- Saulo, C., J. Ruiz, and Y.G. Skabar, 2007: Synergism between the Low-Level Jet and Organized Convection at Its Exit Region. *Mon. Wea. Rev.*, **135**, 1310–1326
- Schubert, S.D., Y. Chang, M.J. Suarez, and P.J. Pegion, 2008: ENSO and Wintertime Extreme Precipitation Events over the Contiguous United States. *J. Climate*, **21**, 22–39
- Smith, H. W., 1897: Recent Publications. *Mon. Wea. Rev.*, **25**, 483
- Stephens, G.L., J. Li, M. Wild, C. A. Clayson, N. Loeb, S. Kato, T. L'Ecuyer, P. W. Stackhouse, M. Lebsock ; T. Andrews, 2012: An update on Earth's energy balance in light of the latest global observations. *Nat. Geosci.* **5**, 691-696
- Stephens, G.L. and T.D. Ellis, 2008: Controls of Global-Mean Precipitation Increases in Global Warming GCM Experiments. *J. Climate*, **21**, 6141–6155
- Stevenson, S. N., & Schumacher, R. S., 2014: A 10-year survey of extreme precipitation events in the central and eastern United States using gridded multisensor precipitation analyses. *Mon. Wea. Rev.*, **142**, 3147–3162.
- Stidd, C. K., 1967: The Use of Eigenvectors for Climatic Estimates. *J. Appl. Meteor.*, **6**, 255–264.
- Trapp, R.J. and K.A. Hoogewind, 2016: The Realization of Extreme Tornadoic Storm Events under Future Anthropogenic Climate Change. *J. Climate*, **29**, 5251–5265
- Wentz, F. J., and L. Ricciardulli, K. Hilburn, and C. Mears, 2007: How much more rain will global warming bring? *Science*, **317**, 233–235
- Zipser, E.J., D.J. Cecil, C. Liu, S.W. Nesbitt, and D.P. Yorty, 2006: Where are the Most Intense Thunderstorms on Earth? *Bull. Amer. Meteor. Soc.*, **87**, 1057–1072